Implications of the mitochondrial interactome of mammalian thioredoxin 2 for normal cellular function and disease

Christos T. Chasapis[1], Manousos Makridakis[2], Anastassios E. Damdimopoulos[3], Jerome Zoidakis[2], Vassiliki Lygirou[2], Manolis Mavroidis[2], Antonia Vlahou[2], Antonio Miranda-Vizuete[4], Giannis Spyrou[5], Alexios Vlamis-Gardikas[6]*

[1] Institute of Chemical Engineering Sciences (ICE-HT), Foundation for Research and Technology, Hellas (FORTH), Platani 26504, Greece

[2] Biomedical Research Foundation, Academy of Athens (BRFAA), Athens, Greece

[3] Department of Biosciences and Nutrition, Center for Innovative Medicine (CIMED), Karolinska Institutet, Huddinge, Sweden

[4] Redox Homeostasis Group, Instituto de Biomedicina de Sevilla (IBIS), Hospital Universitario Virgen del Rocío/CSIC/Universidad de Sevilla, 41013 Sevilla, Spain

[5] Department of Clinical and Experimental Medicine, Division of Clinical Chemistry, Linköping University, S-581 85 Linköping, Sweden

[6] Department of Chemistry, University of Patras, Rion 26504, Greece

*Corresponding author. Email: avlamis@upatras.gr

Running title: The thioredoxin 2 interactome

Abstract

Multiple thioredoxin isoforms exist in all living cells. To explore the possible functions of mammalian mitochondrial thioredoxin 2 (Trx2), an interactome of mouse Trx2 was initially created using (i) a monothiol mouse Trx2 species for capturing protein partners from different organs and (ii) yeast two hybrid screens on human liver and rat brain cDNA libraries. The resulting interactome consisted of 195 proteins (Trx2 included) plus the mitochondrial 16S RNA. 48 of these proteins were classified as mitochondrial (MitoCarta2.0 human inventory). In a second step, the mouse interactome was combined with the current four-membered mitochondrial sub-network of human Trx2 (BioGRID) to give a 53-membered human Trx2 mitochondrial interactome (52 interactor proteins plus the mitochondrial 16S RNA). Although thioredoxins are thiol-employing disulfide oxidoreductases, approximately half of the detected interactions were not due to covalent disulfide bonds. This finding reinstates the extended role of thioredoxins as moderators of protein function by specific non-covalent, protein-protein interactions. Analysis of the mitochondrial interactome suggested that human Trx2 was involved potentially in mitochondrial integrity, formation of iron sulfur clusters, detoxification of aldehydes, mitoribosome assembly and protein synthesis, protein folding, ADP ribosylation, amino acid and lipid metabolism, glycolysis, the TCA cycle and the electron transport chain. The oxidoreductase functions of Trx2 were verified by its detected interactions with mitochondrial peroxiredoxins and methionine sulfoxide reductase. Parkinson's disease, triosephosphate isomerase deficiency, combined oxidative phosphorylation deficiency, and lactate dehydrogenase b deficiency are some of the diseases where the proposed mitochondrial network of Trx2 may be implicated.

Key words: redox, disulfide, interactome, interactor, thiol-disulfide interchange, thioredoxin, mitochondrion

Abbreviations

2D: two dimensional; NADPH: reduced nicotinamide adenine dinucleotide phosphate; Trx: thioredoxin; TrxR: thioredoxin reductase; Y2H: yeast two hybrid.

Introduction

Thioredoxin and glutaredoxin are proteins that maintain the reduction of cytosolic disulfides in most living cells and are implicated in many different functions [1]. Their first discovered pivotal role was their ability to donate electrons to ribonucleotide reductases for the reduction of ribonucleotides to deoxyribonucleotides, the precursors of DNA synthesis [2, 3]. While reducing substrates, thioredoxins and glutaredoxins get oxidized to be in turn reduced by thioredoxin reductase (TrxR) and glutathione respectively. The ultimate electron donor for these systems is NADPH. Their ability to donate electrons places thioredoxins and glutaredoxins in the general category of 'antioxidants' whose specific functions are determined by the particular molecule that receives their electrons. Reduction of methionine sulfoxide reductase by thioredoxins and glutaredoxins is a well known example of such antioxidant function [4, 5]. Thioredoxins and glutaredoxins may have common substrates with the reduction of glutathione mixed disulfides being exclusive for glutaredoxins [6]. In some cases, thioredoxins (and glutaredoxins) may bind non-covalently to other proteins for gain/loss of function. In the case of *Escherichia coli* (*E. coli*), binding of reduced thioredoxin 1 (EcoTrx1) to gene 5 protein of phage T7 gives rise to a functional T7 DNA polymerase [7]. Reduced cytosolic human thioredoxin 1 (Trx1) may bind to apoptosis signaling kinase 1 (ASK1) to keep the kinase inactive. Removal of Trx1 from ASK1 by oxidation of Trx1 or by the thioredoxin-interacting protein (Txnip) promotes apoptosis ([8] and references therein). Reduced mitochondrial thioredoxin 2 (Trx2) will also normally bind to mitochondrial ASK1 and prevent its activation and concomitant apoptosis [9, 10]. Therefore, thioredoxins (and glutaredoxins) may associate with a number of proteins that constitute their interactomes and affect their functions decisively. The thioredoxin and glutaredoxin interactomes, however, are far from complete.

Mammalian cells have two distinct thioredoxin types; one cytosolic (Trx1) and one mitochondrial (Trx2), each protein being reduced by its specific TrxR. Trx1 is reduced by cytosolic TrxR isoforms [11], whereas Trx2 is reduced by a mitochondrial TrxR (thioredoxin reductase 2 or TrxR2) [12]. Although Trx1 is the prominent thioredoxin species in most tissues, it is barely detectable in heart and skeletal muscle where Trx2 is highly expressed [13]. Trx1 and Trx2 may respond differently to external stimuli affecting the redox state of the cell. In the case of increased reactive oxygen species (ROS) via epidermal growth factor addition, selective oxidation of cytoplasmic Trx1 but not Trx2 or the glutathione pools [14]

occurred. On the other hand, tumor necrosis factor α (TNFα) caused preferential oxidation of Trx2 whose overexpression inhibited the TNFα-induced, NF-κB translocation to the nucleus (activation) [15]. Overexpresion of Trx1 or Trx2 may have opposing effets: in the regulation of transcription of hypoxia-inducible factor-1α (Hif-1α) [16], Trx2 overexpression in HEK cells lowered Hif-1α protein levels, whereas Trx1 raised them. Since the mRNA levels of Hif-1α were unaltered, results were explained in view of the activation of transcription factors that regulated cap-dependent translation and by the production of ROS. Overexpression of Trx2 increased the production of mitochondrial ROS and decreased translation of Hif-1α [16].

Thioredoxins (and dithiol glutaredoxins) have an active site composed of two vicinal thiols (CxxC) that is reversibly oxidized/reduced during the catalytic cycle of the enzyme. The electron transfer of the thioredoxin thiols to the substrate disulfide starts with a nucleophilic attack from the thiolate of the N-terminal thiol (catalytic) of reduced thioredoxin. A following attack from the second non-catalytic, resolving thiol to the sulfur of the catalytic that participates in the temporary disulfide with the substrate leads to an oxidized thioredoxin and a reduced substrate. This mechanism has been employed to trap thioredoxin-substrates by using mutant monothiol thioredoxins with the second "resolving" thiol of the active site being changed to Ser (mutant active site: CxxS). The mutated monothiol thioredoxins can attack and bind to their dithiol substrates but cannot be released from them as they lack the second non-catalytic cysteine. Monothiol thioredoxin mutants of EcoTrx1 [17, 18], plant thioredoxins [19], *Plasmodium falciparum* [20] and *Entamoeba histolytica* [21] have been used (among others) to identify their potential substrates. Monothiol mutant glutaredoxins have served the same purpose (e.g. monothiol human glutaredoxin 2 [22]).

Monothiol mouse Trx1 has been used in combination with isotope-coded affinity tags to identify transnitrosylation targets [23] and protein networks [24], while expression of monothiol Trx1 in whole mice has provided the interacting proteome of cytosolic Trx1 [25]. The current experiment-based interactome of human Trx1 is composed of 147 proteins [26] compared to the 59 interactors described for Trx2 [26], with only four of the latter being mitochondrial (MitoCarta [27]). Respective interactomes for the rat and mouse Trx2 are currently not available ([26]). To create an interactome for mouse Trx2, we employed an immobilized monothiol mouse Trx2 lacking its mitochondrial signal sequence, for the detection of strong non-covalent and covalent (disulfides) interactions with proteins from different mouse tissues. In addition, yeast two hybrid (Y2H) screens with rat and human cDNA libraries were used to identify weaker non-covalent interactions. The novel results (194 proteins plus the mitochondrial 16S RNA) were integrated with the described 59 interactors

(BioGRID) of human Trx2 to give an updated human interactome of 253 proteins (excluding Trx2). 52 of these proteins were mitochondrial (four from BioGRID, plus 48 novel hits), while the mitochondrial 16S RNA was identified as an additional interactor by Y2H screens. The possible novel cellular functions of Trx2 and its association with human diseases are discussed within the context of its mitochondrial interactome.

Materials and Methods

Construction of plasmid for the overexpression of ΔTrx2C93S.

A plasmid (pET15b) containing the gene encoding mouse Trx2 [13] was used as a template to initially generate the 5' and 3; parts of the *TXN2* gene, each coding for the C93S mutation and containing some common sequence. The 5' part was amplified with primers F-NdeI (CGA GGA TCC ATA TGA CAA CCT TTA ATA TCC AGG) and C93S-RC (CAG GAT CTT GCT GGG TCC ACA CC) as forward and reverse complementary respectively, while the 3' part was amplified using F-C93S (GGT GTG GAC CCA GCA AGA TCC TG) and EcoRI-RC (CCC TTA GAA TTC CCA ATC AGC TTC TTC AGG) as forward and reverse complementary respectively. The 5' and 3' PCR fragments of the gene containing the C93S mutation were gel-purified, mixed and used as a template for the F-NdeI and EcoRI-RC primers to receive a PCR product encoding Trx2 without its 1-59 mitochondrial targeting signal (now starting as (M)TTF...) and bearing the C93S mutation (ΔTrx2C93S). Insertion of the product in the NdeI and EcoRI of vector pET24a+ gave rise to plasmid pET24a+ΔTrx2C93S coding for ΔTrx2C93S comprised of 107 amino acids. The mouse Trx2 lacking its mitochondrial targeting sequence is identical to the enzyme from rat and differs in only two amino acids from human Trx2.

Purification of ΔTrx2C93S

E. coli BL21(DE3) cells were transformed with plasmid pET24a+ΔTrx2C93S and were grown in LB medium with kanamycin (50 mg/ml), in 1 l cultures in 2 l flasks at 37 ºC, 140 rpm. At A_{600} of ~0.5, IPTG was added (0.5 mM), temperature was set to 25 ºC and cells were further grown for 6 hours after which they were harvested and resuspended in 20 mM Tris (non-buffered) as 100 A_{600}/ml. EDTA (1 mM), lysozyme (0.1 mg/ml) and 2 mercaptoethanol (50 mM) were added and the resuspension was frozen and thawed for three times. The sample was sonicated thoroughly and centrifuged at 10,000 g for 30 min. The occurring total lysate supernatant (TCLS) was filtered through a 2 μm filter and loaded on a DEAE FF column equilibrated with 20 mM Bis-Tris-HCl, pH 6.7. ΔTrx2C93S was eluted in a 0 to 1 M NaCl gradient at ~15 mS/cm (supplementary figures 2 and 3). Fractions containing ΔTrx2C93S (by SDS-PAGE) were concentrated, made up to 5 mM DTT, stood for 30 min at RT and chromatographed on Sephadex G-50 Superfine in 20 mM Hepes-KOH, 1 mM EDTA, 100 mM NaCl, pH 7.0, at 0.1 ml/min. ΔTrx2C93S was obtained in a homogeneous stage after this

purification step. The extinction coefficient ε_{280} of purified ΔTrx2C93S was assumed as $6990 \cdot M^{-1} \cdot cm^{-1}$ (https://web.expasy.org/protparam/).

Immobilization of ΔTrx2C93S on solid phase

Homogeneous ΔTrx2C93S (estimated pI of 4.9) was coupled to Affi-Gel 15 according to the protocol of the manufacturer (Bio-Rad). In experiments concerning interaction of ΔTrx2C93S with crude lysates, ~10 mg ΔTrx2C93S was immobilized/ml of Affi-Gel beads. When mitochondrial extracts were obtained, 1 ml of beads contained ~1 mg ΔTrx2C93S. The conjugated beads were used for a maximum of two affinity experiments after which they were discarded.

Preparation of tissue extracts

Male mice of C57BL/6 genetic background, 5-6 months old, were used. The procedures for the care and treatment of animals were approved by the Animal Care Committee of East Attica County, Athens, Greece, and followed the guidelines of the Association for the Assessment and Accreditation of Laboratory Animal Care and the recommendations of the Federation of European Laboratory Animal Science Association.

Lung, kidney and skeletal muscle were isolated immediately after sacrifice, inserted in liquid N_2 and stored at -80 ºC. Frozen tissue was initially crushed and homogenized by pestle in a liquid N_2 cooled mortar to a fine powder which was transferred to ice cold 50 mM Tris-HCl, 1 mM EDTA, 0.2 M KCl, pH 8.0 with a freshly added cocktail of protease inhibitors (1 mM PMSF, 0.5 mM Na_3VO_4, 5 mM NaF, 1:25 $^{v}/_{v}$ complete (EDTA free) protease inhibitor cocktail in PBS from Roche (catalogue number: 11873580001). The sample was sonicated on ice thoroughly. Triton X-100 (1 % $^{v}/_{v}$) was added and the homogenate was centrifuged at 14.000 g for 45 min to obtain the total cell lysate supernatant (TCLS) fraction. In the case of kidney lysate preparations for example, to 0.647 gr of pulverized kidney tissue, 5 ml of 50 mM Tris-HCl, 1 mM EDTA, 0.2 M KCl, pH 8.0 were added. Typical protein concentrations of the TCLS were in the order of ~10 mg/ml.

Preparation of mitochondrial extracts

Heart and brain (and skeletal muscle in one case: supplementary table 1.13) mitochondrial fractions were prepared according to [28]. In more detail, animals were perfused with ice-cold PBS, and hearts and quadriceps muscle were isolated from six mice. Freshly isolated tissue (1-2 gr muscle/heart, or seven whole brains without their cerebella) was minced in 10 ml ice-

cold MSE (225 mM mannitol, 75 mM sucrose, 1 mM EGTA, 1 mM Tris–HCl pH 8.0, 0.5 mM Na_3VO_4, 5 mM NaF, 1 mM PMSF and and protease inhibitors (Sigma Protease Inhibitor Cocktail P8340). The minced tissue was further homogenized by up to 15 strokes of Teflon head at 1500 rpm on ice using a Glas-Col homogenizer. The homogenate was centrifuged at 800 g for 10 min and the pellet was re-extracted with 6 ml MSE and centrifuged again at 800 g for 10 min at 4 °C. The two resulting supernatants were combined and centrifuged at 12,000 g for 30 min at 4 °C to give crude mitochondria at the pellet and cytoplasm in the supernatant. Crude mitochondria were suspended in 1 ml MSE and placed on the top of a sucrose step gradient (60, 50, 40, 30 and 20 %, 2 ml each) in which were centrifuged at 200,000 g for 30 min at 4 °C using a TH641 (Sorvall) swing out rotor. 0.5 ml fractions were collected from the 40 % and the 50 % sucrose steps. The selected fractions were subjected to Western blotting to ensure the presence of mitochondria. The adenine nucleotide translocator 1 (ANT 1) was considered as a positive mitochondrial marker, while LAMP-1 protein and calsequestrin were considered as markers for late endosomes-lysosomes and endoplasmic reticulum respectively. Representative Western blots with antibodies against ANT 1 (sc 9300, Santa Cruz Biotechnology, 1:300 dilution), LAMP-1 (NB1952 from Novus Biologicals antibody at 1:400 dilution) and calsequestrin (sc 28274, Santa Cruz Biotechnology, 1:400 dilution) are shown in supplementary figure 3 for samples derived from cardiac muscle. Fractions positive for ANT 1 but negative for LAMP-1 and calsequestrin were considered as mitochondrial fractions (supplementary figure 3). This rationale and method were followed to isolate mitochondrial fractions from brain, heart and quadriceps muscle.

Purification of ΔTrx2C93S interacting substrates

Prior to adding to cell lysates, beads-ΔTrx2C93S (1 ml) were reduced with DTT 5 mM for 30 min at RT in 20 mM Tris-HCl, pH 8.0, 1 mM EDTA, 0.2 M KCl. Thereafter beads were transferred to a column and washed extensively in 50 mM Tris-HCl, 1 mM EDTA, 0.2 M KCl, pH 8.0 to remove the DTT. 5 ml of the lysate (~10 mg/ml protein) in 50 mM Tris-HCl, 1 mM EDTA, 0.2 M KCl, pH 8.0 was added to solid phase (1 ml) with bound ΔTrx2C93S and the slurry was left (in 15 ml tubes) on a rocking platform at 4 °C overnight. To complete all nucleophilic attacks of any remaining thiolates of ΔTrx2C93S to possible substrates, selenite (0.1 mM) was added the next day and the suspension was mildly rotated at room temperature for 1 hour after which it was transferred on a glass column. The flow through was discarded and the beads were washed extensively with (2x13 ml) 50 mM Tris-HCl, 1 mM EDTA, 0.2 M KCl, pH 8.0 (high salt wash), (13 ml) 20 mM Hepes-KOH pH 8.0 (low salt wash), 50 mM

Tris-HCl, 1 mM EDTA, 0.2 M KCl, pH 8.0 1 % v/v Triton X-100 (13 ml) (high salt wash with detergent) and finally with 20 mM Hepes-KOH pH 8.0 (4x13 ml). At this stage, the first elution of non-covalently bound material (via hydrophobic interactions) was performed by adding 0.1 M acetic acid-formic acid pH 2.1 (2x1 ml). Immediately after, 1 M Tris-HCl pH 9.0 (0.4 ml) plus 20 mM Hepes-KOH pH 8.0 (1 ml) were sequentially added. The column was further washed with 20 mM Hepes-KOH pH 8.0 (4 ml) and the column temporarily gravity dried. All the above elutions were polled in the "acid wash" fraction (about 7.5 ml) to which KOH 10 M (60 µl) were added to a final pH of ~8. The slightly dried column beads-ΔTrx2C93S after the acid elution were transferred to a new tube (15 ml) where 20 mM Hepes-KOH pH 8.0 with 10 mM DTT (3 ml) were added. The slurry stood at RT for 1 h after which it was reloaded on a glass column and washed with 20 mM Hepes-KOH pH 8.0 (2x4 ml). The whole 11 ml constituted the "DTT fraction" corresponding to covalently bound material (via disulfide bonds) freed from the column by DTT reduction. Acid and DTT fractions were kept on ice. Their proteins were precipitated with TCA (6 % $^{w}/_{v}$) and deoxycholate (125 µg/ml) [29], centrifuged (10.000 g, 30 min, 4 °C), the resulting pellets were washed with acetone, methanol, resuspended in isoelectrofocusing buffer (IEF) and subjected to electrophoresis. All fractions resulting from the different elutions prior and after TCA precipitation were kept on ice.

Electrophoretic separation of fractions

Two dimensional separation of the purified fractions took place as follows: Samples were resuspended in IEF sample buffer (7 M urea, 2 M thiourea, 50 mM Tris-HCl, 2 % CHAPS, 0.4 % DTE, 0.1 % bromophenol blue, pH 7.5) including 3.6 % v/v of protease inhibitors mix (Roche, Cat No: 11873580001) and loaded onto 7 cm strips pH 3-10 (Biorad) using cups. For the first dimensional separation a voltage of 4000 V was applied for a total run of 12,500 VH. Strips were then incubated for 15 min at room temperature with equilibration solution I (6 M urea, 50 mM Tris-HCl, pH 8.8, 30 % glycerol, 2.0 % SDS, 30 mM DTE) followed by a 15 min incubation with equilibration solution II (same composition as in solution I but with 230 mM iodoacetamide instead of DTE) for reduction and alkylation of the proteins. Strips were then applied on the top of 12.5 % polyacrylamide mini gels, by the use of 0.5 % agarose in TGS buffer and SDS-PAGE run at 40 V for 15 min followed by 80 V for 2 hours approximately. 2D gels were stained with colloidal Coomassie blue overnight and destained with ultra pure water.

Protein identification by MALDI-TOF-MS (Peptide Mass Fingerprinting)

Following this procedure gels were scanned, spots were detected and excised. In gel-trypsin digestion was performed according to standard protocols. In brief, destaining of the excised spots took place by 30 min incubation in 150 µl of destaining solution (50 mM ammonium hydrogen carbonate, 30 % acetonitrile). Protein spots were then washed with 150 µl ultra pure water twice and dried with the help of a vacuum centrifuge. Dried protein spots were trypsinized with the addition of 30 ng trypsin (diluted in 10 mM ammonium hydrogen carbonate pH 8.0) and overnight incubation at room temperature. Finally tryptic digests were extracted by the addition of 10 µl extraction solution (50 % $^{v}/_{v}$ acetonitrile, 0.1 % $^{v}/_{v}$ TFA) and 15 min incubation at room temperature. Peptide mixture (1 µl) was applied on an anchor chip MALDI plate with 1 µl matrix solution (50 % $^{v}/_{v}$ acetonitrile, 0.1 % $^{v}/_{v}$ TFA, 0.025 % α-cyano-4-hydroxycinnamicacid) containing the peptides des-Arg-bradykinin (Sigma, 904.4681 Da) and adrenocorticotropic hormone fragment 18–39 (Sigma, 2465.1989 Da) as internal standards. Samples were analysed in a TOF mass spectrometer (Ultraflex, Bruker Daltonics, Bremen, Germany). Peak list was created with Flexanalysis v2.2 software by Bruker by summarizing 400 laser shots at intensity between 40 and 60 %. Smoothing was applied with Savitzky-Golay algorithm (width 0.2 m/z, cycle number 1). Signal to noise was calculated by SNAP algorithm and a threshold ratio of 2.5 was allowed. Peptide matching and protein searches were performed automatically with Mascot Server 2 (Matrix Science). The peptide masses were compared to the theoretical peptide masses of all available proteins from *Mus musculus* in the Swissprot database. Monoisotopic masses were used, 1 miscleavage site was calculated for trypsin proteolytic products, carbamidomethylation of cysteine was calculated as fixed and oxidation of methionine as variable modifications and finally a mass tolerance of 25 ppm was allowed.

Isolation of thioredoxin interacting clones using the yeast two hybrid system

cDNA libraries from human liver and rat brain were cloned into plasmid pGAD10 [*LEU2*, *GAL4* (768–881)] (Clontech). All cDNA clones were therefore expressed as fusion proteins with the *GAL4* activation domain (AD). The human Trx2 gene (without its mitochondrial signal, Trx2 starting as TTF) was cloned into the pGBT9y (Clontech) and expressed as a fusion protein with the DNA binding domain (BD) of the GAL4 transcriptional activator. The fusion site was verified by sequencing (not shown). pGBT9y also contained the gene for Amp resistance but in the place of the *Leu* gene (as in pGAD10) it contained the gene coding for tryptophan (Trp). The Trx2 gene was also cloned into the pAS2 vector which is similar to

pGBT9y but with the ability to express higher amounts of GAL4-Trx2, allowing thus, the detection of weak protein interactions with Trx2. The pGBT9y/Trx2 construct was transformed into yeast HF7C cells. HF7C-pGBT9y/Trx2 cells surviving on plates without Trp were in addition transformed with the human liver or the rat brain library in pGAD10 plasmid using PEG/ lithium acetate. The yeast colonies growing on plates lacking Leu/Trp/His were numbered, picked with an inoculating loop and replated on plates lacking Leu/Trp/His. After three days at 30 °C, growing (positive) colonies were collected and used for preparation of plasmid DNA which was electroporated into the HB 101 bacterial strain. Selection was on M9 Amp-containing plates lacking Leu. Plasmids from distinct growing colonies were isolated and transformed separately into yeast strain Y187 which grown on synthetic defined medium (SD) plates lacking Leu so that only cells containing the same pGAD10/cDNA clone would grow. Growing colonies from each plate were mated with pAS2/Trx2, HF7C yeast cells and spread on SD plates lacking Leu/Trp. All cells that grew contained the same pGAD10/cDNA clone and the pAS2/Trx2 vector. cDNA inserts from the growing clones were sequenced and provided the genes presented in supplementary tables 2.2 and 2.3.

Construction of the Trx2 interactome and diseasome.

Human interactors of Trx2 were mined from the BioGRID web resource [26]. The mitochondrial topology of a protein species was according to Human MitoCarta2.0 (1158 mitochondrial genes [27]). The disease network (diseasome) uncovering disease-disease relationships was reconstructed by the Gene Prioritization and Evidence Collection (GPEC) plug-in of Cytoscape v.3.0.0 [30] taking into consideration the interactions between the mitochondrial Trx2 targets (MitoCarta and BioGRID) and the gene-disease associations retrieved from OMIM [31]. GO annotation of human proteins was performed by DAVID tool [32] and the ClueGO v.2.0.0 plug-in of Cytoscape as described previously [33, 34].

Results

1. Construction of the interactome of human Trx2

Isolation and analysis of Trx2-interacting proteins by proteomics

To isolate Trx2 interacting proteins, mouse total protein extracts from lung, kidney or skeletal muscle and mitochondrial extracts from mouse brain were initially left to interact overnight with Affi-Gel 15 coupled to ΔTrx2C93S. Next, the Affi-Gel slurry was loaded onto a column and washed with a succession of low and high salt washes. Two types of elutions followed. The first elution ("acid wash" by acetic/formic acid) aimed to the isolation of proteins bound strongly but in a non-covalent manner to Trx2. The second elution by DTT aimed at the proteins bound exclusively by a disulfide bond. The eluted proteins were visualized by 2D electrophoresis and picked and analysed by MALDI-TOF. Mouse mitochondrial extracts from cardiac and skeletal muscle were also used but analysed by 1D gels. The proteins identified using the two different elution methods from the different tissues and mitochondrial fractions are presented in supplementary tables 1.1-1.13. A synopsis of the proteomics results (supplementary tables 1.1-1.13) is presented in supplementary table 2.1 (176 protein species).

Trx2-interacting proteins as revealed by Y2H screens

A human liver cDNA library was used in Y2H screens to isolate proteins interacting with Trx2. Approximately $16x10^6$ clones were examined. 110 positive clones (growing on Leu/Trp/His) were analyzed. The Y2H screen of the human liver library gave 11 clones, all novel interacting partners for Trx2 (supplementary table 2.2). Another Y2H screen using a cDNA library from rat brain, gave 7 novel interactors (supplementary table 2.3).

Integration of the mouse, rat and published data for the construction of a probable interactome of human Trx2

The information obtained from the mouse proteomics analysis and the human and rat Y2H experiments were combined to construct an interactome for human Trx2. This is most likely a valid approach as mouse, rat and human Trx2 are practically identical (supplementary figure 1). The resulting combined interactome consisted of 195 proteins (Trx2 itself, plus 176 interactors from the proteomics approach, plus 11+7 protein from the Y2H screens, supplementary tables 2.1, 2.2, and 2.3), plus the mitochondrial 16S RNA. Inclusion of the

known (BioGRID) human Trx2 interactome of 59 proteins (supplementary table 2.4) raised the interactome of human Trx2 to 254 proteins (including Trx2), plus the mitochondrial 16S RNA. Not a single protein species was common between the current and published data.

Selection of Trx2-specific mitochondrial protein interactors

As Trx2 is considered a mitochondrial protein, its potential interactors would be expected to be mitochondrial too. In the protocols used for the isolation of Trx2 interactors, the total cell lysates used contained non-mitochondrial proteins, thus, a number of cytosolic proteins appeared interacting with Trx2 (supplementary table 2.1). The same applied for the Y2H screens (supplementary tables 2.2, 2.3). To overcome these cytosolic interactions, we examined whether the proteomics approach would be more specific if only mitochondrial fractions were examined as the source of Trx2 interactors (supplementary tables 1.9-1.13). However, this approach did not achieve exclusive selectivity for mitochondrial interactors: in the case of the mitochondrial fractions isolated from brain (supplementary tables 1.9, 1.10, 2.1 combined acid and DTT elutions) for example, 16 out of a total of 26 protein species were mitochondrial according to the MitoCarta repository of proteins with strong evidence for mitochondrial localization (MitoCarta2.0 [27]). To overcome the apparently false cytosolic positives, all potential interactors of Trx2 had their localization validated by MitoCarta. According to this approach, the novel mouse, human and rat mitochondrial Trx2 interactors were 48 proteins, plus the mitochondrial 16S RNA (supplementary tables 2.1, 2.2, and 2.3; mitochondrial species in green background). Integration of these 48 proteins with the 4 known human mitochondrial interactors of Trx2 (combination of BioGRID [26] and MitoCarta2.0 [27]) raised the number of human mitochondrial protein species interacting with Trx2 to 52 (table 1). The herein identified mitochondrial interactors included expected hits (peroxiredoxins, methionine sulfoxide reductase) but also proteins participating in the formation of iron sulfur clusters, protein folding in the mitochondrion, and proteins of lipid and carbohydrate metabolism. The novel findings regarding mitochondrial interactors and their potential significance to normal cellular function and disease are further elaborated in the "Discussion" section.

General observations on the proteins that associated with Trx2

A general outcome of the presented data (Fig. 1) is that almost the same number of protein species interacted covalently or non-covalently with Trx2. 19 mitochondrial interactors, were from non-covalent interactions (16 acid-eluted, 3 from Y2H screens), 21 were of the covalent

type, while 7 were common in covalent and non-covalent interactions. Most mitochondrial-specific interactions were derived from the proteomics experiments (46/182) while 3/19 were derived from the Y2H screens and 4/59 from BioGRID. The highest number of interacting proteins was detected in lung lysates, a finding that may correlate with the higher levels of mRNA Trx2 in the tissue [35].

2. The diseasome of human Trx2

Any diseasome (disease network) links the phenotypic features of a disease (human disease phenome) to common molecular mechanisms such as genetic associations and/or protein interactions. Clustering of disease phenotypes is likely due to underlying common pathophysiology mechanisms [36]. Diseasome analysis by the GPEC plug-in of Cytoscape for the mitochondrial interactome of Trx2 showed that the genes encoding Trx2 and its interactors were directly associated with ten different diseases forming four cliques (Figure 2, supplementary table 2.5).

Discussion

The acceptors of the flow of electrons via thioredoxins are *per se* the interacting partners of thioredoxins and constitute the "classical" thiol-reacting substrates such as ribonucleotide reductases, methionine sulfoxide reductases etc. These interactions are fast covalent exchanges of electrons via the active site thiols of thioredoxins and should in principle be detected by a monothiol thioredoxin species. As thioredoxins may associate non-covalently with other proteins, Y2H approaches should be able to detect this type of interactions. Up till now, 59 interactors for human Trx2 are described in the BioGRID interaction repository, with only four of them being mitochondrial (MitoCarta2.0). Using a proteomics approach combined with Y2H screens, the potential mitochondrial interactome of Trx2 was increased herein by 49 additional interactors.

Novelty of the method

While the general principle of the monothiol trapping method has been used for other thioredoxins/glutaredoxins, the current approach differed in subtle aspects. First, immobilization of Trx2 was not directly on activated Sepharose beads but on Affi-Gel resin via a 15 carbon spacer to reduce steric hindrance preventing the interaction of thioredoxin with ligands: binding of EcoTrx1 directly on dextran via N-hydroxy succinimide esters, greatly limited its interaction with gene 5 protein of phage T7 [37]. By adding a spacer of six extra carbons (6-amino-*n*-hexanoic acid), the hindrance was eliminated [37]. Second, the method detected proteins interacting strongly with Trx2 in a non-covalent manner that were removed from Trx2 prior to the reducing step (the latter detecting covalent interactions with Trx2) by a succession of low and high salt washes, finally followed by an acid wash to detect strong hydrophobic interactions. Such washing protocols are used for the affinity purification of antibodies (K_Ds in the low nM range) and in the present case gave a significant number of potential interactors (almost 50 % of total interactome), that might have been overlooked or misinterpreted by a disulfide reducing protocols aiming at the specific detection of covalent redox (S-S) interactions. In addition, acid treatment *before* reduction increased the specificity of the method for the following detection of S-S covalent interactions. Third, selenite was employed to force the oxidative interaction of thioredoxin and ensure the nucleophilic attack to its potential substrates as the compound is a fast oxidant of the thioredoxin system [38]. Fourth, the amounts of protein used in the interaction experiments were generally high for

immobilised Trx2 and lysates to enhance interactions. Finally, material from different tissues was examined, to include the possible tissue-specific expression patterns of potential interactors of Trx2. Apart from the suggested novel interactors (table 1), the greater emerging concept for the Trx2 interactome is that the number of non-covalent interactors is as much if not greater than the number of the covalent ones (figure 1). Assuming some degree of complementarity between the shapes of Trx2 and its interactors, we propose three major types of interactions (Fig. 3): (i) somewhat weak ionic (Fig. 3A), mostly not detected here due to the preceding relatively high salt washes; (ii) strong hydrophobic as revealed by the acidic elutions (Fig. 3B); (iii) covalent (SS bonds, Fig. 3C) due to the thiol oxidoreductase activity of Trx2. The hypothesis should not exclude mixed types of interactions between the contact areas (e.g. mostly hydrophobic and ionic to a lesser extent etc).

On the specificity of the detected interactions

The immediate concern of the applied approach is whether the monothiol motif within the substrate contact area of Trx2 could select for specific interactors. In the case of EcoTrx1 with 3′-phosphoadenosine 5′-phosphosulfate reductase, the interaction was not dependent on the exact active site sequence (CxxC) of thioredoxin but on complementarities in geometry and charges in the contact areas of the two molecules [39]. This finding showed that the very strict characteristics of thioredoxin structure dictate themselves the interaction with specific substrates. Fine details on the catalytic mechanism of thioredoxins revealed that it differed among these oxidoreductases [40]: while all thioredoxins apparently use the Michaelis-Menten mechanism, the eukaryotic species (mithochondrial Trx2 excluded) may also apply single-electron transfer reactions (SET) [40]. Prokaryotic thioredoxins and mitochondrial Trx2 reduce their substrates by nucleophilic substitution (S_N2) and SET reactions [40]. The difference in the reductions mechanism were explained in view of the deeper substrate binding groove of eukaryotic thioredoxins compared to the more shallow one of the prokaryotic enzymes and Trx2 [40].

Under the previous considerations, the overall structure of monothiol Trx2 used herein for monothiol trapping should have been able to recognize specific interactors. However, the mitochondrial interactors identified by the proteomics approach were 46 out of 176. In BioGRID, the common interactors between Trx1 and 2 (147 and 59 interactors respectivly) were eight proteins, suggesting increased specificity for each thioredoxin species. Perhaps, the considered non-specific cytosolic interactors of Trx2 (supplementary table 2.1) could be envisaged as a bycatch of the contact area of a mitochondrial protein exposed to the cytosol

and interacting with complementary surfaces of cytosolic proteins. In case that Trx2 may have hitherto unidentified splicing variants without the mitochondrial targeting sequence, these interactions could be significant: the splice isoforms the *TXN2* gene have not been analysed for all types of cells. In any case, the monothiol method picked *bona fide* interactors of Trxs (e.g. mitochondrial peroxiredoxins, mitochondrial methionine sulfoxide reductase), while classic substrates of Trx1 such as ribonucleotide reductase and cytosolic methionine sulfoxide reductase, were not selected. The latter could reflect the afore-mentioned structural characteristics conferring exclusive specificity on Trx2, or the reducing action of alternative disulfide reductants (the glutaredoxin system or the action of cytosolic Trx1), preventing the formation of the complexes in total cell lysates. Considering the likelihood that the high amounts of Trx2 immobilized on the affinity columns should compete with interferences from other redoxins, the mentioned subtleties in thioredoxin specificity, and the currently believed mitochondrial localisation of Trx2, it could well be that at least the mitochondrial interactors of table 1 represent specific findings of functional significance.

Implications on the possible cellular functions of Trx2 in view of the proposed specific interactions

1. Mitochondrial integrity

MICOS complex subunit Mic60 (IMMT) is one of the major subunits of the mitochondrial intermembrane space bridging complex that is involved in the invaginative folding of inner mitochondrial membranes into cristae [41]. The possible interaction of Trx2 with IMMT suggests the involvement of Trx2 in maintaining the inner mitochondrial membrane structure.

Mitochondrial inorganic pyrophosphatase 2 (PPA2) hydrolyzes inorganic pyrophosphate to pyrophosphate, an essential activity for the regulation of a proper mitochondrial membrane potential, organization and function. *PPA2* mutations are pathogenic and can be related to cardiomyopathy [42]. Overexpression of Trx1 [43], or Trx2 [44, 45] prevent oxidative damage to the heart, while ablation of the TrxR2 in mice resulted in fatal dilated cardiomyopathy [46]. Our data suggest that Trx2 could be the linked to cardiomyopathy via TrxR2 and PPA2.

2. Formation of iron-sulfur clusters

A number of proteins participating in iron-sulfur cluster formation were associated with Trx2. The mitochondrial Stress-70 protein (HSPA9, Uniprot ID: P38646), is a chaperone involved

with iron-sulfur cluster (ISC) biogenesis that occurs exclusively in mitochondria [47]. It interacts with and stabilizes ISC cluster assembly proteins frataxin (FXN, the prokaryotic CyaY, an iron donor), NFU1 (maturation of lipoate synthase and succinate dehydrogenase, prokaryotic equivalents are the C-terminal domains of NifU, NfuA, both scaffold proteins), cysteine desulfurase NFS1 (the equivalent of IscS, a sulfur donor) and ISCU (a scaffold protein for Fe/S cluster synthesis) [47, 48]. Therefore, HSP9 is a central protein in ISC biogenesis whose depletion causes a deficit in mitochondrial ISCs ultimately affecting heme synthesis and differentiation of red blood cells [48, 49]. Its herein detected interaction with Trx2 raises the possibility that the activity of HSP9, hence Fe/S cluster biogenesis (and heme synthesis) in mitochondria may be affected by Trx2. Apart from HSPA9, Trx2 interacted with the Fe/S cluster containing proteins NDUFS2, NDUFS3, and NDUFV1. In the super molecular assembly of the human mitochondrial respiratory mega complex [50], NDUFS3 and NDUFV1 appear accessible to solvent and thus could in principle interact with Trx2. It is tempting to assume that the interaction of Trx2 with these proteins would result in the reduction of their cysteines in a step related to protein folding or the formation/assembly or rearrangement of their iron-sulfur clusters. In fission yeast, the mitochondrial Trx2 system could affect the activity of Fe-S proteins (such as mitochondrial aconitase and cytosolic sulfite reductase but not succinate dehydrogenase) by lowering the levels of free cellular iron [51]. EcoTrx1 along with TrxR were able to supply iron specifically to IscA, the protein (with NFS1 as the eukaryotic homologue) that may provide iron for normal Fe/S cluster assembly on IscU [52]. The mitochondrial Trx2 system could thus affect iron sulfur cluster biogenesis by (i) affecting the activity of HSPA9 (ii) affecting the redox state of cysteines in specific Fe-S enzymes and indirectly by (iii) having an impact on free Fe supply [51]. The proposed interaction of HSPA9 with Trx2 implicates the latter with sideroblastic anemia, the inability to insert iron in the heme of hemoglobin resulting in the characteristic altered phenotype of red blood cells [53].

3. Oxidative stress

Superoxide generated from stray electrons of the electron transport chain may be reduced by superoxide dismutases (SODs) to generate hydrogen peroxide (H_2O_2) that may promote oxidative stress via formation of hydroxyl radicals by the Fenton reaction ([54] and references therein). Trx2 could itself reduce H_2O_2 to H_2O at low rates but is considered as the main electron donor to peroxiredoxins (Prx) 3 and 5 who together with glutathione peroxidases 1 and 4 are on top of the hierarchy for the reduction of H_2O_2 in cells [55]. The central role of

Prx3 in detoxifying H_2O_2 has been demonstrated for cell lines [56] and transgenic mice [57]. Trx2 is the main reductant of Prx3 in mitochondria [58] while human glutaredoxin 2 (hGrx2) may also reduce Prx3 but with lower (double Km) catalytic efficiency. Trx2 (but not hGrx2) may also reduce Prx5 [59], although the complex of a mutated Trx2C93S did not form stable complexes with Prx5 as it did with Prx3 [60]. Cytosolic human Trx1 can reduce Prx3 and Prx5 with better kinetics than Trx2 [59] but this interaction is not likely to happen due to the different compartmentalization of the two thioredoxins. Levels of H_2O_2 were elevated when auranofin, an inhibitor of TrxRs was applied in mouse mitochondrial extracts concomitant with increased levels of oxidized Trx2, Prx3 and ROS (as detected by MitoSOX) [61]. Thus, an intact mitochondrial TrxR2 was essential for the reduction of H_2O_2. The participation of Trx2 is not limited to the elimination of H_2O_2 via Prx3 but also to inhibition of apoptosis: knockdown of Trx2 in lung epithelial cells growing in hyperoxia increased the phosphorylation of ASK1 due to lack of reduced Trx2 binding to it and preventing the serine/threonine kinase activity of ASK1 [62]. In the current work, all peroxiredoxins were picked up as interactors of Trx2. This finding, as well as the interactions with mitochondrial methionine sulfoxide reductase (MSRA) validates the method used. In addition, we present the possible interaction of Trx2 with the peroxisomal bifunctional enzyme (EHHADH) that normally participates in fatty acid β-oxidation by NAD^+. Absence of EHHADH is related to peroxisomal disorders as the enzyme may affect catalase activity and thus the elimination of H_2O_2 produced by the β-oxidation of fatty acids [63].

Trx2 is considered interacting with SOD1 (BioGRID) implicating further Trx2 with reactions involving H_2O_2 and amyotrophic lateral sclerosis [64]. More than a hundred mutations in the human *sod1* have been associated with familial ALS [65]. Reduction of mutant SOD1s by Trx2 1was followed by the formation of aggregates via interaction of the reduced Cys^{57}-Cys^{146} thiols of SOD1s with the Cys^6 and Cys^{111} thiols of neighbouring SOD1s [66]. The toxic effects of mutant SOD1s are considered as a consequence of formation of soluble or insoluble oligomers [67]. In full agreement with the antioxidant functions of Trx2, increased oxidative stress was evident in mitochondria of haploid mice for *TXN2* [68].

4. Detoxification from aldehydes

Trx2 interacted with two detoxifying enzymes: carbonyl reductase [NADPH] 3 (CBR3) and aldehyde dehydrogenase 2 (ALDH2). Aldehyde dehydrogenases catalyse the reduction of aldehydes to carboxylic acids and participate in different biological processes including detoxification. The herein identified partner of Trx2 ALDH2, is crucial for the oxidation of

toxic biogenic aldehydes (e.g. acetaldehyde, catecholaminergic metabolites including DOPAL and DOPEGAL and the principal product of lipid peroxidation 4-HNE) to harmless products [69]. Mutations compromising the catalytic activity of mitochondrial ALDH2 are responsible for increased susceptibility to alcohol intoxication and increased cancer risk due to alcohol consumption [70]. Because of its central role as a phase 1 detoxifying enzyme, dysfunction of ALDH2 has been related to many human diseases and pathologies [71]. The activity of the enzyme may be inhibited by high concentrations of aldehydes such as those occurring at Parkinson's disease [72]. The detoxification of 4-HNE, which is at the beginning of signaling cascades leading to Alzheimer's disease, is dependent on ALDH2 [69]. Activation of ALDH2 has even been proposed as a therapeutic approach for Parkinson's disease [69]. The activity of ALDH2 is redox sensitive: 6-methoxy-2-naphthylaldehyde oxidation by ALDH2 was stimulated by addition of DTT either/or TrxR1 and Trx1 [73]. As TrxR1 and Trx1 are normally cytosolic, these findings most likely reflect the interaction of the mitochondrial thioredoxin system with ALDH2.

CBR3 belongs to the category of monomeric carbonyl reductases that catalyze the reduction of carbonyls in endogenous and xenobiotic compounds, including steroids and prostaglandins [74]. The latter activities are specific for the abundant human CBR1 but not for the highly homologous, less transcribed CBR3 that remains an enigmatic enzyme in terms of substrate specificity and cellular function [74]. CBR3 is somewhat abundant in lung, liver, spleen, pancreas, intestine, and more abundant in the ovary [74]. Trx2 that is known to be inhibited by cyclopentenone-type prostaglandins [75] interacted in the present work covalently with CBR3 from lung tissue preparations. The significance of the proposed interaction between Trx2 and CBR3 is not obvious.

5. Protein synthesis

Trx2 is likely to participate in protein synthesis via its detected interactions with the mitochondrial 16S ribosomal RNA gene (identified here by a Y2H screen), the 40S ribosomal protein S18 (RPS18 gene product) and the mitochondrial elongation factor Tu (mEF-Tu, TUFM gene product). The mitochondrial 16S ribosomal RNA gene is essential for protein synthesis. RPS18 (40S ribosomal protein S18) is a protein of the small ribosomal subunit [76] that has also been identified as an mRNA binding protein [77]. The interaction of the two proteins with Trx2 raises the possibility of the participation of the latter in mitoribosomal assembly. There has been a possible lingering association between thioredoxins and EF-Tu: (i) EcoTrx1 and EF-Tu belong to the same osmotically-sensitive compartment [78]; (ii) EF-

Tu has thioredoxin/protein-disulfide isomerase activity (reduction of insulin) that is dependent on DTT [79]; (iii) Inactive oxidised EF-Tu is reactivated after reduction by thioredoxin [80]. In line to previous publications, this work implies the reduction and therefore concomitant activation of mEF-Tu by Trx2.

6. Protein folding in the mitochondrion

The mitochondrial 60 kDa heat shock protein (HSPD1) together with HSP10 (HSPE1) are implicated in the import, folding and assembly of proteins in the mitochondrial matrix (Uniprot ID: P10809). Hsp60 forms heptameric rings [81] in which protein folding may occur [82]. Hsp60 and Hsp10 are the structural and functional equivalents of prokaryotic GroEL [83] and GroES [84] respectively. HSPD1 rings are properly folded in the mitochondria by the concerted action of the HSP9-Hsp10 complex that binds to the unassembled Hsp60 precursor to promote its assembly into mature Hsp60 complexes [85]. The association of Trx2 with this cytosolic pathway (and PDI or P07237, table 1) points to the direction of Trx2 being involved in the folding of mitochondrial proteins.

7. ADP-ribosylation

Trx2 associated with O-acetyl-ADP-ribose deacetylase MACROD1 (also known as LRP16) that confers post translational modification of the ADP-ribosylation type. The latter is a reversible post-translational modification with wide-ranging biological implications [86]. LRP16/ MACROD1 may hydrolyse the ester bonds forming between glutamate residues in proteins [87] or phosphorylated double-stranded DNA ends and a single ADP-ribose moiety [88]. MACROD1 may interact with estrogen receptor alpha (ERα) [89] and integrate into the NF-κB transcriptional complex and activate it [89]. Trx2 may also interact directly with the p65 subunit of NF-κB [90], while Trx1 may associate with DNA-bound ERα [91]. These observations bring into proximity MACROD1 and Trx2 and suggest that the covalent interaction observed in this work may be of physiological significance and implicate Trx2 in ADP-ribosylation.

8. Glycolysis

Trx2 was associated with triosephosphate isomerase (TPI), glyceraldehyde 3-phosphate dehydrogenase (GAPDH) and lactate dehydrogenases (LDHs) of the glycolytic cycle. TPI catalyzes the reversible interconversion of dihydroxyacetone phosphate and D-glyceraldehyde 3-phosphate in glycolysis [92]. Several studies show that TPI is a target for different plant

thioredoxins and EcoTrx1 ([93] and references therein), making it highly possible that the protein may indeed interact with mammalian Trx1 or Trx2. TPI is of mitochondrial localization in 14 tissues reported in the Human MitoCarta2.0 [27], while cytosolic TPI may have evolved from the mitochondrial form [94]. Therefore, the presently reported covalent and non-covalent interaction of TPI with Trx2 could well mean that TPI may interact *in vivo* with Trx2. The potential interactions of Trx2 with TPI introduces a potential role of Trx2 in the pathogenesis of triosephosphate isomerase deficiency [95] (Fig. 2).

Glyceraldehyde 3-phosphate dehydrogenase (GAPDH), had high prevalence of interaction with Trx2 in different tissues (4 hits, supplementary table 2.1). The cytosolic thioredoxin of *Plasmodium falciparum* [96], EcoTrx1 and plant thioredoxins are known to interact with GAPDH ([93] and references therein). In the case of *Arabidopsis thaliana* cytosolic GAPDH thioredoxin/glutaredoxin could reduce a mixed disulfide forming between GSH and an exposed catalytic cysteine (Cys^{149}), crucial for enzyme function [97]. Trx1 could denitrosylate the active site Cys^{152} of human GAPDH and thus control the pool of free heme [98]. Human Trx1 could also act as an S-desulfhydrase on human GAPDH with the activity residing on the attacking Cys^{32} of Trx1 [99]. Trx1 alone or in combination with TrxR1 and α crystallin were able to revive the activity of GADPH in the cortex and nucleus from cataract lenses [100], although the exact mechanism is not known. These observations may validate (via Trx1) our data regarding the interaction of Trx2 with GAPDH. Both GAPDH and α crystalline B chain were identified as potential targets of Trx2 suggesting that redox interactions between Trx2 with α crystallin and GAPDH may occur simultaneously.

Lactate dehydrogenases (LDHs) A (cytosolic) and B (cytosolic and mitochondrial localization) are glycolytic enzymes that catalyze the reversible oxidation of lactate to pyruvate coupled to the concomitant reduction of NAD^+ to NADH. In the case of LDHD (exclusive mitochondrial localization Uniprot ID: Q86WU2) the electrons for the reduction are derived from ferricytochrome c that is oxidized to ferrocytochrome. The balance of lactate/pyruvate levels may affect levels of intracellular NADH and thus the activity of NADPH oxidase (production of superoxide when higher levels of NADH and lactate) [101]. Higher pyruvate levels can thus promote a reduced intracellular environment [102]. In addition, lactate can enhance hydroxyl radical formation by the Fenton reaction [103]. High LDH levels are thus considered cytotoxic [104]. Higher lactate levels lead to elevation of Trx1 resulting in HIF-1 increase and synthesis of HIF-1-dependent growth factors [105]. The

high reactivity (inhibition) of ebselen with LDH from heart and liver homogenates [106] suggests that LDHs may react with nucleophiles such as thiols. This work presented evidence of possible interactions of the three LDHs with Trx2 (LDHA: non-covalent, LDHB: non-covalent, LDHD: covalent). Considering the promotion of an oxidative environment by LDHs, such interactions would seem biologically logical as a means of interfering directly with the activity of LDHs. In addition, the proposed interaction of Trx2 with LDHB raises the possibility of Trx2 being involved in LDHB deficiency although the condition appears non pathogenic (OMIM entry 614128).

9. Pyruvate dehydrogenase activity

The enzyme complex of pyruvate dehydrogenase catalyzes the decarboxylation of pyruvate to acetyl-CoA [107, 108], linking the glycolytic pathway to the tricarboxylic cycle [109]. It consists of the E1 (pyruvate dehydrogenase activity), the E2 (dihydrolipoamide acetyltransferase) and the E3 (lipoamide dehydrogenase) components ([109], https://www.ebi.ac.uk/interpro/entry/IPR027110). The human E1 component is a heterotetramer of the $\alpha_2\beta_2$ type (α = PDHA1 and β = PDHB) with two catalytic sites [107]. It contains thiamine pyrophosphate as a co factor and catalyses the rate limiting step of the whole reaction [110]. To our knowledge, there is no reported direct interaction of any component of the thioredoxin system with any member of the pyruvate dehydrogenase complex. EcoTrx1 could reduce *in vitro* the disulfides of insulin after receiving electrons from reduced lipoamide [111], a cofactor of the E2 component. However, suppressor mutants of the lipoamide dehydrogenase gene in *E. coli* showed that glutaredoxin 1 (and not EcoTrx1) was able to transfer electrons from oxidized lipoamide to ribonucleotide reductase [112]. Herein, Trx2 was associated to the E1 component subunits PDHA1 and PDHB in a non-covalent and covalent manner respectively. The active site loops of PDHA1 (E1 component subunit alpha) and PDH (E1 component subunit beta) are flexible and may affect the activity of E1 [107, 108, 113]. The detected interaction of Trx2 could perhaps modify their flexibility resulting in alterations of the active sites of E1, raising the possibility of regulation of the whole activity of eukaryotic pyruvate dehydrogenase by the thioredoxin system. The two systems are interconnected in terms of electron transfer as the pyruvate dehydrogenase complex may provide electrons to mitochondrial TrxR via the mitochondrial membrane nicotinamide nucleotide transhydrogenase [114]. The proposed interactions of Trx2 with PDHA1 and PDHB implicate the protein with pyruvate dehydrogenase complex deficiencies (entries 300502 and 179060 respectively in the OMIM data base: www.omim.org).

Trx2 interacted covalently with nucleoside diphosphate-linked moiety X motif 19 (NUDT19) that may hydrolyze *in vitro* the diphosphate bond of free CoA and acyl-CoAs to form 3',5'-ADP and 4'-(acyl)phosphopantetheine, while it contributes to the regulation of CoA levels in the kidney *in vivo* [115]. The interaction of Trx2 with NUDT19 implicates the thioredoxin system in pathways utilizing CoA (the proposed relations of Trx2 with lipid metabolism will be commented later).

10. TCA cycle

Trx2 interacted with mitochondrial aconitate hydratase (aconitase, ACO2) that catalyzes the stereo-specific isomerization of citrate to isocitrate via cis-aconitate in the subpathway synthesizing isocitrate from oxaloacetate in the citric acid cycle. Aconitase contains [4Fe-4S] clusters that do not participate in electron flow but may reversibly loose one Fe atom to obtain a [3Fe-4S] cluster (apo aconitase). In *E. coli*, the cluster is delivered by IscU [116]. In conditions of low iron, apo aconitase may bind to the mRNA of iron responsive elements [117] associated with iron metabolism [118]. In *E. coli*, the respective enzyme binds to its own mRNA and stabilizes it [119]. Mutations in the human gene may result in vision defects [120], while loss of Fe in wild type enzyme due to smoking related oxidants may result in increased iron deposition in arterial cells [121]. In fission yeast, overexpression of Trx2 (but not cytosolic Trx1) was able to restore aconitase activity in glutathione reductase depleted cells, most likely by regulating the levels of free iron [51]. The detected interaction of Trx2 with mitochondrial aconitase suggests that Trx2 may reduce a disulfide forming between the three cysteine residues comprising the coordination site for the Fe-S cluster, allowing thus normal coordination of the cluster.

Trx2 interacted non-covalently with human isocitrate dehydrogenases 1, 2 and 3 (IDH1, 2, 3G) and covalently with IDH3A. The enzymes catalyze the oxidative decarboxylation of isocitrate to alpha-ketoglutarate in the citric acid cycle. In the reaction, IDH1 and IDH2 reduce $NADP^+$ to NADPH, whereas IDH3 reduces NAD^+ to NADH [122, 123]. IDH1 is regarded as cytosolic (although also described with mitochondrial localization [27]), whereas IDH2 and 3 are considered strictly mitochondrial. Due to its role in replenishing NADPH pools, IDH2 may supply electrons for the reduction of mitochondrial TrxR and oxidized glutathione, affecting thus the activity of glutathione peroxidase [123]. Null mutants for *Idh2* had increased loss of hair cells and neurons in the cochlea of male mice due to oxidative stress resulting from a defective mitochondrial thioredoxin system [122]. The interaction of Trx2

with IDH2 could affect the activity of the latter. The possible implication is a feedback between the thioredoxin system and IDH2.

IDH3G may form part of the heterotetramer of IDH3 which has an $\alpha_2\beta\gamma$ composition with α being IDH3A, β IDH3B and γ IDH3G, the allosteric activator of the complex [124]. In this work, Trx2 could interact with IDH3G non- covalently introducing the possibility of an additional, redox regulation of the allosteric activator component IDH3G of IDH3. In *E. coli*, EcoTrx1 is known to associate with isocitrate dehydrogenase (ICD) [17]. ICD shows an approximately 30 % identity to subunits α (IDH3A) and β (IDH3B) and 24 % to IDH3G.

Apart from its interactions with the E1 component subunits PDHA1 and PDHB of pyruvate dehydrogenase, Trx2 interacted non-covalently with IDH1. Since mutant IDH1 perturbs the normal metabolism of pyruvate in glioblastoma cells [125], Trx2 could be affecting pyruvate metabolism by IDHs, PDHA1 and PDHB.

11. Electron transport chain

Complex I

Complex I is a large L-shaped protein complex (almost 1000 kDa [126]), composed of three domains: a dehydrogenase domain (N module) and a hydrogenase domain (Q module) both located at the mitochondrial matrix, and a transmembrane part (P module) located on the inner mitochondrial membrane [126, 127]. Electrons from NADH (produced from the Krebs cycle) are transferred to the dehydrogenase domain (N module), then to the hydrogenase domain (Q module) where reduction of coenzyme Q10 ($CoQH_2$) is performed. The reduction is followed by translocation of protons from the mitochondrial matrix to the intramembrane space by the transmembrane part (P module), resulting in formation of a proton gradient.

Trx2 bound non-covalently to NDUFS1, 2, 3 and NDUFV1, all iron-sulfur cluster containing proteins of the Q module [126]. NDUFS3 along with NDUFS2 [128] initiate the *in vivo* assembly of Complex-I subunits in the mitochondrial matrix [129]. The detected interactions with NDUFS1, 2 and 3 imply a possible contribution of Trx2 to the functional and structural integrity of Complex I.

Complex II

Trx2 interacted non-covalently with SDHA, the flavoprotein (FP) subunit of the enzyme complex of succinate dehydrogenase (SDH), or respiratory Complex II. SDHA is located at the mitochondrial matrix and catalyses the oxidation of succinate to fumarate. The electrons

abstracted, travel via the iron sulfur clusters of adjacent SDHB, to the inner mitochondrial membrane located SDHC and SDHD that reduce CoQ to $CoQH_2$ (exemplified for the enzyme from *E. coli* [130]). The result is an increase of the $CoQH_2$ pool that transfers electrons to the cytochrome bc1 complex (complex III) that in succession relocates electrons to complex IV for the reduction of molecular oxygen to water [131]. A defective SDHA resulted in elevated succinate levels that activated mitochondrial TrxR2 [132]. This finding implicates further the potential interaction of Trx2 with SDHA for the reduction of CoQ in mitochondria and pinpoints TrxR2 as a possible target for the modulation of the electron chain: inhibitors of TrxR2 could affect the normal function of the electron chain at the levels of complex II, possibly via Trx2.

Complex III

Trx2 apparently interacted with UQCRC1 (covalently) and UQCRC2 (non-covalently), both core subunit proteins of the mitochondrial cytochrome b-c1 complex (complex III) of the electron transport chain that catalyzes the reduction of cytochrome *c* by oxidation of $CoQH_2$ to CoQ with simultaneous transfer of protons from the mitochondrial matrix to the intermembrane space [133]. Complex III contains 3 additional respiratory subunits (cytochrome b, cytochrome c1 and Rieske/UQCRFS1) and 6 low-molecular weight proteins. UQCRC1 may mediate formation of the complex between cytochromes c and c1 (Uniprot ID: P31930, [134]), while its normal function is required for spermatogenesis [135]. Overexpression of UQCRC1 may affect mitochondrial morphology/physiology and may lead to development of obesity [136]. UQCRC2 contributes to the assembly of complex III (Uniprot ID: P22695) and may be involved in carcinogenesis [137-139].

Trx2 interacted covalently and non-covalently in brain extracts with UQCRFS1, whose incorporation is the penultimate step in the biogenesis of complex III [140]. Dysfunction of the latter is related to neurological diseases.

Complex IV

Trx2 interacted with cytochrome c oxidase (complex IV) subunits MT-CO1 (cytochrome c oxidase subunit 1 or COX1, data from Y2H) and NDUFA4 (non-covalent binding, proteomics data) of complex IV. MT-CO1 is one of the three core components, (the other two being, COX2, and COX3) that form the core of cytochrome oxidase. COX1 is the nucleus for the biogenesis process of complex IV to which imported subunits (including COX2 and COX3), associate and assemble in a sequential manner [141, 142]. NDUFA4 is required for normal

activity of complex IV [143]. Mutant forms of NDUFA4 may give the neurological phenotype of the Leigh Syndrome [144].

We did not detect any binding of Trx2 to cytochrome c as has been observed in immunoprecipitations [145]. In a previous work, cytochrome c was a substrate for TrxR2 that reduced the protein *in vitro* with similar efficiency in the presence or absence of Trx2 [146] suggesting that Trx2 may not reduce cytochrome c.

ATP synthase and Trx2

The most hits for Trx2 interactions from different tissues were for the β subunit of mitochondrial ATP synthase (ATP5B), while the α subunit (ATP5A) was in the second position (with peroxiredoxin 6). These subunits form a structure within the F_1 domain located in the mitochondrial matrix that binds to ADP to form ATP from the proton gradient that generates a torque on the F_0 domain where the transmembrane rotating c-ring is located ([147] and references therein). Trx2 interacted also covalently with the subunit d of ATP synthase that is part of the peripheral stalk connecting the F_1 and F_0 domains [147]. Although we found reports for redox regulation of the gamma subunit of the F_1 domain [148-150], no data were available for such a mechanism for the alpha and beta subunits. The evidence presented herein, raises this possibility which is likely to be validated by previous work in which overexpression of Trx2 in HEK293 cells was specifically affecting the activity of ATP synthase and therefore, the potential of the mitochondrial membrane [35].

Another possible association of Trx2 with ATP levels is via S-type mitochondrial creatine kinase (CKMT2) with which Trx2 was covalently associated. CKMT2 reversibly catalyzes the transfer of phosphate between ATP and various phosphogens (e.g. creatine phosphate). CKMT2 isoenzymes are involved in energy transduction in tissues with large and fluctuating energy demands (e.g. skeletal muscle, heart, brain, spermatozoa, Uniprot ID: P17540).

Overall, interactors of Trx2 were found in all complexes of the electron transport chain. It is not therefore surprising that the protein is related to combined oxidative phosphorylation deficiency. Decreased activity of the transport chain has been observed in haploid mutants for the gene encoding Trx2 [68]. A possibility of therapeutic interference could be the use of TrxR2 inhibitors, expected to modify the redox state and thus the interactions of Trx2 with its related binding partners within the electron transport chain.

12. Lipid metabolism

Trx2 interacted non-covalently with subunit alpha of the trifunctional protein/enzyme TFP. TFP is an octameric complex composed of four α-subunits (HADHA), each composed of a long-chain enoyl-CoA hydratase and a long-chain L-3-hydroxyacyl-CoA dehydrogenase domain and four β-subunits (HADHB) encoding a long-chain 3-ketoacyl-CoA thiolase domain [151]. The enzyme catalyzes the last three steps of the of long-chain fatty acids β-oxidation. Defects in TFP may result in hepatic steatosis and insulin resistance [152]. So far there has not been any report correlating thioredoxin proteins to TFP. Regulation of fatty acid biosynthesis has been described for Txnip not via thioredoxin but a specific regulatory microRNA (miR-33a), affecting HADHB activity [153].

Trx2 interacted covalently with mitochondrial acetyl-coenzyme A synthetase 2-like (ACSS1) that converts acetate to acetyl-CoA to be oxidized via the tricarboxylic cycle to produce ATP and CO_2. In view of its similarity to ACSL1, ACSS1 is likely to be involved in energy homeostasis and in maintaining normal body temperature during fasting. Deacetylation of ACSS1 by SIRT3 activates the acetyl-CoA synthetase activity of ACSS1 [154]. The interaction with Trx2 reported here raises another potential level of regulation.

13. Amino acid metabolism

The non-covalent interaction of Trx2 with the β chain of mitochondrial methylcrotonoyl-CoA carboxylase (MCCC2), potentially links the thioredoxin system to amino acid metabolism. MCCC2 is the carboxyltransferase subunit of the biotin requiring mitochondrial enzyme 3-methylcrotonyl-CoA carboxylase, that is involved in the catabolism of leucine and isovaleric acid. Deficiency of the holoenzyme leads to an autosomal inherited disease that has a variable phenotype ranging from asymptomatic to death in infancy from neurological disorders [155] [156]. Analysis of the transcriptome of a deficient human skin fibroblast cell line revealed that its mitochondria were dysfunctional (e.g. downregulation of transcripts concerning respiratory complex proteins) leading to oxidative stress [156]. It were the Trx1 transcripts, however, that were upregulated in that study and not the Trx2 ones [156].

Trx2 reacted covalently with cytosolic 10-formyltetrahydrofolate dehydrogenase (ALDH1L1) an abundant enzyme that catalyses the reductive (via NADPH) decarboxylation of 10-formyltetrahydrofolate to tetrahydrofolate and CO_2. Although a mitochondrial form of the enzyme exists (ALDH1L2 with 74 % identity to ALDH1L1 [157]), ALDH1L1 is also considered mitochondrial [27]. Folate participates in one-carbon metabolism and comprises a network of interconnected folate-dependent metabolic pathways that are involved in serine

and glycine interconversion, homocysteine remethylation to methionine and *de novo* biosynthesis of purine an thymidylate [158]. It is not known how the reported interaction between ALDH1L1 and Trx2 may affect the activity of either enzyme.

14. Protein/nucleic acid deglycase DJ-1 and Parkinson's disease

DJ-1/PARK7 is a 2x20 kDa protein localized in the cytosol, nucleus and mitochondria. Autosomal recessive mutations in the *DJ-1* gene causing loss of function, lead to an early start of Parkinson's disease [159]. In this work, Trx2 was able to interact directly with DJ-1. As was the case for human Trx1, it is likely that mitochondrial Trx2 will be able to reduce Cys^{53} of DJ-1 [24, 160]. While the particular residue may help the dimerisation of DJ-1, the redox state of Cys^{106} that is responsible for the delivery of the antioxidant effects of DJ-1, is affected by peroxiredoxin 2 [160] herein, another interactor of Trx2. In an epidemiological study, Parkinson's development after exposure to pesticides was related to defects in Complex I [161]. In this work, Trx2 interacted with four components of the Complex I. Another potential Trx2 interactor, lactate dehydrogenase b was down regulated in midbrain-derived dopaminergic neuronal cells when exposed to 1-methyl-4-phenyl-1, 2, 3, 6-tetrahydropyridine (MPTP) known to promote a Parkinson's phenotype [162]. A 16-year-old adolescent with infantile-onset neurodegenerative disorder had an homozygous stop mutation in the gene encoding Trx2, demonstrating the importance of the protein for neuronal integrity [163]. Taken together these observations provide evidence that Trx2 participates in protein networks with neuroprotective roles.

Prospects

This work aimed at the identification of mainly strong non-covalent and covalent interactions of Trx2 in the context of the mitochondrion. Novel partners were identified and thus increased the spectrum of putative functions for Trx2. The number of interactor species (and concomitant functions) is expected to increase even more with the use of more sensitive detection methods that allow for better resolution and more certain identification of protein species (e.g. Orbitrap LC-MS). Equally relevant are the weaker non-covalent interactions that could have been detected by Y2H screens but here gave only three novel interactors. It is obvious that the "weak" interactome of Trx2 was by no means properly explored. Use of immobilized Trx2, interaction with tissue lysates and elutions by increasing ionic strengths, is likely to reveal more interactions, some of them already known (e.g. ASK1, Txnip) but not detected within the context of this work. Finally, *in vitro* and *in vivo* validation of all these

putative interactors is expected to clarify the effective functional interactome of Trx2 and perhaps provide fine points of therapeutic interference.

Acknowledgements

This investigation was supported by grants from the Greek General Secretariat of Research and Technology in collaboration with the European Union (program Enter, 01EP104).

REFERENCES

1. Miller, C. G., Holmgren, A., Arner, E. S. J. & Schmidt, E. E. (2018) NADPH-dependent and -independent disulfide reductase systems, *Free radical biology & medicine.* **127**, 248-261.
2. Laurent, T. C., Moore, E. C. & Reichard, P. (1964) Enzymatic Synthesis of Deoxyribonucleotides. Iv. Isolation and Characterization of Thioredoxin, the Hydrogen Donor from Escherichia Coli B, *The Journal of biological chemistry.* **239**, 3436-44.
3. Holmgren, A. (1976) Hydrogen donor system for Escherichia coli ribonucleoside-diphosphate reductase dependent upon glutathione, *Proceedings of the National Academy of Sciences of the United States of America.* **73**, 2275-9.
4. Yin, F., Sancheti, H. & Cadenas, E. (2012) Mitochondrial thiols in the regulation of cell death pathways, *Antioxid Redox Signal.* **17**, 1714-27.
5. Couturier, J., Vignols, F., Jacquot, J. P. & Rouhier, N. (2012) Glutathione- and glutaredoxin-dependent reduction of methionine sulfoxide reductase A, *FEBS letters.* **586**, 3894-9.
6. Lundstrom-Ljung, J., Vlamis-Gardikas, A., Aslund, F. & Holmgren, A. (1999) Reactivity of glutaredoxins 1, 2 and 3 from Escherichia coli and protein disulfide isomerase towards glutathionyl-mixed disulfides in ribonuclease A, *FEBS letters.* **443**, 85-8.
7. Mark, D. F. & Richardson, C. C. (1976) Escherichia coli thioredoxin: a subunit of bacteriophage T7 DNA polymerase, *Proceedings of the National Academy of Sciences of the United States of America.* **73**, 780-4.
8. Lu, J. & Holmgren, A. (2012) Thioredoxin system in cell death progression, *Antioxidants & redox signaling.* **17**, 1738-47.
9. Saxena, G., Chen, J. & Shalev, A. (2010) Intracellular shuttling and mitochondrial function of thioredoxin-interacting protein, *The Journal of biological chemistry.* **285**, 3997-4005.
10. Zhang, R., Al-Lamki, R., Bai, L., Streb, J. W., Miano, J. M., Bradley, J. & Min, W. (2004) Thioredoxin-2 inhibits mitochondria-located ASK1-mediated apoptosis in a JNK-independent manner, *Circulation research.* **94**, 1483-91.
11. Dammeyer, P., Damdimopoulos, A. E., Nordman, T., Jimenez, A., Miranda-Vizuete, A. & Arner, E. S. (2008) Induction of cell membrane protrusions by the N-terminal glutaredoxin domain of a rare splice variant of human thioredoxin reductase 1, *The Journal of biological chemistry.* **283**, 2814-21.
12. Vlamis-Gardikas, A. & Holmgren, A. (2002) Thioredoxin and glutaredoxin isoforms, *Methods in enzymology.* **347**, 286-96.
13. Spyrou, G., Enmark, E., Miranda-Vizuete, A. & Gustafsson, J. (1997) Cloning and expression of a novel mammalian thioredoxin, *The Journal of biological chemistry.* **272**, 2936-41.
14. Halvey, P. J., Watson, W. H., Hansen, J. M., Go, Y. M., Samali, A. & Jones, D. P. (2005) Compartmental oxidation of thiol-disulphide redox couples during epidermal growth factor signalling, *The Biochemical journal.* **386**, 215-9.
15. Hansen, J. M., Zhang, H. & Jones, D. P. (2006) Mitochondrial thioredoxin-2 has a key role in determining tumor necrosis factor-alpha-induced reactive oxygen species generation, NF-kappaB activation, and apoptosis, *Toxicological sciences : an official journal of the Society of Toxicology.* **91**, 643-50.
16. Zhou, J., Damdimopoulos, A. E., Spyrou, G. & Brune, B. (2007) Thioredoxin 1 and thioredoxin 2 have opposed regulatory functions on hypoxia-inducible factor-1alpha, *The Journal of biological chemistry.* **282**, 7482-90.
17. Kumar, J. K., Tabor, S. & Richardson, C. C. (2004) Proteomic analysis of thioredoxin-targeted proteins in Escherichia coli, *Proceedings of the National Academy of Sciences of the United States of America.* **101**, 3759-64.
18. Arts, I. S., Vertommen, D., Baldin, F., Laloux, G. & Collet, J. F. (2016) Comprehensively Characterizing the Thioredoxin Interactome In Vivo Highlights the Central Role Played by This Ubiquitous Oxidoreductase in Redox Control, *Molecular & cellular proteomics : MCP.* **15**, 2125-40.

19. Motohashi, K., Romano, P. G. & Hisabori, T. (2009) Identification of thioredoxin targeted proteins using thioredoxin single cysteine mutant-immobilized resin, *Methods in molecular biology.* **479**, 117-31.
20. Sturm, N., Jortzik, E., Mailu, B. M., Koncarevic, S., Deponte, M., Forchhammer, K., Rahlfs, S. & Becker, K. (2009) Identification of proteins targeted by the thioredoxin superfamily in Plasmodium falciparum, *PLoS pathogens.* **5**, e1000383.
21. Schlosser, S., Leitsch, D. & Duchene, M. (2013) Entamoeba histolytica: identification of thioredoxin-targeted proteins and analysis of serine acetyltransferase-1 as a prototype example, *The Biochemical journal.* **451**, 277-88.
22. Schutte, L. D., Baumeister, S., Weis, B., Hudemann, C., Hanschmann, E. M. & Lillig, C. H. (2013) Identification of potential protein dithiol-disulfide substrates of mammalian Grx2, *Biochimica et biophysica acta.* **1830**, 4999-5005.
23. Wu, C., Parrott, A. M., Liu, T., Jain, M. R., Yang, Y., Sadoshima, J. & Li, H. (2011) Distinction of thioredoxin transnitrosylation and denitrosylation target proteins by the ICAT quantitative approach, *Journal of proteomics.* **74**, 2498-509.
24. Fu, C., Wu, C., Liu, T., Ago, T., Zhai, P., Sadoshima, J. & Li, H. (2009) Elucidation of thioredoxin target protein networks in mouse, *Molecular & cellular proteomics : MCP.* **8**, 1674-87.
25. Booze, M. L., Hansen, J. M. & Vitiello, P. F. (2016) A novel mouse model for the identification of thioredoxin-1 protein interactions, *Free radical biology & medicine.* **99**, 533-543.
26. Chatr-Aryamontri, A., Oughtred, R., Boucher, L., Rust, J., Chang, C., Kolas, N. K., O'Donnell, L., Oster, S., Theesfeld, C., Sellam, A., Stark, C., Breitkreutz, B. J., Dolinski, K. & Tyers, M. (2017) The BioGRID interaction database: 2017 update, *Nucleic acids research.* **45**, D369-D379.
27. Calvo, S. E., Clauser, K. R. & Mootha, V. K. (2016) MitoCarta2.0: an updated inventory of mammalian mitochondrial proteins, *Nucleic acids research.* **44**, D1251-7.
28. Diokmetzidou, A., Tsikitis, M., Nikouli, S., Kloukina, I., Tsoupri, E., Papathanasiou, S., Psarras, S., Mavroidis, M. & Capetanaki, Y. (2016) Strategies to Study Desmin in Cardiac Muscle and Culture Systems, *Methods in enzymology.* **568**, 427-59.
29. Bensadoun, A. & Weinstein, D. (1976) Assay of proteins in the presence of interfering materials, *Analytical biochemistry.* **70**, 241-50.
30. Shannon, P., Markiel, A., Ozier, O., Baliga, N. S., Wang, J. T., Ramage, D., Amin, N., Schwikowski, B. & Ideker, T. (2003) Cytoscape: a software environment for integrated models of biomolecular interaction networks, *Genome research.* **13**, 2498-504.
31. Hamosh, A., Scott, A. F., Amberger, J. S., Bocchini, C. A. & McKusick, V. A. (2005) Online Mendelian Inheritance in Man (OMIM), a knowledgebase of human genes and genetic disorders, *Nucleic acids research.* **33**, D514-7.
32. Jiao, X., Sherman, B. T., Huang da, W., Stephens, R., Baseler, M. W., Lane, H. C. & Lempicki, R. A. (2012) DAVID-WS: a stateful web service to facilitate gene/protein list analysis, *Bioinformatics.* **28**, 1805-6.
33. Bindea, G., Mlecnik, B., Hackl, H., Charoentong, P., Tosolini, M., Kirilovsky, A., Fridman, W. H., Pages, F., Trajanoski, Z. & Galon, J. (2009) ClueGO: a Cytoscape plug-in to decipher functionally grouped gene ontology and pathway annotation networks, *Bioinformatics.* **25**, 1091-3.
34. Chasapis, C. T., Andreini, C., Georgiopolou, A. K., Stefanidou, M. E. & Vlamis-Gardikas, A. (2017) Identification of the zinc, copper and cadmium metalloproteome of the protozoon Tetrahymena thermophila by systematic bioinformatics, *Archives of microbiology.* **199**, 1141-1149.
35. Damdimopoulos, A. E., Miranda-Vizuete, A., Pelto-Huikko, M., Gustafsson, J. A. & Spyrou, G. (2002) Human mitochondrial thioredoxin. Involvement in mitochondrial membrane potential and cell death, *The Journal of biological chemistry.* **277**, 33249-57.
36. Goh, K. I., Cusick, M. E., Valle, D., Childs, B., Vidal, M. & Barabasi, A. L. (2007) The human disease network, *Proceedings of the National Academy of Sciences of the United States of America.* **104**, 8685-90.

37. Singha, N. C., Vlamis-Gardikas, A. & Holmgren, A. (2003) Real-time kinetics of the interaction between the two subunits, Escherichia coli thioredoxin and gene 5 protein of phage T7 DNA polymerase, *The Journal of biological chemistry.* **278**, 21421-8.
38. Bjornstedt, M., Kumar, S. & Holmgren, A. (1995) Selenite and selenodiglutathione: reactions with thioredoxin systems, *Methods in enzymology.* **252**, 209-19.
39. Berndt, C., Schwenn, J. D. & Lillig, C. H. (2015) The specificity of thioredoxins and glutaredoxins is determined by electrostatic and geometric complementarity, *Chemical science.* **6**, 7049-7058.
40. Perez-Jimenez, R., Li, J., Kosuri, P., Sanchez-Romero, I., Wiita, A. P., Rodriguez-Larrea, D., Chueca, A., Holmgren, A., Miranda-Vizuete, A., Becker, K., Cho, S. H., Beckwith, J., Gelhaye, E., Jacquot, J. P., Gaucher, E. A., Sanchez-Ruiz, J. M., Berne, B. J. & Fernandez, J. M. (2009) Diversity of chemical mechanisms in thioredoxin catalysis revealed by single-molecule force spectroscopy, *Nature structural & molecular biology.* **16**, 890-6.
41. Ott, C., Dorsch, E., Fraunholz, M., Straub, S. & Kozjak-Pavlovic, V. (2015) Detailed analysis of the human mitochondrial contact site complex indicate a hierarchy of subunits, *PloS one.* **10**, e0120213.
42. Kennedy, H., Haack, T. B., Hartill, V., Matakovic, L., Baumgartner, E. R., Potter, H., Mackay, R., Alston, C. L., O'Sullivan, S., McFarland, R., Connolly, G., Gannon, C., King, R., Mead, S., Crozier, I., Chan, W., Florkowski, C. M., Sage, M., Hofken, T., Alhaddad, B., Kremer, L. S., Kopajtich, R., Feichtinger, R. G., Sperl, W., Rodenburg, R. J., Minet, J. C., Dobbie, A., Strom, T. M., Meitinger, T., George, P. M., Johnson, C. A., Taylor, R. W., Prokisch, H., Doudney, K. & Mayr, J. A. (2016) Sudden Cardiac Death Due to Deficiency of the Mitochondrial Inorganic Pyrophosphatase PPA2, *American journal of human genetics.* **99**, 674-682.
43. Berndt, C., Lillig, C. H. & Holmgren, A. (2007) Thiol-based mechanisms of the thioredoxin and glutaredoxin systems: implications for diseases in the cardiovascular system, *American journal of physiology Heart and circulatory physiology.* **292**, H1227-36.
44. Li, H., Xu, C., Li, Q., Gao, X., Sugano, E., Tomita, H., Yang, L. & Shi, S. (2017) Thioredoxin 2 Offers Protection against Mitochondrial Oxidative Stress in H9c2 Cells and against Myocardial Hypertrophy Induced by Hyperglycemia, *International journal of molecular sciences.* **18**.
45. Chen, C., Chen, H., Zhou, H. J., Ji, W. & Min, W. (2017) Mechanistic Role of Thioredoxin 2 in Heart Failure, *Advances in experimental medicine and biology.* **982**, 265-276.
46. Conrad, M., Jakupoglu, C., Moreno, S. G., Lippl, S., Banjac, A., Schneider, M., Beck, H., Hatzopoulos, A. K., Just, U., Sinowatz, F., Schmahl, W., Chien, K. R., Wurst, W., Bornkamm, G. W. & Brielmeier, M. (2004) Essential role for mitochondrial thioredoxin reductase in hematopoiesis, heart development, and heart function, *Molecular and cellular biology.* **24**, 9414-23.
47. Lill, R., Hoffmann, B., Molik, S., Pierik, A. J., Rietzschel, N., Stehling, O., Uzarska, M. A., Webert, H., Wilbrecht, C. & Muhlenhoff, U. (2012) The role of mitochondria in cellular iron-sulfur protein biogenesis and iron metabolism, *Biochimica et biophysica acta.* **1823**, 1491-508.
48. Shan, Y. & Cortopassi, G. (2016) Mitochondrial Hspa9/Mortalin regulates erythroid differentiation via iron-sulfur cluster assembly, *Mitochondrion.* **26**, 94-103.
49. Chen, T. H., Kambal, A., Krysiak, K., Walshauser, M. A., Raju, G., Tibbitts, J. F. & Walter, M. J. (2011) Knockdown of Hspa9, a del(5q31.2) gene, results in a decrease in hematopoietic progenitors in mice, *Blood.* **117**, 1530-9.
50. Guo, R., Zong, S., Wu, M., Gu, J. & Yang, M. (2017) Architecture of Human Mitochondrial Respiratory Megacomplex I2III2IV2, *Cell.* **170**, 1247-1257 e12.
51. Song, J. Y., Cha, J., Lee, J. & Roe, J. H. (2006) Glutathione reductase and a mitochondrial thioredoxin play overlapping roles in maintaining iron-sulfur enzymes in fission yeast, *Eukaryotic cell.* **5**, 1857-65.
52. Ding, H., Harrison, K. & Lu, J. (2005) Thioredoxin reductase system mediates iron binding in IscA and iron delivery for the iron-sulfur cluster assembly in IscU, *The Journal of biological chemistry.* **280**, 30432-7.
53. Sawicki, K. T., Chang, H. C. & Ardehali, H. (2015) Role of heme in cardiovascular physiology and disease, *Journal of the American Heart Association.* **4**, e001138.

54. Thomas, C., Mackey, M. M., Diaz, A. A. & Cox, D. P. (2009) Hydroxyl radical is produced via the Fenton reaction in submitochondrial particles under oxidative stress: implications for diseases associated with iron accumulation, *Redox report : communications in free radical research.* **14**, 102-8.
55. Cox, A. G., Winterbourn, C. C. & Hampton, M. B. (2009) Mitochondrial peroxiredoxin involvement in antioxidant defence and redox signalling, *The Biochemical journal.* **425**, 313-25.
56. Nonn, L., Berggren, M. & Powis, G. (2003) Increased expression of mitochondrial peroxiredoxin-3 (thioredoxin peroxidase-2) protects cancer cells against hypoxia and drug-induced hydrogen peroxide-dependent apoptosis, *Molecular cancer research : MCR.* **1**, 682-9.
57. Matsushima, S., Ide, T., Yamato, M., Matsusaka, H., Hattori, F., Ikeuchi, M., Kubota, T., Sunagawa, K., Hasegawa, Y., Kurihara, T., Oikawa, S., Kinugawa, S. & Tsutsui, H. (2006) Overexpression of mitochondrial peroxiredoxin-3 prevents left ventricular remodeling and failure after myocardial infarction in mice, *Circulation.* **113**, 1779-86.
58. Watabe, S., Hiroi, T., Yamamoto, Y., Fujioka, Y., Hasegawa, H., Yago, N. & Takahashi, S. Y. (1997) SP-22 is a thioredoxin-dependent peroxide reductase in mitochondria, *European journal of biochemistry.* **249**, 52-60.
59. Hanschmann, E. M., Lonn, M. E., Schutte, L. D., Funke, M., Godoy, J. R., Eitner, S., Hudemann, C. & Lillig, C. H. (2010) Both thioredoxin 2 and glutaredoxin 2 contribute to the reduction of the mitochondrial 2-Cys peroxiredoxin Prx3, *The Journal of biological chemistry.* **285**, 40699-705.
60. Zhang, H., Go, Y. M. & Jones, D. P. (2007) Mitochondrial thioredoxin-2/peroxiredoxin-3 system functions in parallel with mitochondrial GSH system in protection against oxidative stress, *Archives of biochemistry and biophysics.* **465**, 119-26.
61. Stanley, B. A., Sivakumaran, V., Shi, S., McDonald, I., Lloyd, D., Watson, W. H., Aon, M. A. & Paolocci, N. (2011) Thioredoxin reductase-2 is essential for keeping low levels of H(2)O(2) emission from isolated heart mitochondria, *The Journal of biological chemistry.* **286**, 33669-77.
62. Forred, B. J., Daugaard, D. R., Titus, B. K., Wood, R. R., Floen, M. J., Booze, M. L. & Vitiello, P. F. (2017) Detoxification of Mitochondrial Oxidants and Apoptotic Signaling Are Facilitated by Thioredoxin-2 and Peroxiredoxin-3 during Hyperoxic Injury, *PloS one.* **12**, e0168777.
63. Makkar, R. S., Contreras, M. A., Paintlia, A. S., Smith, B. T., Haq, E. & Singh, I. (2006) Molecular organization of peroxisomal enzymes: protein-protein interactions in the membrane and in the matrix, *Archives of biochemistry and biophysics.* **451**, 128-40.
64. Burk, K. & Pasterkamp, R. J. (2019) Disrupted neuronal trafficking in amyotrophic lateral sclerosis, *Acta neuropathologica*.
65. Valentine, J. S., Doucette, P. A. & Zittin Potter, S. (2005) Copper-zinc superoxide dismutase and amyotrophic lateral sclerosis, *Annual review of biochemistry.* **74**, 563-93.
66. Chattopadhyay, M. & Valentine, J. S. (2009) Aggregation of copper-zinc superoxide dismutase in familial and sporadic ALS, *Antioxid Redox Signal.* **11**, 1603-14.
67. Doucette, P. A., Whitson, L. J., Cao, X., Schirf, V., Demeler, B., Valentine, J. S., Hansen, J. C. & Hart, P. J. (2004) Dissociation of human copper-zinc superoxide dismutase dimers using chaotrope and reductant. Insights into the molecular basis for dimer stability, *The Journal of biological chemistry.* **279**, 54558-66.
68. Perez, V. I., Lew, C. M., Cortez, L. A., Webb, C. R., Rodriguez, M., Liu, Y., Qi, W., Li, Y., Chaudhuri, A., Van Remmen, H., Richardson, A. & Ikeno, Y. (2008) Thioredoxin 2 haploinsufficiency in mice results in impaired mitochondrial function and increased oxidative stress, *Free radical biology & medicine.* **44**, 882-92.
69. Deza-Ponzio, R., Herrera, M. L., Bellini, M. J., Virgolini, M. B. & Herenu, C. B. (2018) Aldehyde dehydrogenase 2 in the spotlight: The link between mitochondria and neurodegeneration, *Neurotoxicology.* **68**, 19-24.
70. Seitz, H. K. & Meier, P. (2007) The role of acetaldehyde in upper digestive tract cancer in alcoholics, *Translational research : the journal of laboratory and clinical medicine.* **149**, 293-7.
71. Chen, C. H., Ferreira, J. C., Gross, E. R. & Mochly-Rosen, D. (2014) Targeting aldehyde dehydrogenase 2: new therapeutic opportunities, *Physiological reviews.* **94**, 1-34.

72. Goldstein, D. S., Sullivan, P., Holmes, C., Miller, G. W., Alter, S., Strong, R., Mash, D. C., Kopin, I. J. & Sharabi, Y. (2013) Determinants of buildup of the toxic dopamine metabolite DOPAL in Parkinson's disease, *Journal of neurochemistry.* **126**, 591-603.
73. Oelze, M., Knorr, M., Schell, R., Kamuf, J., Pautz, A., Art, J., Wenzel, P., Munzel, T., Kleinert, H. & Daiber, A. (2011) Regulation of human mitochondrial aldehyde dehydrogenase (ALDH-2) activity by electrophiles in vitro, *The Journal of biological chemistry.* **286**, 8893-900.
74. Miura, T., Nishinaka, T. & Terada, T. (2008) Different functions between human monomeric carbonyl reductase 3 and carbonyl reductase 1, *Molecular and cellular biochemistry.* **315**, 113-21.
75. Shibata, T., Yamada, T., Ishii, T., Kumazawa, S., Nakamura, H., Masutani, H., Yodoi, J. & Uchida, K. (2003) Thioredoxin as a molecular target of cyclopentenone prostaglandins, *The Journal of biological chemistry.* **278**, 26046-54.
76. Ban, N., Beckmann, R., Cate, J. H., Dinman, J. D., Dragon, F., Ellis, S. R., Lafontaine, D. L., Lindahl, L., Liljas, A., Lipton, J. M., McAlear, M. A., Moore, P. B., Noller, H. F., Ortega, J., Panse, V. G., Ramakrishnan, V., Spahn, C. M., Steitz, T. A., Tchorzewski, M., Tollervey, D., Warren, A. J., Williamson, J. R., Wilson, D., Yonath, A. & Yusupov, M. (2014) A new system for naming ribosomal proteins, *Current opinion in structural biology.* **24**, 165-9.
77. Baltz, A. G., Munschauer, M., Schwanhausser, B., Vasile, A., Murakawa, Y., Schueler, M., Youngs, N., Penfold-Brown, D., Drew, K., Milek, M., Wyler, E., Bonneau, R., Selbach, M., Dieterich, C. & Landthaler, M. (2012) The mRNA-bound proteome and its global occupancy profile on protein-coding transcripts, *Molecular cell.* **46**, 674-90.
78. Lunn, C. A. & Pigiet, V. P. (1982) Localization of thioredoxin from Escherichia coli in an osmotically sensitive compartment, *The Journal of biological chemistry.* **257**, 11424-30.
79. Richarme, G. (1998) Protein-disulfide isomerase activity of elongation factor EF-Tu, *Biochemical and biophysical research communications.* **252**, 156-61.
80. Yutthanasirikul, R., Nagano, T., Jimbo, H., Hihara, Y., Kanamori, T., Ueda, T., Haruyama, T., Konno, H., Yoshida, K., Hisabori, T. & Nishiyama, Y. (2016) Oxidation of a Cysteine Residue in Elongation Factor EF-Tu Reversibly Inhibits Translation in the Cyanobacterium Synechocystis sp. PCC 6803, *The Journal of biological chemistry.* **291**, 5860-70.
81. Viitanen, P. V., Lorimer, G. H., Seetharam, R., Gupta, R. S., Oppenheim, J., Thomas, J. O. & Cowan, N. J. (1992) Mammalian mitochondrial chaperonin 60 functions as a single toroidal ring, *The Journal of biological chemistry.* **267**, 695-8.
82. Nielsen, K. L. & Cowan, N. J. (1998) A single ring is sufficient for productive chaperonin-mediated folding in vivo, *Molecular cell.* **2**, 93-9.
83. McMullin, T. W. & Hallberg, R. L. (1988) A highly evolutionarily conserved mitochondrial protein is structurally related to the protein encoded by the Escherichia coli groEL gene, *Molecular and cellular biology.* **8**, 371-80.
84. Lubben, T. H., Gatenby, A. A., Donaldson, G. K., Lorimer, G. H. & Viitanen, P. V. (1990) Identification of a groES-like chaperonin in mitochondria that facilitates protein folding, *Proceedings of the National Academy of Sciences of the United States of America.* **87**, 7683-7.
85. Bottinger, L., Oeljeklaus, S., Guiard, B., Rospert, S., Warscheid, B. & Becker, T. (2015) Mitochondrial heat shock protein (Hsp) 70 and Hsp10 cooperate in the formation of Hsp60 complexes, *The Journal of biological chemistry.* **290**, 11611-22.
86. Jankevicius, G., Hassler, M., Golia, B., Rybin, V., Zacharias, M., Timinszky, G. & Ladurner, A. G. (2013) A family of macrodomain proteins reverses cellular mono-ADP-ribosylation, *Nature structural & molecular biology.* **20**, 508-14.
87. Rack, J. G., Perina, D. & Ahel, I. (2016) Macrodomains: Structure, Function, Evolution, and Catalytic Activities, *Annual review of biochemistry.* **85**, 431-54.
88. Agnew, T., Munnur, D., Crawford, K., Palazzo, L., Mikoc, A. & Ahel, I. (2018) MacroD1 Is a Promiscuous ADP-Ribosyl Hydrolase Localized to Mitochondria, *Frontiers in microbiology.* **9**, 20.
89. Han, W. D., Zhao, Y. L., Meng, Y. G., Zang, L., Wu, Z. Q., Li, Q., Si, Y. L., Huang, K., Ba, J. M., Morinaga, H., Nomura, M. & Mu, Y. M. (2007) Estrogenically regulated LRP16 interacts with estrogen

receptor alpha and enhances the receptor's transcriptional activity, *Endocrine-related cancer.* **14**, 741-53.
90. Psarra, A. M., Hermann, S., Panayotou, G. & Spyrou, G. (2009) Interaction of mitochondrial thioredoxin with glucocorticoid receptor and NF-kappaB modulates glucocorticoid receptor and NF-kappaB signalling in HEK-293 cells, *The Biochemical journal.* **422**, 521-31.
91. Rao, A. K., Ziegler, Y. S., McLeod, I. X., Yates, J. R. & Nardulli, A. M. (2009) Thioredoxin and thioredoxin reductase influence estrogen receptor alpha-mediated gene expression in human breast cancer cells, *Journal of molecular endocrinology.* **43**, 251-61.
92. Orosz, F., Olah, J. & Ovadi, J. (2006) Triosephosphate isomerase deficiency: facts and doubts, *IUBMB life.* **58**, 703-15.
93. Michelet, L., Zaffagnini, M., Massot, V., Keryer, E., Vanacker, H., Miginiac-Maslow, M., Issakidis-Bourguet, E. & Lemaire, S. D. (2006) Thioredoxins, glutaredoxins, and glutathionylation: new crosstalks to explore, *Photosynthesis research.* **89**, 225-45.
94. Liaud, M. F., Lichtle, C., Apt, K., Martin, W. & Cerff, R. (2000) Compartment-specific isoforms of TPI and GAPDH are imported into diatom mitochondria as a fusion protein: evidence in favor of a mitochondrial origin of the eukaryotic glycolytic pathway, *Molecular biology and evolution.* **17**, 213-23.
95. Orosz, F., Olah, J. & Ovadi, J. (2009) Triosephosphate isomerase deficiency: new insights into an enigmatic disease, *Biochimica et biophysica acta.* **1792**, 1168-74.
96. Kawazu, S., Takemae, H., Komaki-Yasuda, K. & Kano, S. (2010) Target proteins of the cytosolic thioredoxin in Plasmodium falciparum, *Parasitology international.* **59**, 298-302.
97. Bedhomme, M., Adamo, M., Marchand, C. H., Couturier, J., Rouhier, N., Lemaire, S. D., Zaffagnini, M. & Trost, P. (2012) Glutathionylation of cytosolic glyceraldehyde-3-phosphate dehydrogenase from the model plant Arabidopsis thaliana is reversed by both glutaredoxins and thioredoxins in vitro, *The Biochemical journal.* **445**, 337-47.
98. Chakravarti, R. & Stuehr, D. J. (2012) Thioredoxin-1 regulates cellular heme insertion by controlling S-nitrosation of glyceraldehyde-3-phosphate dehydrogenase, *The Journal of biological chemistry.* **287**, 16179-86.
99. Ju, Y., Wu, L. & Yang, G. (2016) Thioredoxin 1 regulation of protein S-desulfhydration, *Biochemistry and biophysics reports.* **5**, 27-34.
100. Yan, H., Lou, M. F., Fernando, M. R. & Harding, J. J. (2006) Thioredoxin, thioredoxin reductase, and alpha-crystallin revive inactivated glyceraldehyde 3-phosphate dehydrogenase in human aged and cataract lens extracts, *Molecular vision.* **12**, 1153-9.
101. Gupte, S. A., Rupawalla, T., Mohazzab, H. K. & Wolin, M. S. (1999) Regulation of NO-elicited pulmonary artery relaxation and guanylate cyclase activation by NADH oxidase and SOD, *The American journal of physiology.* **276**, H1535-42.
102. Lee, Y. J., Kang, I. J., Bunger, R. & Kang, Y. H. (2004) Enhanced survival effect of pyruvate correlates MAPK and NF-kappaB activation in hydrogen peroxide-treated human endothelial cells, *Journal of applied physiology.* **96**, 793-801; discussion 792.
103. Ali, M. A., Yasui, F., Matsugo, S. & Konishi, T. (2000) The lactate-dependent enhancement of hydroxyl radical generation by the Fenton reaction, *Free radical research.* **32**, 429-38.
104. Leong, P. K. & Ko, K. M. (2015) Schisandrin B induces an Nrf2-mediated thioredoxin expression and suppresses the activation of inflammasome in vitro and in vivo, *BioFactors.* **41**, 314-23.
105. Milovanova, T. N., Bhopale, V. M., Sorokina, E. M., Moore, J. S., Hunt, T. K., Hauer-Jensen, M., Velazquez, O. C. & Thom, S. R. (2008) Lactate stimulates vasculogenic stem cells via the thioredoxin system and engages an autocrine activation loop involving hypoxia-inducible factor 1, *Molecular and cellular biology.* **28**, 6248-61.
106. Lugokenski, T. H., Muller, L. G., Taube, P. S., Rocha, J. B. & Pereira, M. E. (2011) Inhibitory effect of ebselen on lactate dehydrogenase activity from mammals: a comparative study with diphenyl diselenide and diphenyl ditelluride, *Drug and chemical toxicology.* **34**, 66-76.

107. Ciszak, E. M., Korotchkina, L. G., Dominiak, P. M., Sidhu, S. & Patel, M. S. (2003) Structural basis for flip-flop action of thiamin pyrophosphate-dependent enzymes revealed by human pyruvate dehydrogenase, *The Journal of biological chemistry.* **278**, 21240-6.
108. Kato, M., Wynn, R. M., Chuang, J. L., Tso, S. C., Machius, M., Li, J. & Chuang, D. T. (2008) Structural basis for inactivation of the human pyruvate dehydrogenase complex by phosphorylation: role of disordered phosphorylation loops, *Structure.* **16**, 1849-59.
109. Patel, M. S. & Roche, T. E. (1990) Molecular biology and biochemistry of pyruvate dehydrogenase complexes, *FASEB journal : official publication of the Federation of American Societies for Experimental Biology.* **4**, 3224-33.
110. Balakrishnan, A., Nemeria, N. S., Chakraborty, S., Kakalis, L. & Jordan, F. (2012) Determination of pre-steady-state rate constants on the Escherichia coli pyruvate dehydrogenase complex reveals that loop movement controls the rate-limiting step, *Journal of the American Chemical Society.* **134**, 18644-55.
111. Holmgren, A. (1979) Thioredoxin catalyzes the reduction of insulin disulfides by dithiothreitol and dihydrolipoamide, *The Journal of biological chemistry.* **254**, 9627-32.
112. Feeney, M. A., Veeravalli, K., Boyd, D., Gon, S., Faulkner, M. J., Georgiou, G. & Beckwith, J. (2011) Repurposing lipoic acid changes electron flow in two important metabolic pathways of Escherichia coli, *Proceedings of the National Academy of Sciences of the United States of America.* **108**, 7991-6.
113. Jordan, F., Arjunan, P., Kale, S., Nemeria, N. S. & Furey, W. (2009) Multiple roles of mobile active center loops in the E1 component of the Escherichia coli pyruvate dehydrogenase complex - Linkage of protein dynamics to catalysis, *Journal of molecular catalysis B, Enzymatic.* **61**, 14-22.
114. Fisher-Wellman, K. H., Lin, C. T., Ryan, T. E., Reese, L. R., Gilliam, L. A., Cathey, B. L., Lark, D. S., Smith, C. D., Muoio, D. M. & Neufer, P. D. (2015) Pyruvate dehydrogenase complex and nicotinamide nucleotide transhydrogenase constitute an energy-consuming redox circuit, *The Biochemical journal.* **467**, 271-80.
115. Shumar, S. A., Kerr, E. W., Geldenhuys, W. J., Montgomery, G. E., Fagone, P., Thirawatananond, P., Saavedra, H., Gabelli, S. B. & Leonardi, R. (2018) Nudt19 is a renal CoA diphosphohydrolase with biochemical and regulatory properties that are distinct from the hepatic Nudt7 isoform, *The Journal of biological chemistry.* **293**, 4134-4148.
116. Kim, J. H., Fuzery, A. K., Tonelli, M., Ta, D. T., Westler, W. M., Vickery, L. E. & Markley, J. L. (2009) Structure and dynamics of the iron-sulfur cluster assembly scaffold protein IscU and its interaction with the cochaperone HscB, *Biochemistry.* **48**, 6062-71.
117. Kaptain, S., Downey, W. E., Tang, C., Philpott, C., Haile, D., Orloff, D. G., Harford, J. B., Rouault, T. A. & Klausner, R. D. (1991) A regulated RNA binding protein also possesses aconitase activity, *Proceedings of the National Academy of Sciences of the United States of America.* **88**, 10109-13.
118. Moeder, W., Del Pozo, O., Navarre, D. A., Martin, G. B. & Klessig, D. F. (2007) Aconitase plays a role in regulating resistance to oxidative stress and cell death in Arabidopsis and Nicotiana benthamiana, *Plant molecular biology.* **63**, 273-87.
119. Tang, Y. & Guest, J. R. (1999) Direct evidence for mRNA binding and post-transcriptional regulation by Escherichia coli aconitases, *Microbiology.* **145 (Pt 11)**, 3069-79.
120. Metodiev, M. D., Gerber, S., Hubert, L., Delahodde, A., Chretien, D., Gerard, X., Amati-Bonneau, P., Giacomotto, M. C., Boddaert, N., Kaminska, A., Desguerre, I., Amiel, J., Rio, M., Kaplan, J., Munnich, A., Rotig, A., Rozet, J. M. & Besmond, C. (2014) Mutations in the tricarboxylic acid cycle enzyme, aconitase 2, cause either isolated or syndromic optic neuropathy with encephalopathy and cerebellar atrophy, *Journal of medical genetics.* **51**, 834-8.
121. Talib, J. & Davies, M. J. (2016) Exposure of aconitase to smoking-related oxidants results in iron loss and increased iron response protein-1 activity: potential mechanisms for iron accumulation in human arterial cells, *Journal of biological inorganic chemistry : JBIC : a publication of the Society of Biological Inorganic Chemistry.* **21**, 305-17.

122. White, K., Kim, M. J., Han, C., Park, H. J., Ding, D., Boyd, K., Walker, L., Linser, P., Meneses, Z., Slade, C., Hirst, J., Santostefano, K., Terada, N., Miyakawa, T., Tanokura, M., Salvi, R. & Someya, S. (2018) Loss of IDH2 Accelerates Age-related Hearing Loss in Male Mice, *Scientific reports.* **8**, 5039.
123. Xu, Y., Liu, L., Nakamura, A., Someya, S., Miyakawa, T. & Tanokura, M. (2017) Studies on the regulatory mechanism of isocitrate dehydrogenase 2 using acetylation mimics, *Scientific reports.* **7**, 9785.
124. Ma, T., Peng, Y., Huang, W., Liu, Y. & Ding, J. (2017) The beta and gamma subunits play distinct functional roles in the alpha2betagamma heterotetramer of human NAD-dependent isocitrate dehydrogenase, *Scientific reports.* **7**, 41882.
125. Izquierdo-Garcia, J. L., Viswanath, P., Eriksson, P., Cai, L., Radoul, M., Chaumeil, M. M., Blough, M., Luchman, H. A., Weiss, S., Cairncross, J. G., Phillips, J. J., Pieper, R. O. & Ronen, S. M. (2015) IDH1 Mutation Induces Reprogramming of Pyruvate Metabolism, *Cancer research.* **75**, 2999-3009.
126. Vartak, R. S., Semwal, M. K. & Bai, Y. (2014) An update on complex I assembly: the assembly of players, *Journal of bioenergetics and biomembranes.* **46**, 323-8.
127. Moparthi, V. K. & Hagerhall, C. (2011) The evolution of respiratory chain complex I from a smaller last common ancestor consisting of 11 protein subunits, *Journal of molecular evolution.* **72**, 484-97.
128. Andrews, B., Carroll, J., Ding, S., Fearnley, I. M. & Walker, J. E. (2013) Assembly factors for the membrane arm of human complex I, *Proceedings of the National Academy of Sciences of the United States of America.* **110**, 18934-9.
129. Jaokar, T. M., Patil, D. P., Shouche, Y. S., Gaikwad, S. M. & Suresh, C. G. (2013) Human mitochondrial NDUFS3 protein bearing Leigh syndrome mutation is more prone to aggregation than its wild-type, *Biochimie.* **95**, 2392-403.
130. Yankovskaya, V., Horsefield, R., Tornroth, S., Luna-Chavez, C., Miyoshi, H., Leger, C., Byrne, B., Cecchini, G. & Iwata, S. (2003) Architecture of succinate dehydrogenase and reactive oxygen species generation, *Science.* **299**, 700-4.
131. Sharma, L. K., Lu, J. & Bai, Y. (2009) Mitochondrial respiratory complex I: structure, function and implication in human diseases, *Current medicinal chemistry.* **16**, 1266-77.
132. Du, Z., Liu, X., Chen, T., Gao, W., Wu, Z., Hu, Z., Wei, D., Gao, C. & Li, Q. (2018) Targeting a Sirt5-Positive Subpopulation Overcomes Multidrug Resistance in Wild-Type Kras Colorectal Carcinomas, *Cell reports.* **22**, 2677-2689.
133. Crofts, A. R. (2004) The cytochrome bc1 complex: function in the context of structure, *Annual review of physiology.* **66**, 689-733.
134. Hoffman, G. G., Lee, S., Christiano, A. M., Chung-Honet, L. C., Cheng, W., Katchman, S., Uitto, J. & Greenspan, D. S. (1993) Complete coding sequence, intron/exon organization, and chromosomal location of the gene for the core I protein of human ubiquinol-cytochrome c reductase, *The Journal of biological chemistry.* **268**, 21113-9.
135. Huang, S., Wang, J. & Cui, Y. (2016) 2,2',4,4'-Tetrabromodiphenyl ether injures cell viability and mitochondrial function of mouse spermatocytes by decreasing mitochondrial proteins Atp5b and Uqcrc1, *Environmental toxicology and pharmacology.* **46**, 301-310.
136. Kunej, T., Wang, Z., Michal, J. J., Daniels, T. F., Magnuson, N. S. & Jiang, Z. (2007) Functional UQCRC1 polymorphisms affect promoter activity and body lipid accumulation, *Obesity.* **15**, 2896-901.
137. Shang, Y., Zhang, F., Li, D., Li, C., Li, H., Jiang, Y. & Zhang, D. (2018) Overexpression of UQCRC2 is correlated with tumor progression and poor prognosis in colorectal cancer, *Pathology, research and practice*.
138. Bai, Y. H., Zhan, Y. B., Yu, B., Wang, W. W., Wang, L., Zhou, J. Q., Chen, R. K., Zhang, F. J., Zhao, X. W., Duan, W. C., Wang, Y. M., Liu, J., Bao, J. J., Zhang, Z. Y. & Liu, X. Z. (2018) A Novel Tumor-Suppressor, CDH18, Inhibits Glioma Cell Invasiveness Via UQCRC2 and Correlates with the Prognosis of Glioma Patients, *Cellular physiology and biochemistry : international journal of experimental cellular physiology, biochemistry, and pharmacology.* **48**, 1755-1770.
139. Ellinger, J., Gromes, A., Poss, M., Bruggemann, M., Schmidt, D., Ellinger, N., Tolkach, Y., Dietrich, D., Kristiansen, G. & Muller, S. C. (2016) Systematic expression analysis of the mitochondrial complex

III subunits identifies UQCRC1 as biomarker in clear cell renal cell carcinoma, *Oncotarget.* **7**, 86490-86499.
140. Bottani, E., Cerutti, R., Harbour, M. E., Ravaglia, S., Dogan, S. A., Giordano, C., Fearnley, I. M., D'Amati, G., Viscomi, C., Fernandez-Vizarra, E. & Zeviani, M. (2017) TTC19 Plays a Husbandry Role on UQCRFS1 Turnover in the Biogenesis of Mitochondrial Respiratory Complex III, *Molecular cell.* **67**, 96-105 e4.
141. Dennerlein, S., Oeljeklaus, S., Jans, D., Hellwig, C., Bareth, B., Jakobs, S., Deckers, M., Warscheid, B. & Rehling, P. (2015) MITRAC7 Acts as a COX1-Specific Chaperone and Reveals a Checkpoint during Cytochrome c Oxidase Assembly, *Cell reports.* **12**, 1644-55.
142. Dennerlein, S. & Rehling, P. (2015) Human mitochondrial COX1 assembly into cytochrome c oxidase at a glance, *Journal of cell science.* **128**, 833-7.
143. Balsa, E., Marco, R., Perales-Clemente, E., Szklarczyk, R., Calvo, E., Landazuri, M. O. & Enriquez, J. A. (2012) NDUFA4 is a subunit of complex IV of the mammalian electron transport chain, *Cell metabolism.* **16**, 378-86.
144. Pitceathly, R. D., Rahman, S., Wedatilake, Y., Polke, J. M., Cirak, S., Foley, A. R., Sailer, A., Hurles, M. E., Stalker, J., Hargreaves, I., Woodward, C. E., Sweeney, M. G., Muntoni, F., Houlden, H., Taanman, J. W., Hanna, M. G. & Consortium, U. K. (2013) NDUFA4 mutations underlie dysfunction of a cytochrome c oxidase subunit linked to human neurological disease, *Cell reports.* **3**, 1795-805.
145. Tanaka, T., Hosoi, F., Yamaguchi-Iwai, Y., Nakamura, H., Masutani, H., Ueda, S., Nishiyama, A., Takeda, S., Wada, H., Spyrou, G. & Yodoi, J. (2002) Thioredoxin-2 (TRX-2) is an essential gene regulating mitochondria-dependent apoptosis, *The EMBO journal.* **21**, 1695-703.
146. Nalvarte, I., Damdimopoulos, A. E. & Spyrou, G. (2004) Human mitochondrial thioredoxin reductase reduces cytochrome c and confers resistance to complex III inhibition, *Free radical biology & medicine.* **36**, 1270-8.
147. Jonckheere, A. I., Smeitink, J. A. & Rodenburg, R. J. (2012) Mitochondrial ATP synthase: architecture, function and pathology, *Journal of inherited metabolic disease.* **35**, 211-25.
148. Buchert, F., Konno, H. & Hisabori, T. (2015) Redox regulation of CF1-ATPase involves interplay between the gamma-subunit neck region and the turn region of the betaDELSEED-loop, *Biochimica et biophysica acta.* **1847**, 441-450.
149. Kim, Y., Konno, H., Sugano, Y. & Hisabori, T. (2011) Redox regulation of rotation of the cyanobacterial F1-ATPase containing thiol regulation switch, *The Journal of biological chemistry.* **286**, 9071-8.
150. Belogrudov, G. I. & Hatefi, Y. (2002) Factor B and the mitochondrial ATP synthase complex, *The Journal of biological chemistry.* **277**, 6097-103.
151. Spiekerkoetter, U., Khuchua, Z., Yue, Z., Bennett, M. J. & Strauss, A. W. (2004) General mitochondrial trifunctional protein (TFP) deficiency as a result of either alpha- or beta-subunit mutations exhibits similar phenotypes because mutations in either subunit alter TFP complex expression and subunit turnover, *Pediatric research.* **55**, 190-6.
152. Ibdah, J. A., Perlegas, P., Zhao, Y., Angdisen, J., Borgerink, H., Shadoan, M. K., Wagner, J. D., Matern, D., Rinaldo, P. & Cline, J. M. (2005) Mice heterozygous for a defect in mitochondrial trifunctional protein develop hepatic steatosis and insulin resistance, *Gastroenterology.* **128**, 1381-90.
153. Chen, J., Young, M. E., Chatham, J. C., Crossman, D. K., Dell'Italia, L. J. & Shalev, A. (2016) TXNIP regulates myocardial fatty acid oxidation via miR-33a signaling, *American journal of physiology Heart and circulatory physiology.* **311**, H64-75.
154. Schwer, B., Bunkenborg, J., Verdin, R. O., Andersen, J. S. & Verdin, E. (2006) Reversible lysine acetylation controls the activity of the mitochondrial enzyme acetyl-CoA synthetase 2, *Proceedings of the National Academy of Sciences of the United States of America.* **103**, 10224-10229.
155. Forsyth, R., Vockley, C. W., Edick, M. J., Cameron, C. A., Hiner, S. J., Berry, S. A., Vockley, J., Arnold, G. L. & Inborn Errors of Metabolism, C. (2016) Outcomes of cases with 3-methylcrotonyl-CoA carboxylase (3-MCC) deficiency - Report from the Inborn Errors of Metabolism Information System, *Molecular genetics and metabolism.* **118**, 15-20.

156. Zandberg, L., van Dyk, H. C., van der Westhuizen, F. H. & van Dijk, A. A. (2016) A 3-methylcrotonyl-CoA carboxylase deficient human skin fibroblast transcriptome reveals underlying mitochondrial dysfunction and oxidative stress, *The international journal of biochemistry & cell biology.* **78**, 116-129.
157. Strickland, K. C., Krupenko, N. I., Dubard, M. E., Hu, C. J., Tsybovsky, Y. & Krupenko, S. A. (2011) Enzymatic properties of ALDH1L2, a mitochondrial 10-formyltetrahydrofolate dehydrogenase, *Chemico-biological interactions.* **191**, 129-36.
158. Lan, X., Field, M. S. & Stover, P. J. (2018) Cell cycle regulation of folate-mediated one-carbon metabolism, *Wiley interdisciplinary reviews Systems biology and medicine*, e1426.
159. Bonifati, V., Rizzu, P., van Baren, M. J., Schaap, O., Breedveld, G. J., Krieger, E., Dekker, M. C., Squitieri, F., Ibanez, P., Joosse, M., van Dongen, J. W., Vanacore, N., van Swieten, J. C., Brice, A., Meco, G., van Duijn, C. M., Oostra, B. A. & Heutink, P. (2003) Mutations in the DJ-1 gene associated with autosomal recessive early-onset parkinsonism, *Science.* **299**, 256-9.
160. Fernandez-Caggiano, M., Schroder, E., Cho, H. J., Burgoyne, J., Barallobre-Barreiro, J., Mayr, M. & Eaton, P. (2016) Oxidant-induced Interprotein Disulfide Formation in Cardiac Protein DJ-1 Occurs via an Interaction with Peroxiredoxin 2, *The Journal of biological chemistry.* **291**, 10399-410.
161. Terron, A., Bal-Price, A., Paini, A., Monnet-Tschudi, F., Bennekou, S. H., Members, E. W. E., Leist, M. & Schildknecht, S. (2018) An adverse outcome pathway for parkinsonian motor deficits associated with mitochondrial complex I inhibition, *Archives of toxicology.* **92**, 41-82.
162. Wang, J., Duhart, H. M., Xu, Z., Patterson, T. A., Newport, G. D. & Ali, S. F. (2008) Comparison of the time courses of selective gene expression and dopaminergic depletion induced by MPP+ in MN9D cells, *Neurochemistry international.* **52**, 1037-43.
163. Holzerova, E., Danhauser, K., Haack, T. B., Kremer, L. S., Melcher, M., Ingold, I., Kobayashi, S., Terrile, C., Wolf, P., Schaper, J., Mayatepek, E., Baertling, F., Friedmann Angeli, J. P., Conrad, M., Strom, T. M., Meitinger, T., Prokisch, H. & Distelmaier, F. (2016) Human thioredoxin 2 deficiency impairs mitochondrial redox homeostasis and causes early-onset neurodegeneration, *Brain : a journal of neurology.* **139**, 346-54.
164. Havugimana, P. C., Hart, G. T., Nepusz, T., Yang, H., Turinsky, A. L., Li, Z., Wang, P. I., Boutz, D. R., Fong, V., Phanse, S., Babu, M., Craig, S. A., Hu, P., Wan, C., Vlasblom, J., Dar, V. U., Bezginov, A., Clark, G. W., Wu, G. C., Wodak, S. J., Tillier, E. R., Paccanaro, A., Marcotte, E. M. & Emili, A. (2012) A census of human soluble protein complexes, *Cell.* **150**, 1068-81.
165. Rolland, T., Tasan, M., Charloteaux, B., Pevzner, S. J., Zhong, Q., Sahni, N., Yi, S., Lemmens, I., Fontanillo, C., Mosca, R., Kamburov, A., Ghiassian, S. D., Yang, X., Ghamsari, L., Balcha, D., Begg, B. E., Braun, P., Brehme, M., Broly, M. P., Carvunis, A. R., Convery-Zupan, D., Corominas, R., Coulombe-Huntington, J., Dann, E., Dreze, M., Dricot, A., Fan, C., Franzosa, E., Gebreab, F., Gutierrez, B. J., Hardy, M. F., Jin, M., Kang, S., Kiros, R., Lin, G. N., Luck, K., MacWilliams, A., Menche, J., Murray, R. R., Palagi, A., Poulin, M. M., Rambout, X., Rasla, J., Reichert, P., Romero, V., Ruyssinck, E., Sahalie, J. M., Scholz, A., Shah, A. A., Sharma, A., Shen, Y., Spirohn, K., Tam, S., Tejeda, A. O., Trigg, S. A., Twizere, J. C., Vega, K., Walsh, J., Cusick, M. E., Xia, Y., Barabasi, A. L., Iakoucheva, L. M., Aloy, P., De Las Rivas, J., Tavernier, J., Calderwood, M. A., Hill, D. E., Hao, T., Roth, F. P. & Vidal, M. (2014) A proteome-scale map of the human interactome network, *Cell.* **159**, 1212-1226.
166. Wan, C., Borgeson, B., Phanse, S., Tu, F., Drew, K., Clark, G., Xiong, X., Kagan, O., Kwan, J., Bezginov, A., Chessman, K., Pal, S., Cromar, G., Papoulas, O., Ni, Z., Boutz, D. R., Stoilova, S., Havugimana, P. C., Guo, X., Malty, R. H., Sarov, M., Greenblatt, J., Babu, M., Derry, W. B., Tillier, E. R., Wallingford, J. B., Parkinson, J., Marcotte, E. M. & Emili, A. (2015) Panorama of ancient metazoan macromolecular complexes, *Nature.* **525**, 339-44.

Table 1. Human mitochondrial proteins interacting with Trx2 as revealed by proteomics, Y2H screens and BioGRID. NC corresponds to non-covalent interaction; C to covalent. The four protein species in gray background correspond to mitochondrial proteins (combination of MitoCarta2.0 and BioGRID) described as interacting with Trx2.

#	UniProt KB	Protein species	Gene	Interaction confirmed by	Type of interaction (NC or C)
1	Q99798	Aconitate hydratase, mitochondrial,	ACO2	DTT	C
2	Q9NUB1	Acetyl-coenzyme A synthetase 2-like, mitochondrial	ACSS1	DTT	C
3	O75891	Cytosolic 10-formyltetrahydrofolate dehydrogenase	ALDH1L1	DTT	C
4	P05091	Aldehyde dehydrogenase, mitochondrial	ALDH2	Acid	NC
5	P25705	ATP synthase subunit alpha, mitochondrial	ATP5F1A	Acid, DTT	NC, C
6	P06576	ATP synthase subunit beta, mitochondrial	ATP5F1B	Acid, DTT	NC, C
7	O75947	ATP synthase subunit d, mitochondrial	ATP5PD	Acid, DTT	NC, C
8	O75828	Carbonyl reductase [NADPH] 3	CBR3	DTT	C
9	P17540	Creatine kinase S-type, mitochondrial	CKMT2	DTT	C
10	P47985	Cytochrome b-c1 complex subunit Rieske, mitochondrial	UQCRFS1	Acid, DTT	NC, C
11	Q08426	Peroxisomal bifunctional enzyme	EHHADH	DTT	C
12	P04406	Glyceraldehyde-3-phosphate dehydrogenase	GAPDH	Acid, DTT	NC, C
13	P40939	Trifunctional enzyme subunit alpha, mitochondrial	HADHA	Acid	NC
14	P38646	Stress-70 protein, mitochondrial	HSPA9	DTT	C
15	P10809	60 kDa heat shock protein, mitochondrial	HSPD1	DTT	C
16	O75874	Isocitrate dehydrogenase [NADP] cytoplasmic	IDH1	Acid	NC
17	P48735	Isocitrate dehydrogenase [NADP], mitochondrial	IDH2	Acid	NC
18	P50213	Isocitrate dehydrogenase [NAD] subunit alpha, mitochondrial	IDH3A	DTT	C
19	P51553	Isocitrate dehydrogenase [NAD] subunit gamma, mitochondrial	IDH3G	Acid	NC
20	Q16891	MICOS complex subunit MIC60	IMMT	DTT	C
21	P07195	L-lactate dehydrogenase B chain, LDH-B	LDHB	Acid	NC
22	Q86WU2	Probable D-lactate dehydrogenase, mitochondrial	LDHD	DTT	C
23	Q9BQ69	O-acetyl-ADP-ribose deacetylase MACROD1	MACROD 1	DTT	C
24	Q9HCC0	Methylcrotonoyl-CoA carboxylase beta chain, mitochondrial,	MCCC2	Acid	NC
25		Mitochondrially encoded 16S RNA	*MT-RNR2*	Y2H rat	NC
26	Q9UJ68	Mitochondrial peptide methionine sulfoxide reductase	MSRA	DTT	C
27	P00395	Cytochrome c oxidase subunit 1	MT-CO1	Y2H rat	NC
28	O00483	Cytochrome c oxidase subunit NDUFA4	NDUFA4	Acid	NC
29	P28331	NADH-ubiquinone oxidoreductase 75 kDa subunit, mitochondrial	NDUFS1	Acid	NC

30	O75306	NADH dehydrogenase [ubiquinone] iron-sulfur protein 2, mitochondrial	NDUFS2	Acid	NC
31	O75489	NADH dehydrogenase [ubiquinone] iron-sulfur protein 3, mitochondrial	NDUFS3	Acid	NC
32	P49821	NADH dehydrogenase [ubiquinone] flavoprotein 1, mitochondrial	NDUFV1	Acid	NC
33	A8MXV4	Nucleoside diphosphate-linked moiety X motif 19	NUDT19	DTT	C
34	P07237	Protein disulfide-isomerase	P4HB	Y2H human	NC
35	Q99497	Protein/nucleic acid deglycase DJ-1	PARK7	DTT	C
36	P08559	Pyruvate dehydrogenase E1 component subunit alpha, somatic form, mitochondrial	PDHA1	Acid	NC
37	P11177	Pyruvate dehydrogenase E1 component subunit beta, mitochondrial	PDHB	DTT	C
38	Q9H2U2	Inorganic pyrophosphatase 2, mitochondrial	PPA2	DTT	C
39	P32119	Peroxiredoxin-2	PRDX2	Acid, DTT	NC, C
40	P30048	Thioredoxin-dependent peroxide reductase, mitochondrial (Peroxiredoxin-3)	PRDX3	DTT	C
41	Q13162	Peroxiredoxin-4	PRDX4	Acid, DTT	NC, C
42	P30044	Peroxiredoxin-5	PRDX5	Acid, DTT	NC, C
43	P30041	Peroxiredoxin-6	PRDX6	DTT	C
44	P62269	40S ribosomal protein S18	RPS18	Acid	NC
45	P31040	Succinate dehydrogenase [ubiquinone] flavoprotein subunit	SDHA	Acid	NC
46	P60174	Triosephosphate isomerase	TPI1	Acid, DTT	NC, C
47	P49411	Elongation factor Tu, mitochondrial, EF-Tu	TUFM	DTT	C
48	P31930	Cytochrome b-c1 complex subunit 1, mitochondrial	UQCRC1	DTT	C
49	P22695	Cytochrome b-c1 complex subunit 2, mitochondrial	UQCRC2	Acid	NC
50	Q16540	Mitochondrial ribosomal protein L23	MRPL23	Co fractionation/BioGRID [164]	
51	P49247	Ribose 5-phosphate isomerase A	RPIA	BioGRID [165]	
52	P00441	Superoxide dismutase 1, soluble	SOD1	Co fractionation/BioGRID [166]	
53	Q9NS69	Translocase of outer mitochondrial membrane 22 homolog	TOMM22	Co fractionation/BioGRID [164]	

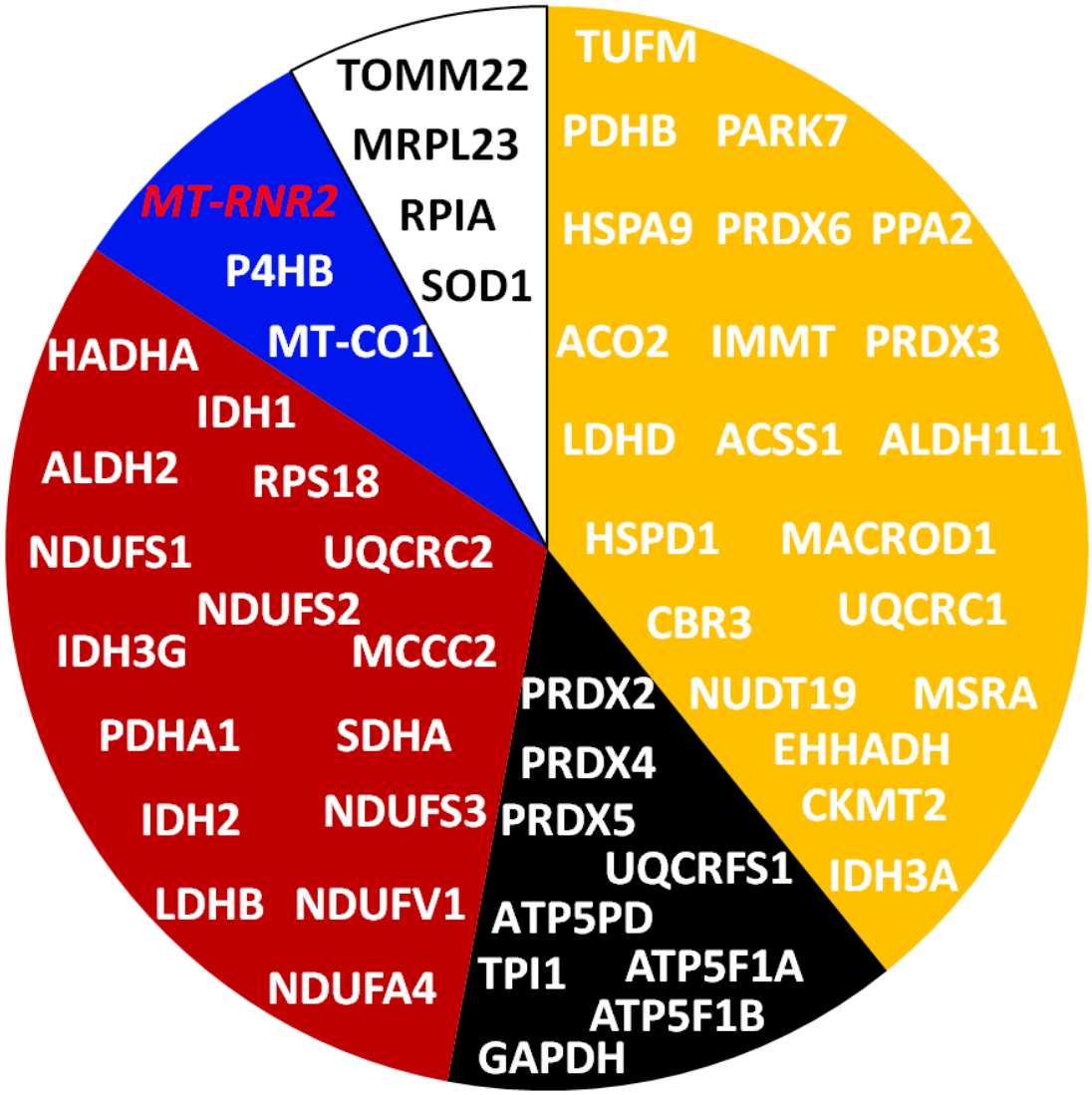

Figure 1: The human Trx2 mitochondrial interactome. Proteins are presented by their primary gene names (table 1). In summary, 21 proteins were eluted by DTT (yellow), 16 by acid (red), and 9 proteins were eluted by both acid and DTT (black). The blue slice represents data from Y2H screens where the mitochondrial 16S RNA gene is in red letters. The white slice contains the four mitochondrial interactors of Trx2 from the BioGRID data base [26].

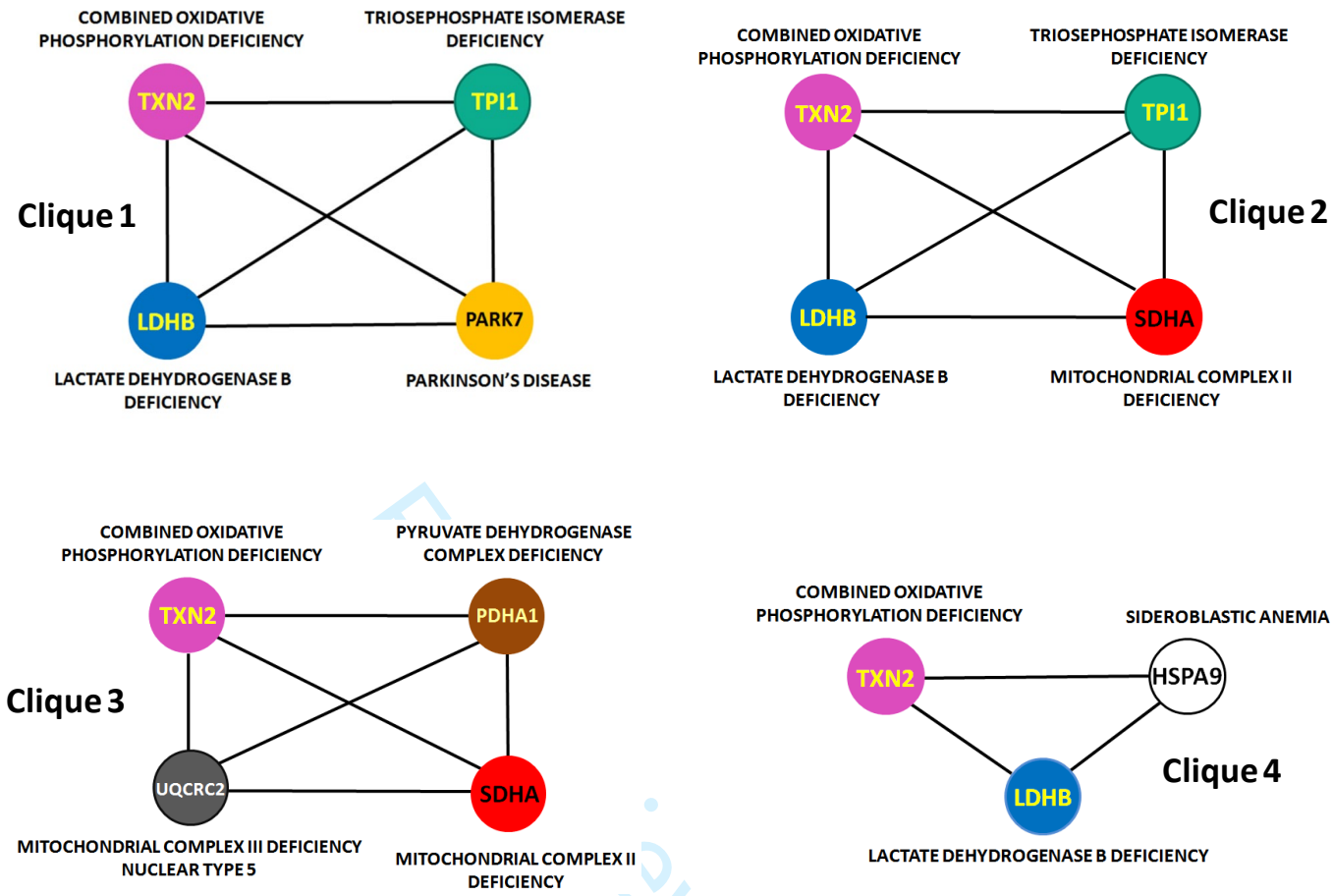

Fig 2: Four cliques of the diseasome of Trx2. The diseasome is based on the Trx2 mitochondrial interactome. The disease-related genes/proteins are shown with capital letters within the circular nodes of each clique (Unipot IDs are provided on supplementary table 2.5). The lines connecting different nodes (genes) indicate the herein supported interactions for Trx2 and the interactions among the interactors of Trx2 (data from BioGRID).

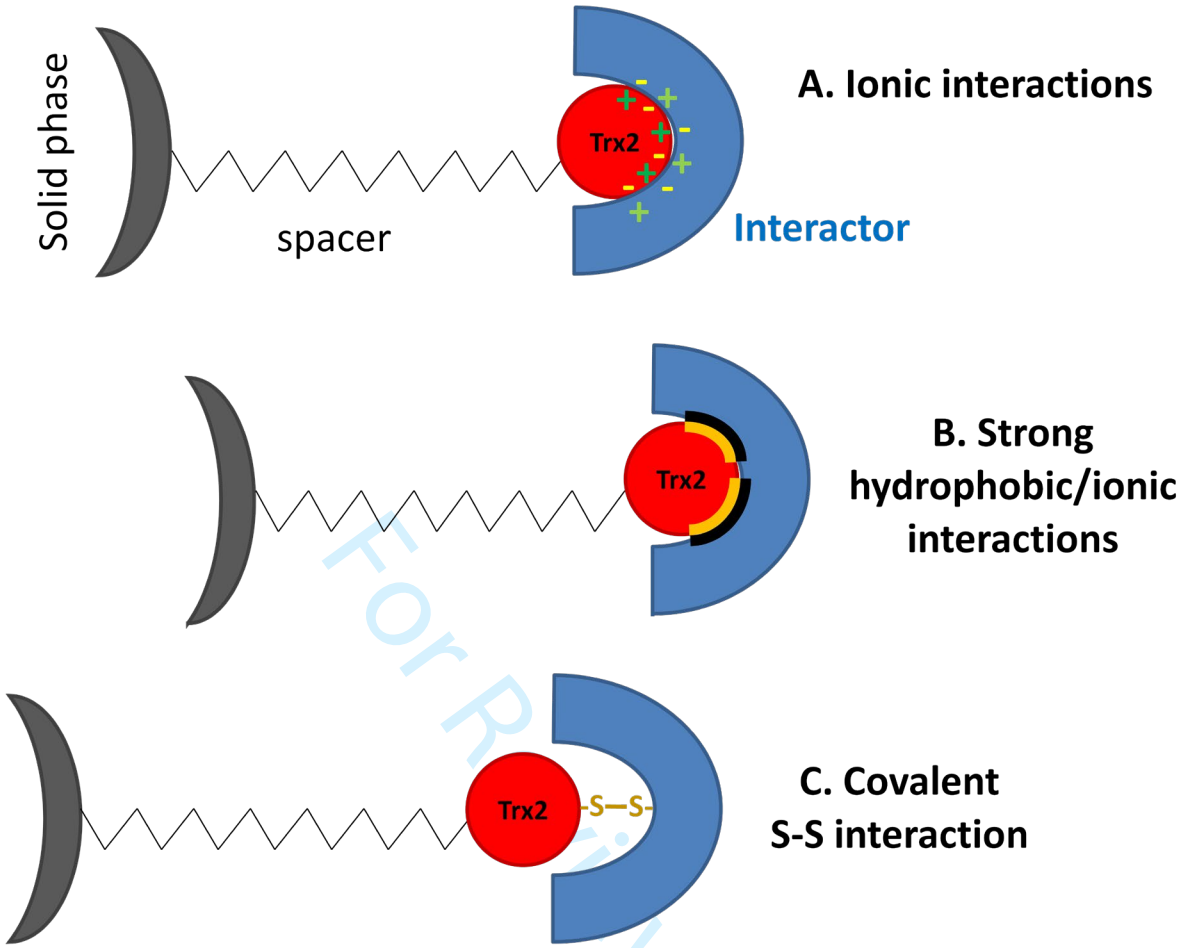

Fig. 3. Proposed interactions of Trx2 with potential substrates. 3A: weak ionic interactions; 3B: strong hydrophobic interactions (interacting hydrophobic areas in black and yellow); 3C: covalent interactions via a disulfide between ΔTrx2C93S and interactor.

Supplementary figures

Supplementary figure 1. Alignment of mouse, rat and human Trx2 lacking their mitochondrial targeting sequene. All different amino acids are highlighted in yellow background. Alignment was performed using the CLUSTAL O(1.2.4) multiple sequence alignment tool (https://www.ebi.ac.uk/Tools/msa/clustalo/).

Supplementary figure 2. Elution profile of ΔTrx2C93S on a DEAE FF column. Chromatography was carried out in 20 mM Bis-Tris-HCl, pH 6,7 and a 0-1 M NaCl gradient (light green line). The other shown lines correspond to: conductivity (brown line); A_{280} (blue); A_{254} (magenta); A_{310} (red). ΔTrx2C93S was eluted at ~15 mS/cm (black arrow). (i) whole chromatogram, (ii) partial chromatogram.

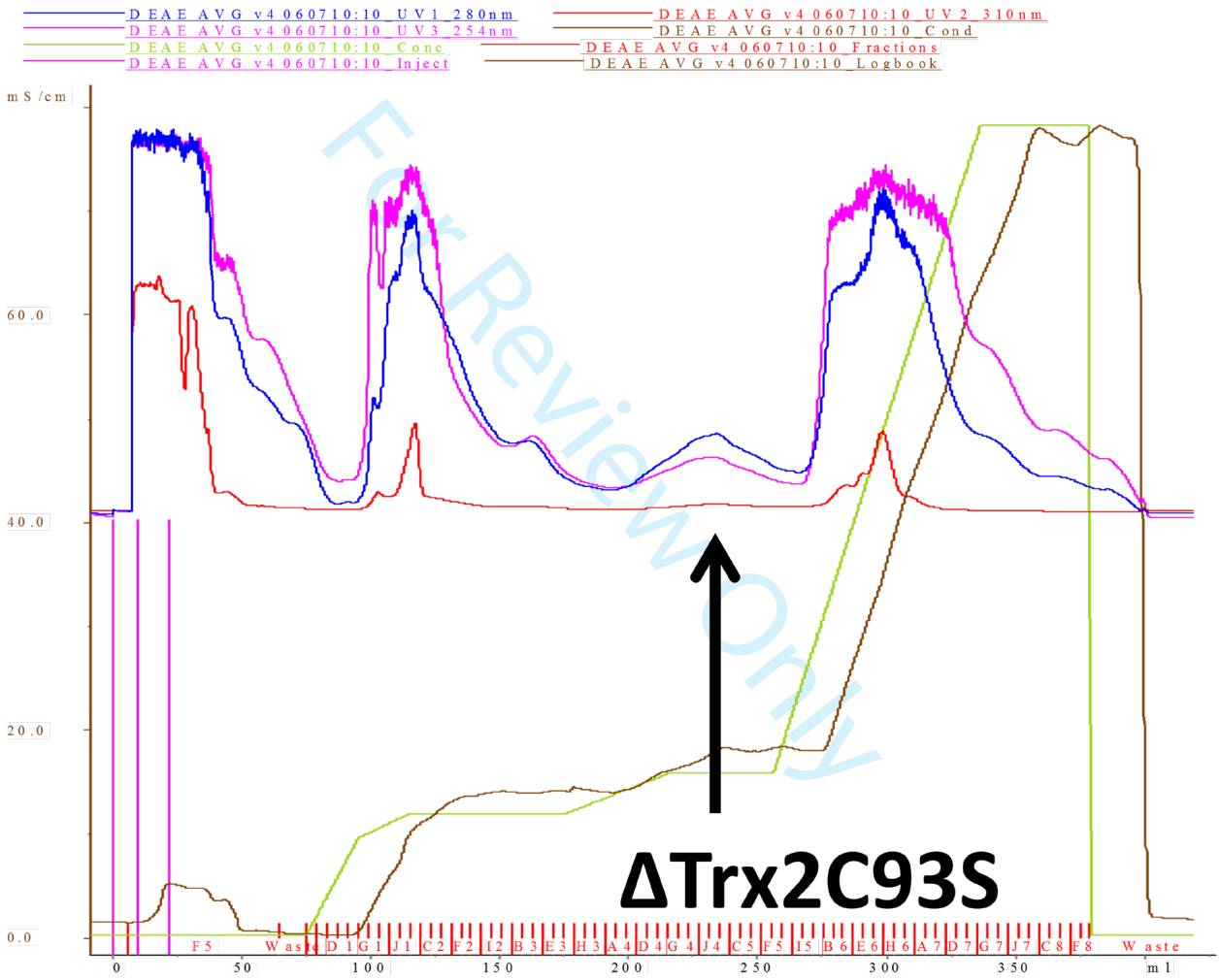

Supplementary figure 2 (i).

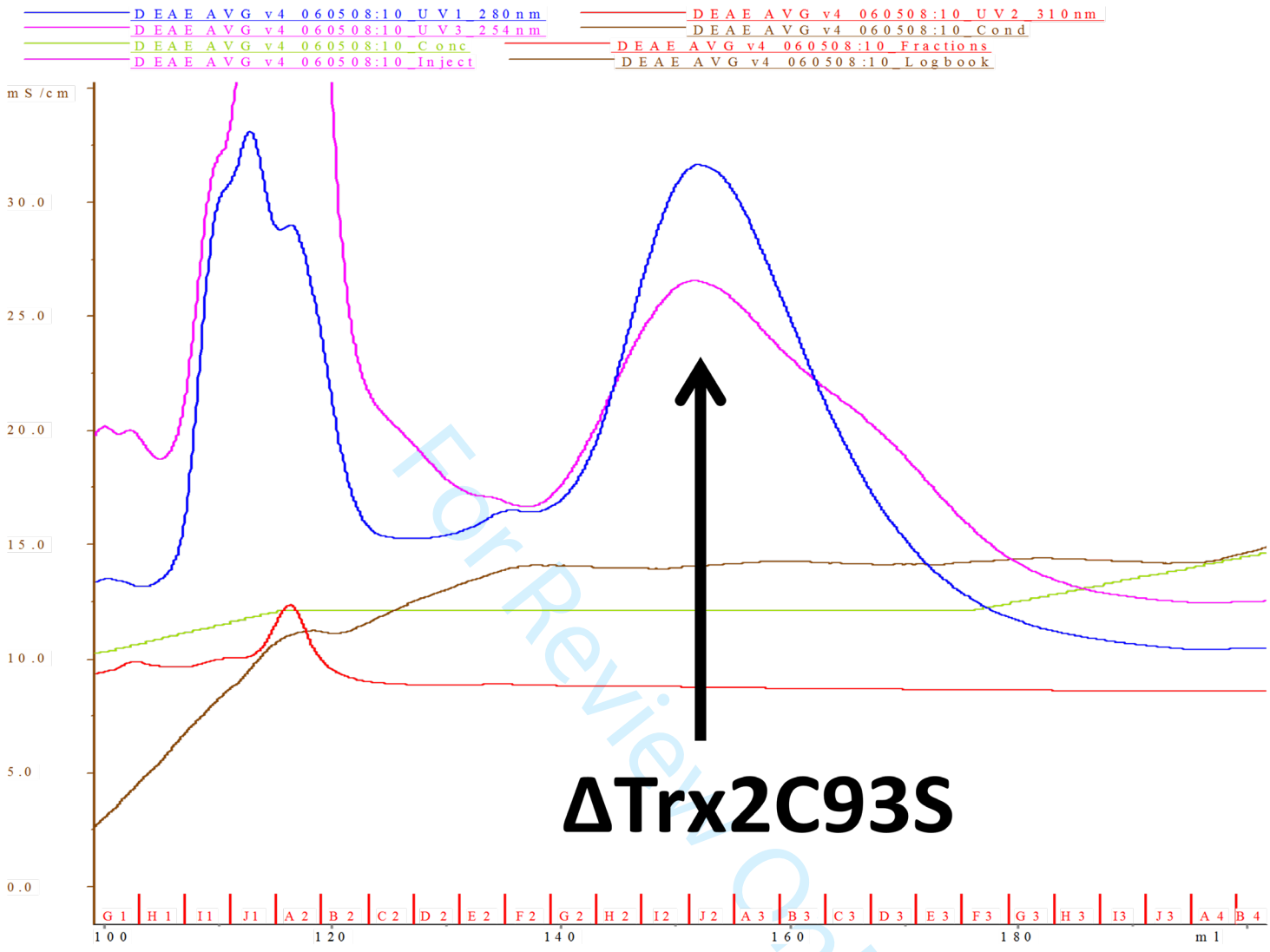

Supplementary figure 2 (ii).

Supplementary figure 3. Western blots of fractions derived by centrifugation gradient from cardiac muscle.

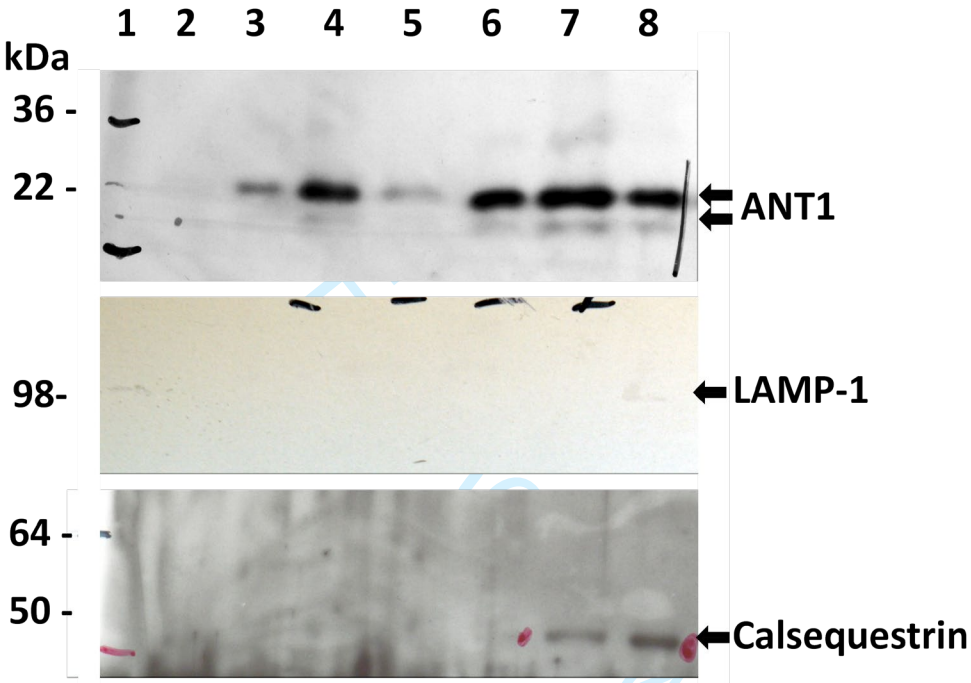

Analysis of sucrose gradient fractions, for mitochondrial (ANT1), lysosomal (LAMP-1) and ER (calsequestrin) proteins by Western blot in 10 % SDS-PAGE. Lane 1: molecular weight protein markers, lanes 2-8: fractions from sucrose gradient. The respective antibody together with an arrow indicting the detected antigen (ANT 1, LAMP1, calsequestrin) are shown at the right side of each Western blot. Fractions corresponding to lanes 3, 4, and 6 were pooled as "mitochondrial" fractions and chromatographed on the ΔTrx2C93S affinity columns. The same criteria were set for the selection of mitochondrial fractions from brain, skeletal muscle.

Supplementary tables 1. Mass spec analysis of individual spots obtained from 2D (and 1D) electrophoresis

MS data for the interactors of Trx2 in different mouse tissues.

Proteins were isolated and identified from 2D gels by MALDI-TOF-MS analysis, using the parameters described under Materials and Methods: % coverage represents the percentage of total protein sequence by the identified peptides. The probability of a false identity was usually lower than 10^{-5}. Spot numbering (Spot #, left column) corresponds to the different spots/bands identified per experiment. The numbering is according to the alphabetical order of the protein species identified. The protein species identified according to the set criteria are numbered in the right column (# of species) and are coloured in red. The individual experiments and their corresponding results are presented in the following tables.

Table 1.1: mass spec analysis of a 2D gel, of an acid-eluted fraction from a lysate derived from mouse lungs.

Spot #	Protein species	Mascot Score	% Coverage	Protein MW	Accession	Uniprot ID	# of species
1	12 days embryo spinal ganglion cDNA, RIKEN full-length enriched library, clone:D130020I06 product:2	27	13	33405.48	Q8BJI0_MOUSE		
2	16 days embryo head cDNA, RIKEN full-length enriched library, clone:C130079C10 product:carbonyl red	42	26	26055.66	Q542P5_MOUSE		
3	40S ribosomal protein S4, X isoform - Mus musculus (Mouse)	106	49	29807.14	RS4X_MOUSE	P62702	1
4	40S ribosomal protein SA - Mus musculus (Mouse)	151	54	32931.48	RSSA_MOUSE	P14206	2
5	Actin, cytoplasmic 1 - Mus musculus (Mouse)	160	63	42051.86	ACTB_MOUSE	P60710	3
6	Adult male testis cDNA, RIKEN full-length enriched library, clone:4930427I11 product:similar to ZIN	47	21	61098.16	Q9D5K8_MOUSE		
7	Aldehyde dehydrogenase, mitochondrial precursor - Mus musculus (Mouse)	247	50	57014.94	ALDH2_MOUSE	P47738	4
8	Aldehyde dehydrogenase, mitochondrial precursor - Mus musculus (Mouse)	194	48	57014.94	ALDH2_MOUSE		
9	Alpha crystallin B chain - Mus musculus (Mouse)	109	54	20056.41	CRYAB_MOUSE	P23927	5

10	Alpha-centractin - Mus musculus (Mouse)	107	45	42700.95	ACTZ_MOUSE	P61164	6
11	Alpha-enolase - Mus musculus (Mouse)	167	63	47453.34	ENOA_MOUSE	P17182	7
12	ATP synthase subunit alpha, mitochondrial precursor - Mus musculus (Mouse)	152	45	59829.63	ATPA_MOUSE	Q03265	8
13	ATP synthase subunit beta, mitochondrial precursor - Mus musculus (Mouse)	144	56	56265.46	ATPB_MOUSE	P56480	9
14	Dihydropyrimidinase-related protein 2 - Mus musculus (Mouse)	189	59	62637.74	DPYL2_MOUSE	Q62188	10
15	Dihydropyrimidinase-related protein 2 - Mus musculus (Mouse)	201	57	62637.74	DPYL2_MOUSE		
16	Dihydropyrimidinase-related protein 3 - Mus musculus (Mouse)	221	64	62296.23	DPYL3_MOUSE		
17	F-actin capping protein subunit alpha-1 - Mus musculus (Mouse)	103	63	33090.37	CAZA1_MOUSE	P47753	11
18	F-actin capping protein subunit alpha-2 - Mus musculus (Mouse)	136	82	33117.68	CAZA2_MOUSE	P47754	12
19	F-actin capping protein subunit alpha-2 - Mus musculus (Mouse)	166	76	33117.68	CAZA2_MOUSE		
20	Gelsolin precursor - Mus musculus (Mouse)	118	34	86287.23	GELS_MOUSE	P13020	13
21	Gelsolin precursor - Mus musculus (Mouse)	134	35	86287.23	GELS_MOUSE		
22	Glyceraldehyde-3-phosphate dehydrogenase - Mus musculus (Mouse)	68	34	36072.32	G3P_MOUSE	P16858	14
23	GTP-binding nuclear protein Ran - Mus musculus (Mouse)	159	50	24578.68	RAN_MOUSE	P62827	15
24	Hist1h2bj protein - Mus musculus (Mouse)	43	42	13570.43	A0JLV3_MOUSE		
25	Indolethylamine N-methyltransferase - Mus musculus (Mouse)	125	58	30068.05	INMT_MOUSE	P40936	17
26	Indolethylamine N-methyltransferase - Mus musculus (Mouse)	89	50	30068.05	INMT_MOUSE		
27	Indolethylamine N-methyltransferase - Mus musculus (Mouse)	119	52	30068.05	INMT_MOUSE		
28	Isocitrate dehydrogenase [NADP] cytoplasmic - Mus musculus (Mouse)	131	38	47029.56	IDHC_MOUSE	P70404	18
29	Isocitrate dehydrogenase [NADP], mitochondrial precursor - Mus musculus (Mouse)	123	38	59419.05	IDHP_MOUSE	O88844	19

30	Keratin, type II cytoskeletal 8 - Mus musculus (Mouse)	149	48	54531.46	K2C8_MOUSE	P11679	20
31	Keratin, type II cytoskeletal 8 - Mus musculus (Mouse)	148	48	54531.46	K2C8_MOUSE		
32	Lung carbonyl reductase [NADPH] - Mus musculus (Mouse)	96	55	26055.66	CBR2_MOUSE	Q8K354	21
33	M-calpain large subunit - Mus musculus (Mouse)	33	45	4173.06	Q920R9_MOUSE		
34	Methylcrotonoyl-CoA carboxylase beta chain, mitochondrial precursor - Mus musculus (Mouse)	166	48	61910.42	MCCC2_MOUSE	Q3ULD5	22
35	Myosin-9 - Mus musculus (Mouse)	160	25	227414.02	MYH9_MOUSE	Q8VDD5	23
36	Myosin-Ib - Mus musculus (Mouse)	93	23	129473.30	MYO1B_MOUSE	P46735	24
37	Myosin-Ic - Mus musculus (Mouse)	218	31	118880.08	MYO1C_MOUSE	Q9WTI7	25
38	Peroxiredoxin-2 - Mus musculus (Mouse)	104	51	21936.12	PRDX2_MOUSE	Q61171	26
39	Peroxiredoxin-4 - Mus musculus (Mouse)	118	53	31261.23	PRDX4_MOUSE	O08807	27
40	Plastin-3 - Mus musculus (Mouse)	131	40	70835.27	PLST_MOUSE	Q99K51	28
41	Plastin-3 - Mus musculus (Mouse)	171	39	70835.27	PLST_MOUSE		
42	Ras suppressor protein 1 - Mus musculus (Mouse)	71	25	31530.74	RSU1_MOUSE	Q01730	29
43	Retinal dehydrogenase 1 - Mus musculus (Mouse)	156	32	55060.08	AL1A1_MOUSE	P24549	30
44	Ribosomal protein L26 - Mus musculus (Mouse)	46	24	17247.53	Q5SWS8_MOUSE		
45	Ribosomal protein S3 - Mus musculus (Mouse)	45	30	26828.48	Q5YLW3_MOUSE		
46	RuvB-like 2 - Mus musculus (Mouse)	147	53	51251.59	RUVB2_MOUSE	Q9WTM5	31
47	Selenium-binding protein 1 - Mus musculus (Mouse)	149	54	53050.58	SBP1_MOUSE	Q63836	32
48	Septin-11 - Mus musculus (Mouse)	128	42	50005.44	SEP11_MOUSE	Q8C1B7	33
49	Septin-7 - Mus musculus (Mouse)	69	37	50860.03	SEPT7_MOUSE	O55131	34
50	Serum albumin precursor - Mus musculus (Mouse)	182	46	70700.48	ALBU_MOUSE	P07724	35
51	Serum albumin precursor - Mus musculus (Mouse)	261	54	70700.48	ALBU_MOUSE		
52	Trifunctional enzyme subunit alpha, mitochondrial	84	22	83275.66	ECHA_MOUSE	Q8BMS1	16
53	Tubulin beta-5 chain - Mus musculus (Mouse)	233	69	50095.14	TBB5_MOUSE	Q7TMM9	36
54	Ubiquinol-cytochrome-c reductase complex core protein 2, mitochondrial precursor - Mus musculus (Mo	60	30	48262.03	UQCR2_MOUSE	Q9DB77	37

55	Vacuolar ATP synthase catalytic subunit A - Mus musculus (Mouse)	153	47	68624.68	VATA_MOUSE	P50516	38
56	Vimentin - Mus musculus (Mouse)	163	52	53712.08	VIME_MOUSE	P20152	39
57	14-3-3 protein zeta/delta - Mus musculus (Mouse)	139	62	27924.81	1433Z_MOUSE	P62259	40

Table 1.2: mass spec analysis of a 2D gel of a DTT-eluted fraction from a lysate derived from mouse lungs. The analysis is for the proteins remaining on the affinity column after acidic elution has taken place.

Spot #	Protein species	Mascot Score	% Coverage	Protein MW	Accession	Uniprot ID	# of species
1	0 day neonate cerebellum cDNA, RIKEN full-length enriched library, clone:C230064E07 product:VIGILIN	50	19	47099.10	Q8BX68_MOUSE		
2	0 day neonate eyeball cDNA, RIKEN full-length enriched library, clone:E130303L10 product:acetyl-Coe	35	16	44425.81	Q3UPU8_MOUSE		
3	11 days embryo whole body cDNA, RIKEN full-length enriched library, clone:2700001D14 product:Hypoth	46	10	42224.17	Q3V274_MOUSE		
4	12 days embryo female mullerian duct includes surrounding region cDNA, RIKEN full-length enriched l	40	20	37475.98	Q3UXL1_MOUSE		
5	13 days embryo head cDNA, RIKEN full-length enriched library, clone:3110001F06 product:cofilin 1, n	39	27	18775.76	Q544Y7_MOUSE		
6	16 days embryo heart cDNA, RIKEN full-length enriched library, clone:I920194A06 product:cofilin 2,	32	18	18811.88	Q3UHW9_MOUSE		
7	16 days neonate cerebellum cDNA, RIKEN full-length enriched library, clone:9630058I18 product:weakl	29	20	17699.11	Q8BZ86_MOUSE		
8	182 kDa tankyrase 1-binding protein - Mus musculus (Mouse)	316	36	183025.90	TB182_MOUSE	P58871	1
9	26S proteasome non-ATPase regulatory subunit 4 - Mus musculus (Mouse)	89	36	40906.24	PSMD4_MOUSE	O35226	2
10	26S proteasome non-ATPase	64	28	24875.63	PSMD9_MOUSE	Q9CR00	3

	regulatory subunit 9 - Mus musculus (Mouse)						
11	3 days neonate thymus cDNA, RIKEN full-length enriched library, clone:A630013A09 product:KINESIN SU	30	9	64928.87	Q8BY99_MOUSE		
12	8 days embryo whole body cDNA, RIKEN full-length enriched library, clone:5730531E12 product:CHLORID	41	23	27313.68	Q9CYD1_MOUSE		
13	9.5 days embryo parthenogenote cDNA, RIKEN full-length enriched library, clone:B130044C16 product:h	44	18	54104.92	Q8BRB8_MOUSE		
14	9.5 days embryo parthenogenote cDNA, RIKEN full-length enriched library, clone:B130044C16 product:h	46	22	54104.92	Q8BRB8_MOUSE		
15	9.5 days embryo parthenogenote cDNA, RIKEN full-length enriched library, clone:B130044C16 product:h	60	15	54104.92	Q8BRB8_MOUSE		
16	9.5 days embryo parthenogenote cDNA, RIKEN full-length enriched library, clone:B130044C16 product:h	64	24	54104.92	Q8BRB8_MOUSE	Q8BRB8	4
17	9.5 days embryo parthenogenote cDNA, RIKEN full-length enriched library, clone:B130044C16 product:h	82	18	54104.92	Q8BRB8_MOUSE		
18	Acid phosphatase 1, soluble - Mus musculus (Mouse)	39	24	18636.05	Q4VAI2_MOUSE		
19	Adult male kidney cDNA, RIKEN full-length enriched library, clone:0610039M20 product:ribosomal prot	48	31	14904.63	Q6ZWZ6_MOUSE		
20	Adult male testis cDNA, RIKEN full-length enriched library, clone:4922505E06 product:calpastatin, f	50	12	47508.65	Q3TTN2_MOUSE		
21	Adult male testis cDNA, RIKEN full-length enriched library, clone:4930429C23 product:hypothetical p	27	17	29785.00	Q8CDS7_MOUSE		
22	Akap8l protein - Mus musculus (Mouse)	36	18	39279.30	Q80XE9_MOUSE		
23	A-kinase anchor protein 2 - Mus musculus (Mouse)	237	37	99089.83	AKAP2_MOUSE	O54931	5

24	A-kinase anchor protein 2 - Mus musculus (Mouse)	203	34	99089.83	AKAP2_MOUSE		
25	A-kinase anchor protein 2 - Mus musculus (Mouse)	154	24	99089.83	AKAP2_MOUSE		
26	A-kinase anchor protein 2 - Mus musculus (Mouse)	139	25	99089.83	AKAP2_MOUSE		
27	A-kinase anchor protein 2 - Mus musculus (Mouse)	129	20	99089.83	AKAP2_MOUSE		
28	Aldh1a3 protein - Mus musculus (Mouse)	34	28	18949.69	Q810V9_MOUSE		
29	Aldh1a3 protein - Mus musculus (Mouse)	37	28	18949.69	Q810V9_MOUSE		
30	Aldh1a3 protein - Mus musculus (Mouse)	38	28	18949.69	Q810V9_MOUSE		
31	Aldh1a3 protein - Mus musculus (Mouse)	30	28	18949.69	Q810V9_MOUSE		
32	Aldh1a3 protein - Mus musculus (Mouse)	32	28	18949.69	Q810V9_MOUSE		
33	Aldh1a3 protein - Mus musculus (Mouse)	31	28	18949.69	Q810V9_MOUSE		
34	Aldh1a3 protein - Mus musculus (Mouse)	30	28	18949.69	Q810V9_MOUSE		
35	Aldh1a3 protein - Mus musculus (Mouse)	27	28	18949.69	Q810V9_MOUSE		
36	Aldh1a3 protein - Mus musculus (Mouse)	32	28	18949.69	Q810V9_MOUSE		
37	Aldh1a3 protein - Mus musculus (Mouse)	39	30	18949.69	Q810V9_MOUSE		
38	Aldh1a3 protein - Mus musculus (Mouse)	39	30	18949.69	Q810V9_MOUSE		
39	Aldh1a3 protein - Mus musculus (Mouse)	37	28	18949.69	Q810V9_MOUSE		
40	Aldh1a3 protein - Mus musculus (Mouse)	38	33	18949.69	Q810V9_MOUSE		
41	Aldh1a3 protein - Mus musculus (Mouse)	32	28	18949.69	Q810V9_MOUSE		
42	Alpha-enolase - Mus musculus (Mouse)	147	41	47453.34	ENOA_MOUSE	P17182	6
43	Alpha-enolase - Mus musculus (Mouse)	65	23	47453.34	ENOA_MOUSE		
44	Annexin A2 - Mus musculus (Mouse)	151	48	38936.95	ANXA2_MOUSE	P07356	7
45	Annexin A2 - Mus musculus (Mouse)	127	46	38936.95	ANXA2_MOUSE		
46	Annexin A2 - Mus musculus (Mouse)	154	46	38936.95	ANXA2_MOUSE		
47	Annexin A2 - Mus musculus (Mouse)	134	47	38936.95	ANXA2_MOUSE		
48	Annexin A2 - Mus musculus (Mouse)	164	52	38936.95	ANXA2_MOUSE		
49	Caldesmon 1 - Mus musculus (Mouse)	67	20	60530.80	Q8VCQ8_MOUSE	Q8VCQ8	8
50	Caldesmon 1 - Mus musculus (Mouse)	114	23	60530.80	Q8VCQ8_MOUSE		

51	Caldesmon 1 - Mus musculus (Mouse)	101	19	60530.80	Q8VCQ8_MOUSE		
52	Calpastatin - Mus musculus (Mouse)	74	17	85098.73	ICAL_MOUSE	P51125	9
53	Calpastatin - Mus musculus (Mouse)	161	31	85098.73	ICAL_MOUSE		
54	Calponin-2 - Mus musculus (Mouse)	62	27	33590.21	CNN2_MOUSE	Q08093	10
55	Calponin-2 - Mus musculus (Mouse)	105	49	33590.21	CNN2_MOUSE		
56	Calponin-2 - Mus musculus (Mouse)	63	41	33590.21	CNN2_MOUSE		
57	Calponin-2 - Mus musculus (Mouse)	79	41	33590.21	CNN2_MOUSE		
58	Calponin-3 - Mus musculus (Mouse)	113	39	36576.90	CNN3_MOUSE	Q9DAW9	11
59	Calponin-3 - Mus musculus (Mouse)	96	35	36576.90	CNN3_MOUSE		
60	Calponin-3 - Mus musculus (Mouse)	59	21	36576.90	CNN3_MOUSE		
61	Capping protein - Mus musculus (Mouse)	61	19	39029.78	Q99LB4_MOUSE		
62	Carbonyl reductase 3 - Mus musculus (Mouse)	78	33	31333.07	Q8K354_MOUSE	Q8K354	12
63	Cellular nucleic acid-binding protein - Mus musculus (Mouse)	67	40	20833.08	CNBP_MOUSE	P53996	13
64	Cellular nucleic acid-binding protein - Mus musculus (Mouse)	62	33	20833.08	CNBP_MOUSE		
65	Clathrin light polypeptide - Mus musculus (Mouse)	29	17	23521.36	A2AJ56_MOUSE		
66	Cofilin-1 - Mus musculus (Mouse)	138	65	18775.76	COF1_MOUSE	P18760	14
67	Cofilin-1 - Mus musculus (Mouse)	87	48	18775.76	COF1_MOUSE		
68	Cofilin-1 - Mus musculus (Mouse)	107	48	18775.76	COF1_MOUSE		
69	Cofilin-1 - Mus musculus (Mouse)	73	26	18775.76	COF1_MOUSE		
70	CRL-1722 L5178Y-R cDNA, RIKEN full-length enriched library, clone:I730098K12 product:deoxynucleotid	28	15	37056.85	Q3THA4_MOUSE		
71	Destrin - Mus musculus (Mouse)	68	32	18851.61	DEST_MOUSE	Q9R0P5	15
72	Destrin - Mus musculus (Mouse)	59	35	18851.61	DEST_MOUSE		
73	Dihydropyrimidinase-related protein 2 - Mus musculus (Mouse)	159	35	62637.74	DPYL2_MOUSE	O08553	16
74	Dihydropyrimidinase-related protein 2 - Mus musculus (Mouse)	204	48	62637.74	DPYL2_MOUSE		
75	Dihydropyrimidinase-related	85	39	62637.74	DPYL2_MOUSE		

	protein 2 - Mus musculus (Mouse)						
76	Dstn protein - Mus musculus (Mouse)	48	38	18851.61	Q4FK36_MOUSE		
77	Dstn protein - Mus musculus (Mouse)	32	28	18851.61	Q4FK36_MOUSE		
78	Dual specificity protein phosphatase 3 - Mus musculus (Mouse)	64	40	20687.29	DUS3_MOUSE	Q9D7X3	17
79	Extracellular superoxide dismutase [Cu-Zn] precursor - Mus musculus (Mouse)	58	29	27716.81	SODE_MOUSE	O09164	18
80	Filamin-A - Mus musculus (Mouse)	58	7	283868.91	FLNA_MOUSE	Q8BTM8	19
81	Galectin-1 - Mus musculus (Mouse)	71	45	15198.33	LEG1_MOUSE	P16045	20
82	Glucocorticoid modulatory element binding protein 2 - Mus musculus (Mouse)	36	22	23370.57	A2AS07_MOUSE		
83	Glycine N-methyltransferase - Mus musculus (Mouse)	32	16	33070.48	Q5I0T9_MOUSE		
84	H2-K1 protein - Mus musculus (Mouse)	33	19	20819.69	Q66JU6_MOUSE		
85	Hemoglobin subunit beta-1 - Mus musculus (Mouse)	71	58	15944.19	HBB1_MOUSE	P02088	21
86	Heterogeneous nuclear ribonucleoprotein D0 - Mus musculus (Mouse)	73	27	38501.35	HNRPD_MOUSE	Q60668	22
87	Heterogeneous nuclear ribonucleoprotein F - Mus musculus (Mouse)	138	42	46043.04	HNRPF_MOUSE	Q9Z2X1	23
88	Heterogeneous nuclear ribonucleoprotein F - Mus musculus (Mouse)	131	42	46043.04	HNRPF_MOUSE		
89	Heterogeneous nuclear ribonucleoprotein H - Mus musculus (Mouse)	86	26	49453.50	HNRH1_MOUSE	O35737	24
90	Heterogeneous nuclear ribonucleoprotein L - Mus musculus (Mouse)	72	16	60712.34	HNRPL_MOUSE	Q8R081	25
91	Immunoglobulin-binding protein 1 - Mus musculus (Mouse)	71	23	39117.65	IGBP1_MOUSE	Q61249	26
92	In vitro fertilized eggs cDNA, RIKEN full-length enriched library, clone:7420408C23 product:heterog	37	13	19898.71	Q3UXC8_MOUSE		
93	Inorganic pyrophosphatase - Mus musculus (Mouse)	91	35	33102.33	IPYR_MOUSE	Q91VM9	27
94	Leukocyte elastase inhibitor A - Mus musculus (Mouse)	138	35	42718.83	ILEUA_MOUSE	Q9D154	28
95	LIM and SH3 domain protein 1 - Mus musculus (Mouse)	62	29	30374.46	LASP1_MOUSE	Q61792	29
96	LIM and SH3 domain protein 1 - Mus musculus (Mouse)	127	39	30374.46	LASP1_MOUSE		

97	Lymphocyte-specific protein 1 - Mus musculus (Mouse)	106	48	36805.87	LSP1_MOUSE		30
98	Melanocyte cDNA, RIKEN full-length enriched library, clone:G270138C06 product:caldesmon 1, full ins	36	15	44189.84	Q3UGC3_MOUSE		
99	MFLJ00400 protein - Mus musculus (Mouse)	28	4	68989.33	Q571H8_MOUSE		
100	Mszf77 - Mus musculus (Mouse)	33	62	3417.61	O88227_MOUSE		
101	Myl6 protein - Mus musculus (Mouse)	55	22	17121.20	Q642K0_MOUSE		
102	Myosin regulatory light chain 2, atrial isoform - Mus musculus (Mouse)	76	55	19608.63	MLRA_MOUSE	Q9QVP4	31
103	Myosin, heavy polypeptide 1, skeletal muscle, adult - Mus musculus (Mouse)	29	4	224115.73	Q32P18_MOUSE		
104	Na(+)/H(+) exchange regulatory cofactor NHE-RF2 - Mus musculus (Mouse)	96	32	37721.99	NHRF2_MOUSE	Q9JHL1	32
105	Na(+)/H(+) exchange regulatory cofactor NHE-RF2 - Mus musculus (Mouse)	173	43	37721.99	NHRF2_MOUSE		
106	Na(+)/H(+) exchange regulatory cofactor NHE-RF2 - Mus musculus (Mouse)	214	58	37721.99	NHRF2_MOUSE		
107	Na(+)/H(+) exchange regulatory cofactor NHE-RF2 - Mus musculus (Mouse)	269	66	37721.99	NHRF2_MOUSE		
108	Na(+)/H(+) exchange regulatory cofactor NHE-RF2 - Mus musculus (Mouse)	244	61	37721.99	NHRF2_MOUSE		
109	Na(+)/H(+) exchange regulatory cofactor NHE-RF2 - Mus musculus (Mouse)	174	49	37721.99	NHRF2_MOUSE		
110	Novel protein putative orthologue to human mitochondrial carrier triple repeat 6 - Mus musculus (Mo	28	21	21020.77	A2AF35_MOUSE		
111	Nucleoredoxin - Mus musculus (Mouse)	38	82	3538.83	Q5H8T6_MOUSE		
112	Osteoclast-like cell cDNA, RIKEN full-length enriched library, clone:I420020N05 product:clathrin, l	53	16	23274.25	Q3TWZ9_MOUSE		
113	Peroxiredoxin 1 - Mus musculus (Mouse)	36	22	22390.44	A2AP16_MOUSE		
114	Peroxiredoxin-1 - Mus musculus (Mouse)	145	57	22390.44	PRDX1_MOUSE		
115	Peroxiredoxin-1 - Mus musculus (Mouse)	75	49	22390.44	PRDX1_MOUSE	P35700	33
116	Peroxiredoxin-1 - Mus musculus (Mouse)	158	63	22390.44	PRDX1_MOUSE		
117	Peroxiredoxin-1 - Mus	96	44	22390.44	PRDX1_MOUSE		

	musculus (Mouse)						
118	Peroxiredoxin-2 - Mus musculus (Mouse)	73	40	21936.12	PRDX2_MOUSE	Q61171	34
119	Peroxiredoxin-4 - Mus musculus (Mouse)	61	40	31261.23	PRDX4_MOUSE	O08807	35
120	Peroxiredoxin-4 - Mus musculus (Mouse)	58	25	31261.23	PRDX4_MOUSE		
121	Peroxiredoxin-6 - Mus musculus (Mouse)	67	40	24969.02	PRDX6_MOUSE	O08709	36
122	Peroxiredoxin-6 - Mus musculus (Mouse)	149	66	24969.02	PRDX6_MOUSE		
123	Peroxiredoxin-6 - Mus musculus (Mouse)	79	56	24969.02	PRDX6_MOUSE		
124	Peroxiredoxin-6 - Mus musculus (Mouse)	172	76	24969.02	PRDX6_MOUSE		
125	Peroxiredoxin-6 - Mus musculus (Mouse)	96	45	24969.02	PRDX6_MOUSE		
126	Peroxiredoxin-6 - Mus musculus (Mouse)	87	50	24969.02	PRDX6_MOUSE		
127	Poly(rC)-binding protein 1 - Mus musculus (Mouse)	134	59	37987.14	PCBP1_MOUSE	P60335	37
128	Poly(rC)-binding protein 1 - Mus musculus (Mouse)	110	43	37987.14	PCBP1_MOUSE		
129	Predicted - Mus musculus (Mouse)	56	14	47453.34	Q5FW97_MOUSE		
130	Selenium-binding protein 1 - Mus musculus (Mouse)	80	20	53050.58	SBP1_MOUSE	P17563	38
131	Selenium-binding protein 1 - Mus musculus (Mouse)	98	40	53050.58	SBP1_MOUSE		
132	Selenium-binding protein 1 - Mus musculus (Mouse)	136	50	53050.58	SBP1_MOUSE		
133	Selenium-binding protein 1 - Mus musculus (Mouse)	288	82	53050.58	SBP1_MOUSE		
134	Selenium-binding protein 1 - Mus musculus (Mouse)	181	54	53050.58	SBP1_MOUSE		
135	Selenium-binding protein 1 - Mus musculus (Mouse)	284	75	53050.58	SBP1_MOUSE		
136	Selenium-binding protein 1 - Mus musculus (Mouse)	290	61	53050.58	SBP1_MOUSE		
137	Selenium-binding protein 1 - Mus musculus (Mouse)	309	87	53050.58	SBP1_MOUSE		
138	Selenium-binding protein 1 - Mus musculus (Mouse)	249	73	53050.58	SBP1_MOUSE		
139	Selenium-binding protein 1 - Mus musculus (Mouse)	145	60	53050.58	SBP1_MOUSE		
140	Selenium-binding protein 1 - Mus musculus (Mouse)	192	48	53050.58	SBP1_MOUSE		
141	Selenium-binding protein 1 - Mus musculus (Mouse)	189	50	53050.58	SBP1_MOUSE		
142	Selenium-binding protein 1 - Mus musculus (Mouse)	155	43	53050.58	SBP1_MOUSE		
143	Selenium-binding protein 1 - Mus musculus (Mouse)	58	13	53050.58	SBP1_MOUSE		
144	Serum albumin precursor -	113	33	70700.48	ALBU_MOUSE	P07724	39

	Mus musculus (Mouse)						
145	Serum albumin precursor - Mus musculus (Mouse)	78	23	70700.48	ALBU_MOUSE		
146	Serum albumin precursor - Mus musculus (Mouse)	225	46	70700.48	ALBU_MOUSE		
147	Serum albumin precursor - Mus musculus (Mouse)	221	42	70700.48	ALBU_MOUSE		
148	Serum albumin precursor - Mus musculus (Mouse)	113	25	70700.48	ALBU_MOUSE		
149	Serum albumin precursor - Mus musculus (Mouse)	255	52	70700.48	ALBU_MOUSE		
150	Serum albumin precursor - Mus musculus (Mouse)	170	43	70700.48	ALBU_MOUSE		
151	Src substrate cortactin - Mus musculus (Mouse)	219	43	61393.52	SRC8_MOUSE	Q60598	40
152	Src substrate cortactin - Mus musculus (Mouse)	63	18	61393.52	SRC8_MOUSE		
153	Stress-induced-phosphoprotein 1 - Mus musculus (Mouse)	97	32	63169.63	STIP1_MOUSE	Q60864	41
154	Synapse-associated protein 1 - Mus musculus (Mouse)	67	17	41381.51	SYAP1_MOUSE	Q9D5V6	42
155	Talin-1 - Mus musculus (Mouse)	114	17	271831.92	TLN1_MOUSE	P26039	43
156	Thioredoxin 1 - Mus musculus (Mouse)	44	42	12009.77	A2AV97_MOUSE		
157	Uncharacterized protein C1orf198 homolog - Mus musculus (Mouse)	95	31	35408.68	CA198_MOUSE	Q8C3W1	44
158	Uridine phosphorylase 2 - Mus musculus (Mouse)	30	14	36623.21	A2AIG1_MOUSE		
159	Vigilin - Mus musculus (Mouse)	64	8	142225.48	VIGLN_MOUSE	Q8VDJ3	45
160	Vimentin - Mus musculus (Mouse)	111	42	53712.08	VIME_MOUSE	P20152	46
161	Zinc finger protein 248 - Mus musculus (Mouse)	36	10	68338.20	Q640N4_MOUSE		
162	Zinc finger protein 248 - Mus musculus (Mouse)	41	13	68338.20	Q640N4_MOUSE		

Table 1.3: mass spec analysis of a 2D gel, of an acid-eluted fraction from lysate 1 derived from mouse skeletal muscles.

Spot #	Protein species	Mascot Score	% Coverage	Protein MW	Accession	Uniprot ID	# of species
1	10 days neonate cerebellum cDNA, RIKEN full-length enriched library, clone:6530402D11 product:hypot	30	25	12035.14	Q8C5H4_MOUSE		
2	13 days embryo male testis cDNA, RIKEN full-length	37	15	40784.43	Q8CD30_MOUSE		

	enriched library, clone:6030456D20 product:heat						
3	14 days embryo liver cDNA, RIKEN full-length enriched library, clone:4432406E13 product:zinc finger	41	70	2544.24	Q8CEE9_MOUSE		
4	15 days embryo head cDNA, RIKEN full-length enriched library, clone:D930027M19 product:NUCLEOPORIN	34	7	89621.14	Q8BUA6_MOUSE		
5	16 days embryo head cDNA, RIKEN full-length enriched library, clone:C130026O10 product:weakly simil	44	37	11570.81	Q8C4P8_MOUSE		
6	16 days neonate cerebellum cDNA, RIKEN full-length enriched library, clone:9630059H04 product:neure	27	14	17873.27	Q3V3R0_MOUSE		
7	18-day embryo whole body cDNA, RIKEN full-length enriched library, clone:1110036D22 product:hypothe	46	26	41740.31	Q9D102_MOUSE		
8	18-day embryo whole body cDNA, RIKEN full-length enriched library, clone:1110029E05 product:thiosul	34	13	33672.90	Q545S0_MOUSE		
9	9830124H08Rik protein - Mus musculus (Mouse)	41	24	27961.68	Q6PDL1_MOUSE		
10	Actin, alpha cardiac muscle 1 - Mus musculus (Mouse)	75	23	42334.01	ACTC_MOUSE	P68033	1
11	Actin, alpha cardiac muscle 1 - Mus musculus (Mouse)	65	23	42334.01	ACTC_MOUSE		
12	Actin, alpha skeletal muscle - Mus musculus (Mouse)	125	46	42365.98	ACTS_MOUSE	P68134	2
13	Actin, aortic smooth muscle - Mus musculus (Mouse)	61	15	42380.96	ACTA_MOUSE	P62737	3
14	Activated spleen cDNA, RIKEN full-length enriched library, clone:F830207J03 product:yes-associated	37	27	25090.58	Q3U046_MOUSE		
15	Activated spleen cDNA, RIKEN full-length enriched library, clone:F830207J03 product:yes-associated	36	27	25090.58	Q3U046_MOUSE		
16	Activated spleen cDNA, RIKEN full-length enriched library, clone:F830207J03 product:yes-associated	32	27	25090.58	Q3U046_MOUSE		
17	Adult male cerebellum cDNA, RIKEN full-length enriched library, clone:1520402A20	31	29	18159.84	Q8CEI4_MOUSE		

	product:hypothetic						
18	Adult male testis cDNA, RIKEN full-length enriched library, clone:4930429C23 product:hypothetical p	31	18	29785.00	Q8CDS7_MOUSE		
19	Adult male thymus cDNA, RIKEN full-length enriched library, clone:5830406G23 product:deoxynucleotid	38	11	58684.92	Q3UZ80_MOUSE		
20	Adult male tongue cDNA, RIKEN full-length enriched library, clone:2310051N24 product:myosin light c	42	21	16703.17	Q545G5_MOUSE		
21	Adult retina cDNA, RIKEN full-length enriched library, clone:A930038E24 product:hypothetical protei	38	34	17208.90	Q8C8P3_MOUSE		
22	Ahdc1 protein - Mus musculus (Mouse)	26	13	26700.08	Q8VCU7_MOUSE		
23	Aldh1a3 protein - Mus musculus (Mouse)	29	28	18949.69	Q810V9_MOUSE		
24	Aldh1a3 protein - Mus musculus (Mouse)	33	28	18949.69	Q810V9_MOUSE		
25	Aldh1a3 protein - Mus musculus (Mouse)	34	28	18949.69	Q810V9_MOUSE		
26	Aldh1a3 protein - Mus musculus (Mouse)	26	28	18949.69	Q810V9_MOUSE		
27	Aldh1a3 protein - Mus musculus (Mouse)	31	28	18949.69	Q810V9_MOUSE		
28	Aldh1a3 protein - Mus musculus (Mouse)	29	28	18949.69	Q810V9_MOUSE		
29	Aldh1a3 protein - Mus musculus (Mouse)	30	28	18949.69	Q810V9_MOUSE		
30	Aldh1a3 protein - Mus musculus (Mouse)	37	28	18949.69	Q810V9_MOUSE		
31	Aldh1a3 protein - Mus musculus (Mouse)	32	28	18949.69	Q810V9_MOUSE		
32	Aldolase 1, A isoform - Mus musculus (Mouse)	50	25	39787.45	Q5FWB7_MOUSE		
33	Aldolase 1, A isoform - Mus musculus (Mouse)	32	11	39743.43	Q6NY00_MOUSE		
34	Alpha crystallin B chain - Mus musculus (Mouse)	90	50	20056.41	CRYAB_MOUSE	P23927	4
35	Alpha crystallin B chain - Mus musculus (Mouse)	80	48	20056.41	CRYAB_MOUSE		
36	Alpha-actin - Mus musculus (Mouse)	52	24	39453.86	Q61275_MOUSE		
37	ATP synthase subunit alpha, mitochondrial precursor - Mus musculus (Mouse)	59	16	59829.63	ATPA_MOUSE	Q03265	5
38	ATP synthase subunit alpha, mitochondrial precursor - Mus musculus (Mouse)	84	16	59829.63	ATPA_MOUSE		
39	ATP synthase subunit beta, mitochondrial precursor - Mus	78	25	56265.46	ATPB_MOUSE	P56480	6

	musculus (Mouse)						
40	ATP synthase subunit beta, mitochondrial precursor - Mus musculus (Mouse)	60	22	56265.46	ATPB_MOUSE		
41	ATP synthase subunit beta, mitochondrial precursor - Mus musculus (Mouse)	191	42	56265.46	ATPB_MOUSE		
42	Beta-enolase - Mus musculus (Mouse)	62	13	47337.43	ENOB_MOUSE	P21550	7
43	Beta-enolase - Mus musculus (Mouse)	103	29	47337.43	ENOB_MOUSE		
44	Beta-enolase - Mus musculus (Mouse)	128	30	47337.43	ENOB_MOUSE		
45	Bone marrow macrophage cDNA, RIKEN full-length enriched library, clone:I830036L09 product:peroxired	36	21	22358.46	Q3U9J9_MOUSE		
46	Creatine kinase M-type - Mus musculus (Mouse)	61	25	43245.88	KCRM_MOUSE	P07310	8
47	Fructose-bisphosphate aldolase A - Mus musculus (Mouse)	70	21	39787.45	ALDOA_MOUSE	P05064	9
48	Fructose-bisphosphate aldolase A - Mus musculus (Mouse)	108	51	39787.45	ALDOA_MOUSE		
49	G patch domain and KOW motifs - Mus musculus (Mouse)	32	12	54083.43	A2AEU7_MOUSE		
50	Glyceraldehyde-3-phosphate dehydrogenase - Mus musculus (Mouse)	90	34	36072.32	G3P_MOUSE	P16858	10
51	Glyceraldehyde-3-phosphate dehydrogenase - Mus musculus (Mouse)	93	41	36072.32	G3P_MOUSE		
52	Glyceraldehyde-3-phosphate dehydrogenase - Mus musculus (Mouse)	96	41	36072.32	G3P_MOUSE		
53	Hair keratin acidic 5 - Mus musculus (Mouse)	32	6	48983.58	Q9Z2T8_MOUSE		
54	Heat-shock protein beta-1 - Mus musculus (Mouse)	89	42	23056.74	HSPB1_MOUSE	P14602	11
55	Keratin complex 1, acidic, gene 10 - Mus musculus (Mouse)	49	16	57177.78	A2A513_MOUSE		
56	LATS2B - Mus musculus (Mouse)	42	20	19476.01	Q8VHE2_MOUSE		
57	L-lactate dehydrogenase A chain - Mus musculus (Mouse)	87	27	36817.35	LDHA_MOUSE	P06151	12
58	Low-voltage-activated calcium channel alpha13.2 subunit - Mus musculus (Mouse)	31	32	12283.98	Q99P43_MOUSE		
59	NADH dehydrogenase [ubiquinone] flavoprotein 1, mitochondrial precursor - Mus	73	14	51485.97	NDUV1_MOUSE	Q91YT0	13

	musculus (Mouse)						
60	NALP12 - Mus musculus (Mouse)	38	8	83710.93	Q6UQE6_MOUSE		
61	NOD-derived CD11c +ve dendritic cells cDNA, RIKEN full-length enriched library, clone:F630103L03 pr	32	12	42883.29	Q3U3L3_MOUSE		
62	NOD-derived CD11c +ve dendritic cells cDNA, RIKEN full-length enriched library, clone:F630113L23 pr	27	9	24492.13	Q3U317_MOUSE		
63	Puromycin-sensitive aminopeptidase - Mus musculus (Mouse)	30	23	6408.20	A2A9T3_MOUSE		
64	Serine proteinase inhibitor mBM17 - Mus musculus (Mouse)	46	39	16994.47	O08799_MOUSE		
65	Succinate dehydrogenase [ubiquinone] flavoprotein subunit, mitochondrial precursor - Mus musculus (	114	24	73622.58	DHSA_MOUSE	Q8K2B3	14
66	Synaptobrevin-like protein - Mus musculus (Mouse)	32	13	25293.13	P70280_MOUSE		
67	Telokin - Mus musculus (Mouse)	39	49	7968.95	Q8CIY6_MOUSE		
68	Triosephosphate isomerase - Mus musculus (Mouse)	131	53	27037.89	TPIS_MOUSE	P17751	15
69	Type I keratin KA22 - Mus musculus (Mouse)	38	21	50444.02	Q6IFX2_MOUSE		
70	Upf3b protein - Mus musculus (Mouse)	36	16	29749.13	Q149I6_MOUSE		
71	ZFP421 - Mus musculus (Mouse)	44	22	50248.87	Q8CG23_MOUSE		

Table 1.4: mass spec analysis of a 2D gel of a DTT-eluted fraction from lysate 1 derived from mouse skeletal muscles. The analysis is for the proteins remaining on the affinity column after acidic elution has occurred.

Spot #	Protein species	Mascot Score	% Coverage	Protein MW	Accession	Uniprot ID	# of species
1	18-day embryo whole body cDNA, RIKEN full-length enriched library, clone:1110056B09 product:weakly	82	32	24405.14	Q8BK84_MOUSE	Q8BK84	1
2	60 kDa heat shock protein, mitochondrial precursor - Mus musculus (Mouse)	59	22	61088.45	CH60_MOUSE	P63038	2
3	Adenylate kinase isoenzyme 1 - Mus musculus (Mouse)	68	52	21640.16	KAD1_MOUSE	Q9R0Y5	3

4	Adenylate kinase isoenzyme 1 - Mus musculus (Mouse)	130	56	21640.16	KAD1_MOUSE		
5	Aldh1a3 protein - Mus musculus (Mouse)	28	28	18949.69	Q810V9_MOUSE		
6	Aldh1a3 protein - Mus musculus (Mouse)	37	30	18949.69	Q810V9_MOUSE		
7	Carbonic anhydrase 3 - Mus musculus (Mouse)	60	31	29632.75	CAH3_MOUSE	P16015	4
8	Creatine kinase M-type - Mus musculus (Mouse)	74	22	43245.88	KCRM_MOUSE	P07310	5
9	Creatine kinase M-type - Mus musculus (Mouse)	120	34	43245.88	KCRM_MOUSE		
10	Creatine kinase, sarcomeric mitochondrial precursor - Mus musculus (Mouse)	158	38	47899.49	KCRS_MOUSE	Q6P8J7	6
11	Creatine kinase, sarcomeric mitochondrial precursor - Mus musculus (Mouse)	156	38	47899.49	KCRS_MOUSE		
12	Crip2 protein - Mus musculus (Mouse)	53	40	23510.36	Q4FJU3_MOUSE		
13	Fbxo33 protein - Mus musculus (Mouse)	37	17	31480.00	A0JLR4_MOUSE		
14	Galectin-1 - Mus musculus (Mouse)	70	58	15198.33	LEG1_MOUSE	P16045	7
15	Galectin-1 - Mus musculus (Mouse)	65	45	15198.33	LEG1_MOUSE		
16	Glyceraldehyde-3-phosphate dehydrogenase - Mus musculus (Mouse)	93	48	36072.32	G3P_MOUSE	P16858	8
17	Glyceraldehyde-3-phosphate dehydrogenase - Mus musculus (Mouse)	98	51	36072.32	G3P_MOUSE		
18	Glyceraldehyde-3-phosphate dehydrogenase - Mus musculus (Mouse)	124	51	36072.32	G3P_MOUSE		
19	Glyceraldehyde-3-phosphate dehydrogenase - Mus musculus (Mouse)	58	40	36072.32	G3P_MOUSE		
20	Glyceraldehyde-3-phosphate dehydrogenase - Mus musculus (Mouse)	100	57	36072.32	G3P_MOUSE		
21	Glyceraldehyde-3-phosphate dehydrogenase - Mus musculus (Mouse)	106	47	36072.32	G3P_MOUSE		
22	Glyceraldehyde-3-phosphate dehydrogenase - Mus musculus (Mouse)	81	40	36072.32	G3P_MOUSE		
23	Glyceraldehyde-3-phosphate dehydrogenase - Mus musculus (Mouse)	83	36	36072.32	G3P_MOUSE		
24	Glyceraldehyde-3-phosphate dehydrogenase - Mus musculus (Mouse)	92	45	36072.32	G3P_MOUSE		
25	Glyceraldehyde-3-phosphate dehydrogenase - Mus	74	48	36072.32	G3P_MOUSE		

	musculus (Mouse)						
26	Glyceraldehyde-3-phosphate dehydrogenase - Mus musculus (Mouse)	117	49	36072.32	G3P_MOUSE		
27	Glyceraldehyde-3-phosphate dehydrogenase - Mus musculus (Mouse)	101	51	36072.32	G3P_MOUSE		
28	Glyceraldehyde-3-phosphate dehydrogenase - Mus musculus (Mouse)	76	42	36072.32	G3P_MOUSE		
29	Glyceraldehyde-3-phosphate dehydrogenase - Mus musculus (Mouse)	67	28	36072.32	G3P_MOUSE		
30	Glyceraldehyde-3-phosphate dehydrogenase - Mus musculus (Mouse)	88	45	36072.32	G3P_MOUSE		
31	Glyceraldehyde-3-phosphate dehydrogenase - Mus musculus (Mouse)	104	45	36072.32	G3P_MOUSE		
32	Glyceraldehyde-3-phosphate dehydrogenase - Mus musculus (Mouse)	97	51	36072.32	G3P_MOUSE		
33	Glyceraldehyde-3-phosphate dehydrogenase - Mus musculus (Mouse)	95	51	36072.32	G3P_MOUSE		
34	Glyceraldehyde-3-phosphate dehydrogenase - Mus musculus (Mouse)	69	30	36072.32	G3P_MOUSE		
35	Glyceraldehyde-3-phosphate dehydrogenase - Mus musculus (Mouse)	67	34	36072.32	G3P_MOUSE		
36	Glyceraldehyde-3-phosphate dehydrogenase - Mus musculus (Mouse)	85	52	36072.32	G3P_MOUSE		
37	Glyceraldehyde-3-phosphate dehydrogenase - Mus musculus (Mouse)	103	51	36072.32	G3P_MOUSE		
38	Glyceraldehyde-3-phosphate dehydrogenase - Mus musculus (Mouse)	119	42	36072.32	G3P_MOUSE		
39	Glyceraldehyde-3-phosphate dehydrogenase - Mus musculus (Mouse)	103	45	36072.32	G3P_MOUSE		
40	Glyceraldehyde-3-phosphate dehydrogenase - Mus musculus (Mouse)	89	45	36072.32	G3P_MOUSE		
41	Glyceraldehyde-3-phosphate dehydrogenase - Mus musculus (Mouse)	102	48	36072.32	G3P_MOUSE		
42	Glyceraldehyde-3-phosphate dehydrogenase - Mus musculus (Mouse)	93	45	36072.32	G3P_MOUSE		
43	Glyceraldehyde-3-phosphate dehydrogenase - Mus musculus (Mouse)	76	45	36072.32	G3P_MOUSE		

44	Glyceraldehyde-3-phosphate dehydrogenase - Mus musculus (Mouse)	90	48	36072.32	G3P_MOUSE		
45	Glyceraldehyde-3-phosphate dehydrogenase - Mus musculus (Mouse)	90	41	36072.32	G3P_MOUSE		
46	Glyceraldehyde-3-phosphate dehydrogenase - Mus musculus (Mouse)	105	51	36072.32	G3P_MOUSE		
47	Glyceraldehyde-3-phosphate dehydrogenase - Mus musculus (Mouse)	106	51	36072.32	G3P_MOUSE		
48	Glyceraldehyde-3-phosphate dehydrogenase - Mus musculus (Mouse)	58	25	36072.32	G3P_MOUSE		
49	Glyceraldehyde-3-phosphate dehydrogenase - Mus musculus (Mouse)	70	34	36072.32	G3P_MOUSE		
50	Glyceraldehyde-3-phosphate dehydrogenase - Mus musculus (Mouse)	108	45	36072.32	G3P_MOUSE		
51	M-calpain large subunit - Mus musculus (Mouse)	30	45	4173.06	Q920R9_MOUSE		
52	M-calpain large subunit - Mus musculus (Mouse)	33	45	4173.06	Q920R9_MOUSE		
53	Myomesin-1 - Mus musculus (Mouse)	100	14	186470.45	MYOM1_MOUSE	Q62234	9
54	Myosin light chain 1, skeletal muscle isoform - Mus musculus (Mouse)	105	63	20695.45	MLE1_MOUSE	P05977	10
55	Myosin regulatory light chain 2, skeletal muscle isoform - Mus musculus (Mouse)	133	70	19057.39	MLRS_MOUSE	P97457	11
56	Myosin-binding protein C, fast-type - Mus musculus (Mouse)	79	19	128127.87	MYPC2_MOUSE	Q5XKE0	12
57	Myosin-binding protein C, fast-type - Mus musculus (Mouse)	114	19	128127.87	MYPC2_MOUSE		
58	Myosin-binding protein C, fast-type - Mus musculus (Mouse)	291	38	128127.87	MYPC2_MOUSE		
59	Myosin-binding protein C, fast-type - Mus musculus (Mouse)	193	34	128127.87	MYPC2_MOUSE		
60	Myosin-binding protein C, fast-type - Mus musculus (Mouse)	82	13	128127.87	MYPC2_MOUSE		
61	Myosin-binding protein H - Mus musculus (Mouse)	115	38	53068.82	MYBPH_MOUSE	P70402	13
62	Myosin-binding protein H - Mus musculus (Mouse)	146	49	53068.82	MYBPH_MOUSE		
63	Myosin-binding protein H - Mus musculus (Mouse)	115	49	53068.82	MYBPH_MOUSE		
64	Myosin-binding protein H - Mus musculus (Mouse)	136	49	53068.82	MYBPH_MOUSE		
65	Myotilin - Mus musculus (Mouse)	173	43	55738.03	MYOTI_MOUSE	Q9JIF9	14
66	Peroxiredoxin-1 - Mus musculus (Mouse)	112	47	22390.44	PRDX1_MOUSE	P35700	15

67	Peroxiredoxin-1 - Mus musculus (Mouse)	160	63	22390.44	PRDX1_MOUSE		
68	Peroxiredoxin-1 - Mus musculus (Mouse)	83	35	22390.44	PRDX1_MOUSE		
69	Peroxiredoxin-1 - Mus musculus (Mouse)	133	58	22390.44	PRDX1_MOUSE		
70	Peroxiredoxin-1 - Mus musculus (Mouse)	161	63	22390.44	PRDX1_MOUSE		
71	Peroxiredoxin-1 - Mus musculus (Mouse)	165	63	22390.44	PRDX1_MOUSE		
72	Peroxiredoxin-1 - Mus musculus (Mouse)	130	53	22390.44	PRDX1_MOUSE		
73	Peroxiredoxin-1 - Mus musculus (Mouse)	121	53	22390.44	PRDX1_MOUSE		
74	Peroxiredoxin-2 - Mus musculus (Mouse)	95	51	21936.12	PRDX2_MOUSE	Q61171	16
75	Peroxiredoxin-6 - Mus musculus (Mouse)	153	73	24969.02	PRDX6_MOUSE		
76	Peroxiredoxin-6 - Mus musculus (Mouse)	132	57	24969.02	PRDX6_MOUSE	O08709	17
77	Peroxiredoxin-6 - Mus musculus (Mouse)	149	73	24969.02	PRDX6_MOUSE		
78	Protein DJ-1 - Mus musculus (Mouse)	88	56	20236.47	PARK7_MOUSE	Q99LX0	18
79	Thioredoxin-dependent peroxide reductase, mitochondrial precursor - Mus musculus (Mouse)	77	36	28337.49	PRDX3_MOUSE	P20108	19

Table 1.5: mass spec analysis of a 2D gel of a DTT-eluted fraction from a lysate 2 derived from mouse skeletal muscles. The analysis is for the proteins remaining on the affinity column after acidic elution.

Spot #	Protein species	Mascot Score	% Coverage	Protein MW	Accession	Uniprot ID	# of species
1	1 cell embryo 1 cell cDNA, RIKEN full-length enriched library, clone:I0C0026C19 product:hypothetica	32	21	15783.77	Q3TLD8_MOUSE		
2	13 days embryo male testis cDNA, RIKEN full-length enriched library, clone:6030400N17 product:CGMP-	31	14	32360.93	Q8BJ62_MOUSE		
3	13 days embryo male testis cDNA, RIKEN full-length enriched library, clone:6030400N17 product:CGMP-	30	14	32360.93	Q8BJ62_MOUSE		
4	15 days embryo head cDNA,	31	22	15219.59	Q3TNY2_MOUSE		

	RIKEN full-length enriched library, clone:D930049J08 product:spectrin alp						
5	17 days pregnant adult female amnion cDNA, RIKEN full-length enriched library, clone:I920038I15 pro	47	12	57406.91	Q3TGS0_MOUSE		
6	26S proteasome non-ATPase regulatory subunit 4 - Mus musculus (Mouse)	75	19	40906.24	PSMD4_MOUSE	O35226	1
7	4833405L16Rik protein - Mus musculus (Mouse)	33	19	26899.60	Q4FZF0_MOUSE		
8	60 kDa heat shock protein, mitochondrial precursor - Mus musculus (Mouse)	61	21	61088.45	CH60_MOUSE	P63038	2
9	60 kDa heat shock protein, mitochondrial precursor - Mus musculus (Mouse)	131	32	61088.45	CH60_MOUSE		
10	60 kDa heat shock protein, mitochondrial precursor - Mus musculus (Mouse)	74	22	61088.45	CH60_MOUSE		
11	6-phosphofructokinase, muscle type - Mus musculus (Mouse)	71	12	86069.88	K6PF_MOUSE	P47857	3
12	Aconitate hydratase, mitochondrial precursor - Mus musculus (Mouse)	67	15	86151.30	ACON_MOUSE	Q99KI0	4
13	Aconitate hydratase, mitochondrial precursor - Mus musculus (Mouse)	108	20	86151.30	ACON_MOUSE		
14	Aconitate hydratase, mitochondrial precursor - Mus musculus (Mouse)	136	27	86151.30	ACON_MOUSE		
15	Aconitate hydratase, mitochondrial precursor - Mus musculus (Mouse)	127	20	86151.30	ACON_MOUSE		
16	Aconitate hydratase, mitochondrial precursor - Mus musculus (Mouse)	130	25	86151.30	ACON_MOUSE		
17	Aconitate hydratase, mitochondrial precursor - Mus musculus (Mouse)	180	40	86151.30	ACON_MOUSE		
18	Aconitate hydratase, mitochondrial precursor - Mus musculus (Mouse)	151	28	86151.30	ACON_MOUSE		
19	Actin, aortic smooth muscle - Mus musculus (Mouse)	64	15	42380.96	ACTA_MOUSE	P62737	5
20	Activated spleen cDNA, RIKEN full-length enriched library, clone:F830207J03 product:yes-associated	32	20	25090.58	Q3U046_MOUSE		
21	Adult male testis cDNA, RIKEN full-length enriched library, clone:4930512B01 product:hypothetical p	34	41	12324.27	Q9D556_MOUSE		

22	Aldh1a3 protein - Mus musculus (Mouse)	30	28	18949.69	Q810V9_MOUSE		
23	Aldh1a3 protein - Mus musculus (Mouse)	30	28	18949.69	Q810V9_MOUSE		
24	Aldh1a3 protein - Mus musculus (Mouse)	35	28	18949.69	Q810V9_MOUSE		
25	Aldh1a3 protein - Mus musculus (Mouse)	35	28	18949.69	Q810V9_MOUSE		
26	ATP synthase subunit beta, mitochondrial precursor - Mus musculus (Mouse)	167	46	56265.46	ATPB_MOUSE	P56480	6
27	Beta-enolase - Mus musculus (Mouse)	93	26	47337.43	ENOB_MOUSE	P21550	7
28	Beta-enolase - Mus musculus (Mouse)	186	61	47337.43	ENOB_MOUSE		
29	Beta-enolase - Mus musculus (Mouse)	211	64	47337.43	ENOB_MOUSE		
30	Beta-taxilin - Mus musculus (Mouse)	58	13	77729.63	TXLNB_MOUSE	Q8VBT1	8
31	Bone marrow macrophage cDNA, RIKEN full-length enriched library, clone:I830001B16 product:vimentin,	62	17	47204.99	Q3UD36_MOUSE		
32	cAMP-dependent protein kinase type I-alpha regulatory subunit - Mus musculus (Mouse)	67	21	43443.14	KAP0_MOUSE	Q9DBC7	9
33	Creatine kinase M-type - Mus musculus (Mouse)	170	53	43245.88	KCRM_MOUSE	P07310	10
34	Creatine kinase, sarcomeric mitochondrial precursor - Mus musculus (Mouse)	92	25	47899.49	KCRS_MOUSE	Q6P8J7	11
35	Creatine kinase, sarcomeric mitochondrial precursor - Mus musculus (Mouse)	101	28	47899.49	KCRS_MOUSE		
36	Creatine kinase, sarcomeric mitochondrial precursor - Mus musculus (Mouse)	172	55	47899.49	KCRS_MOUSE		
37	Creatine kinase, sarcomeric mitochondrial precursor - Mus musculus (Mouse)	211	64	47899.49	KCRS_MOUSE		
38	Creatine kinase, sarcomeric mitochondrial precursor - Mus musculus (Mouse)	101	28	47899.49	KCRS_MOUSE		
39	Creatine kinase, sarcomeric mitochondrial precursor - Mus musculus (Mouse)	129	43	47899.49	KCRS_MOUSE		
40	Creatine kinase, sarcomeric mitochondrial precursor - Mus musculus (Mouse)	121	32	47899.49	KCRS_MOUSE		
41	Dehydrogenase/reductase - Mus musculus (Mouse)	38	18	35504.86	Q148Q4_MOUSE		
42	Glyceraldehyde-3-phosphate dehydrogenase - Mus	69	34	36072.32	G3P_MOUSE	P16858	12

	musculus (Mouse)						
43	Glyceraldehyde-3-phosphate dehydrogenase - Mus musculus (Mouse)	138	55	36072.32	G3P_MOUSE		
44	Glyceraldehyde-3-phosphate dehydrogenase - Mus musculus (Mouse)	128	54	36072.32	G3P_MOUSE		
45	Lethal(3)malignant brain tumor-like protein - Mus musculus (Mouse)	28	56	5938.85	Q3V555_MOUSE		
46	Low-voltage-activated calcium channel alpha13.2 subunit - Mus musculus (Mouse)	36	41	12283.98	Q99P43_MOUSE		
47	Myomesin-1 - Mus musculus (Mouse)	193	24	186470.45	MYOM1_MOUSE	Q62234	13
48	Myomesin-1 - Mus musculus (Mouse)	315	34	186470.45	MYOM1_MOUSE		
49	Myomesin-1 - Mus musculus (Mouse)	306	35	186470.45	MYOM1_MOUSE		
50	Myomesin-1 - Mus musculus (Mouse)	251	33	186470.45	MYOM1_MOUSE		
51	Myomesin-1 - Mus musculus (Mouse)	326	36	186470.45	MYOM1_MOUSE		
52	Myomesin-1 - Mus musculus (Mouse)	245	28	186470.45	MYOM1_MOUSE		
53	Myomesin-1 - Mus musculus (Mouse)	219	30	186470.45	MYOM1_MOUSE		
54	Myomesin-1 - Mus musculus (Mouse)	91	14	186470.45	MYOM1_MOUSE		
55	Myosin heavy chain IIB - Mus musculus (Mouse)	84	18	61050.65	Q9JHR4_MOUSE	Q9JHR4	14
56	Myosin-binding protein C, fast-type - Mus musculus (Mouse)	217	33	128127.87	MYPC2_MOUSE	Q5XKE0	15
57	Myosin-binding protein C, fast-type - Mus musculus (Mouse)	275	42	128127.87	MYPC2_MOUSE		
58	Myosin-binding protein C, fast-type - Mus musculus (Mouse)	150	31	128127.87	MYPC2_MOUSE		
59	Myosin-binding protein C, fast-type - Mus musculus (Mouse)	178	33	128127.87	MYPC2_MOUSE		
60	Myosin-binding protein C, fast-type - Mus musculus (Mouse)	293	39	128127.87	MYPC2_MOUSE		
61	Myosin-binding protein H - Mus musculus (Mouse)	81	29	53068.82	MYBPH_MOUSE	P70402	
62	Myosin-binding protein H - Mus musculus (Mouse)	71	14	53068.82	MYBPH_MOUSE		
63	Myosin-binding protein H - Mus musculus (Mouse)	68	14	53068.82	MYBPH_MOUSE		
64	Myosin-binding protein H - Mus musculus (Mouse)	79	28	53068.82	MYBPH_MOUSE		
65	Otc protein - Mus musculus (Mouse)	30	12	39511.45	Q8R1A8_MOUSE		
66	RAS-like family 11 member A - Mus musculus (Mouse)	31	7	27221.18	Q6IMB1_MOUSE		
67	Stress-70 protein, mitochondrial precursor - Mus	71	18	73767.84	GRP75_MOUSE	P38647	16

	musculus (Mouse)						
68	Stress-induced-phosphoprotein 1 - Mus musculus (Mouse)	132	28	63169.63	STIP1_MOUSE	Q60864	17
69	Stress-induced-phosphoprotein 1 - Mus musculus (Mouse)	212	43	63169.63	STIP1_MOUSE		
70	Stress-induced-phosphoprotein 1 - Mus musculus (Mouse)	177	37	63169.63	STIP1_MOUSE		
71	Stress-induced-phosphoprotein 1 - Mus musculus (Mouse)	97	19	63169.63	STIP1_MOUSE		
72	Thioredoxin-like 2 - Mus musculus (Mouse)	33	15	38039.48	Q5I0V8_MOUSE		
73	Zinc finger protein 52 - Mus musculus (Mouse)	37	6	83721.30	Q8VDL3_MOUSE		

Table 1.6: mass spec analysis of a 2D gel of a DTT-eluted fraction from lysate 2 (continued) derived from mouse skeletal muscles. The analysis is for the proteins remaining on the affinity column after acidic elution.

Spot #	Protein species	Mascot Score	% Coverage	Protein MW	Accession	Uniprot ID	# species
1	0 day neonate cerebellum cDNA, RIKEN full-length enriched library, clone:C230089I12 product:hypothe	43	28	14380.01	Q8C4A2_MOUSE		
2	10 days neonate skin cDNA, RIKEN full-length enriched library, clone:4732482K20 product:TITIN, HEAR	62	20	47977.68	Q8C139_MOUSE		
3	13 days embryo head cDNA, RIKEN full-length enriched library, clone:3110001F06 product:cofilin 1, n	30	21	18775.76	Q544Y7_MOUSE		
4	6430706D22Rik protein - Mus musculus (Mouse)	38	54	8161.08	Q99KB1_MOUSE		
5	Adenylate kinase isoenzyme 1 - Mus musculus (Mouse)	76	39	21640.16	KAD1_MOUSE	Q9R0Y5	1
6	Adenylate kinase isoenzyme 1 - Mus musculus (Mouse)	87	60	21640.16	KAD1_MOUSE		
7	Adenylate kinase isoenzyme 1 - Mus musculus (Mouse)	83	55	21640.16	KAD1_MOUSE		
8	Adenylate kinase isoenzyme 1 - Mus musculus (Mouse)	63	24	21640.16	KAD1_MOUSE		
9	Adenylate kinase isoenzyme 1 - Mus musculus (Mouse)	65	30	21640.16	KAD1_MOUSE		
10	Adult male diencephalon	26	21	11469.66	Q3TRY6_MOUSE		

	cDNA, RIKEN full-length enriched library, clone:9330101M15 product:hypothet						
11	Adult male hypothalamus cDNA, RIKEN full-length enriched library, clone:A230060C20 product:ubiquiti	30	7	22094.09	Q8CAH4_MOUSE		
12	Adult male urinary bladder cDNA, RIKEN full-length enriched library, clone:9530003A05 product:hypot	36	7	133509.27	Q8CBV3_MOUSE		
13	Aldh1a3 protein - Mus musculus (Mouse)	31	28	18949.69	Q810V9_MOUSE		
14	Aldh1a3 protein - Mus musculus (Mouse)	28	28	18949.69	Q810V9_MOUSE		
15	Aldh1a3 protein - Mus musculus (Mouse)	30	28	18949.69	Q810V9_MOUSE		
16	Aldh1a3 protein - Mus musculus (Mouse)	30	28	18949.69	Q810V9_MOUSE		
17	Aldh1a3 protein - Mus musculus (Mouse)	45	30	18949.69	Q810V9_MOUSE		
18	Aldh1a3 protein - Mus musculus (Mouse)	40	30	18949.69	Q810V9_MOUSE		
19	Aldh1a3 protein - Mus musculus (Mouse)	31	28	18949.69	Q810V9_MOUSE		
20	Aldh1a3 protein - Mus musculus (Mouse)	29	28	18949.69	Q810V9_MOUSE		
21	Aldh1a3 protein - Mus musculus (Mouse)	30	28	18949.69	Q810V9_MOUSE		
22	Aldh3b2 protein - Mus musculus (Mouse)	29	23	20242.26	Q497U8_MOUSE		
23	Aldolase 1, A isoform - Mus musculus (Mouse)	54	36	39787.45	Q5FWB7_MOUSE		
24	Blastocyst blastocyst cDNA, RIKEN full-length enriched library, clone:I1C0024B03 product:UPF0183 pr	27	17	26557.13	Q3TKL5_MOUSE		
25	Bone marrow macrophage cDNA, RIKEN full-length enriched library, clone:I830044A19 product:cellular	37	22	19983.72	Q3U935_MOUSE		
26	Carbonic anhydrase 3 - Mus musculus (Mouse)	59	40	29632.75	CAH3_MOUSE		
27	Carbonic anhydrase 3 - Mus musculus (Mouse)	106	41	29632.75	CAH3_MOUSE	P16015	2
28	Carbonic anhydrase 3 - Mus musculus (Mouse)	81	45	29632.75	CAH3_MOUSE		
29	Cellular nucleic acid-binding protein - Mus musculus (Mouse)	76	40	20833.08	CNBP_MOUSE	P53996	3
30	Cpsf4 protein - Mus musculus	32	30	4626.31	Q8R3L9_MOUSE		

	(Mouse)						
31	Dual specificity protein phosphatase 3 - Mus musculus (Mouse)	87	47	20687.29	DUS3_MOUSE	Q9D7X3	4
32	ES cells cDNA, RIKEN full-length enriched library, clone:2410014J02 product:myosin light chain, pho	50	31	19057.39	Q545G1_MOUSE		
33	ES cells cDNA, RIKEN full-length enriched library, clone:2410014J02 product:myosin light chain, pho	39	21	19057.39	Q545G1_MOUSE		
34	FERM domain containing 4A - Mus musculus (Mouse)	35	28	21080.99	A3KGJ1_MOUSE		
35	Galectin-1 - Mus musculus (Mouse)	80	52	15198.33	LEG1_MOUSE	P16045	5
36	Galectin-1 - Mus musculus (Mouse)	72	45	15198.33	LEG1_MOUSE		
37	Glyceraldehyde-3-phosphate dehydrogenase - Mus musculus (Mouse)	99	48	36072.32	G3P_MOUSE		
38	Glyceraldehyde-3-phosphate dehydrogenase - Mus musculus (Mouse)	62	18	36072.32	G3P_MOUSE		
39	Glyceraldehyde-3-phosphate dehydrogenase - Mus musculus (Mouse)	58	17	36072.32	G3P_MOUSE		
40	Glyceraldehyde-3-phosphate dehydrogenase - Mus musculus (Mouse)	92	41	36072.32	G3P_MOUSE		
41	Glyceraldehyde-3-phosphate dehydrogenase - Mus musculus (Mouse)	85	44	36072.32	G3P_MOUSE		
42	Glyceraldehyde-3-phosphate dehydrogenase - Mus musculus (Mouse)	105	54	36072.32	G3P_MOUSE	P16858	6
43	Glyceraldehyde-3-phosphate dehydrogenase - Mus musculus (Mouse)	72	41	36072.32	G3P_MOUSE		
44	Glyceraldehyde-3-phosphate dehydrogenase - Mus musculus (Mouse)	96	37	36072.32	G3P_MOUSE		
45	Glyceraldehyde-3-phosphate dehydrogenase - Mus musculus (Mouse)	95	42	36072.32	G3P_MOUSE		
46	Glyceraldehyde-3-phosphate dehydrogenase - Mus musculus (Mouse)	91	38	36072.32	G3P_MOUSE		
47	Glyceraldehyde-3-phosphate dehydrogenase - Mus musculus (Mouse)	82	35	36072.32	G3P_MOUSE		
48	Glycerol-3-phosphate dehydrogenase [NAD+],	140	44	38175.66	GPDA_MOUSE	P13707	7

	cytoplasmic - Mus musculus (Mouse)						
49	Hemoglobin subunit beta-1 - Mus musculus (Mouse)	72	40	15944.19	HBB1_MOUSE	P02088	8
50	Keratin 16 - Mus musculus (Mouse)	48	18	51973.48	Q3SYP5_MOUSE		
51	Mercaptopyruvate sulfurtransferase - Mus musculus (Mouse)	29	11	33246.61	Q505N7_MOUSE		
52	Myomesin-1 - Mus musculus (Mouse)	160	18	186470.45	MYOM1_MOUSE	Q62234	9
53	Myomesin-1 - Mus musculus (Mouse)	159	22	186470.45	MYOM1_MOUSE		
54	Myosin light chain 1, skeletal muscle isoform - Mus musculus (Mouse)	119	75	20695.45	MLE1_MOUSE	P05977	10
55	Myosin regulatory light chain 2, skeletal muscle isoform - Mus musculus (Mouse)	115	55	19057.39	MLRS_MOUSE	P97457	11
56	Myosin regulatory light chain 2, skeletal muscle isoform - Mus musculus (Mouse)	58	40	19057.39	MLRS_MOUSE		
57	Myosin, heavy polypeptide 1, skeletal muscle, adult - Mus musculus (Mouse)	31	5	224115.73	Q32P18_MOUSE		
58	Myosin-binding protein C, fast-type - Mus musculus (Mouse)	97	28	128127.87	MYPC2_MOUSE	Q5XKE0	12
59	Peroxiredoxin-1 - Mus musculus (Mouse)	86	41	22390.44	PRDX1_MOUSE	P35700	13
60	Peroxiredoxin-1 - Mus musculus (Mouse)	158	63	22390.44	PRDX1_MOUSE		
61	Polymerase kappa isoform 1 - Mus musculus (Mouse)	34	22	60850.15	Q5Q9H8_MOUSE		
62	Protein DJ-1 - Mus musculus (Mouse)	96	56	20236.47	PARK7_MOUSE	Q99LX0	14
63	Protein LRP16 - Mus musculus (Mouse)	72	26	35842.59	LRP16_MOUSE	Q922B1	15
64	Triosephosphate isomerase - Mus musculus (Mouse)	128	53	27037.89	TPIS_MOUSE	P17751	16
65	Triosephosphate isomerase - Mus musculus (Mouse)	108	53	27037.89	TPIS_MOUSE		
66	Triosephosphate isomerase - Mus musculus (Mouse)	118	61	27037.89	TPIS_MOUSE		
67	Triosephosphate isomerase - Mus musculus (Mouse)	104	46	27037.89	TPIS_MOUSE		
68	Troponin C, skeletal muscle - Mus musculus (Mouse)	109	50	18155.38	TNNC2_MOUSE	P20801	17
69	Troponin C, skeletal muscle - Mus musculus (Mouse)	81	40	18155.38	TNNC2_MOUSE		
70	Ttn protein - Mus musculus (Mouse)	78	24	39353.95	Q8R112_MOUSE	Q8R112	18
71	Zinc finger protein 248 - Mus musculus (Mouse)	38	17	68338.20	Q640N4_MOUSE		

Table 1.7: mass spec analysis of a 2D gel of an acid-eluted fraction from a lysate derived from mouse kidneys.

Spot #	Protein species	Score	% Coverage	Protein MW	Accession	Uniprot ID	# of species
1	14-3-3 protein epsilon - Mus musculus (Mouse)	77	34	29326.48	1433E_MOUSE	P62259	1
2	2210023G05Rik protein - Mus musculus (Mouse)	28	73	3312.91	Q8K197_MOUSE		
3	40S ribosomal protein S18 - Mus musculus (Mouse)	63	40	17707.86	RS18_MOUSE	P62270	2
4	6 days neonate head cDNA, RIKEN full-length enriched library, clone:5430417M15 product:hypothetical	48	14	85514.92	Q8C0L4_MOUSE		
5	Activated spleen cDNA, RIKEN full-length enriched library, clone:F830207J03 product:yes-associated	35	24	25090.58	Q3U046_MOUSE		
6	Aldehyde dehydrogenase, mitochondrial precursor - Mus musculus (Mouse)	145	39	57014.94	ALDH2_MOUSE	P47738	3
7	Aldehyde dehydrogenase, mitochondrial precursor - Mus musculus (Mouse)	87	20	57014.94	ALDH2_MOUSE		
8	Aldh1a3 protein - Mus musculus (Mouse)	33	32	18949.69	Q810V9_MOUSE		
9	Aldh1a3 protein - Mus musculus (Mouse)	34	32	18949.69	Q810V9_MOUSE		
10	Alpha-actinin-4 - Mus musculus (Mouse)	65	12	105367.59	ACTN4_MOUSE	P57780	4
11	Argininosuccinate synthase - Mus musculus (Mouse)	91	34	46840.12	ASSY_MOUSE	P16460	5
12	Argininosuccinate synthase - Mus musculus (Mouse)	69	15	46840.12	ASSY_MOUSE		
13	ARL-6 interacting protein-2 - Mus musculus (Mouse)	28	9	16442.39	Q9WUG4_MOUSE		
14	Aspartoacylase-2 - Mus musculus (Mouse)	74	38	35719.76	ACY3_MOUSE	Q91XE4	6
15	ATP synthase subunit beta, mitochondrial precursor - Mus musculus (Mouse)	77	25	56265.46	ATPB_MOUSE	P56480	7
16	ATP synthase subunit beta, mitochondrial precursor - Mus musculus (Mouse)	166	45	56265.46	ATPB_MOUSE		
17	ATP synthase, H+ transporting, mitochondrial F0 complex, subunit d - Mus musculus (Mouse)	56	41	18794.61	A2A8X4_MOUSE		
18	Cytidine deaminase - Mus musculus (Mouse)	85	73	16520.10	CDD_MOUSE	P56389	8
19	Dihydropyrimidinase-related protein 2 - Mus musculus	130	31	62637.74	DPYL2_MOUSE	O08553	9

	(Mouse)						
20	Dihydropyrimidinase-related protein 2 - Mus musculus (Mouse)	164	54	62637.74	DPYL2_MOUSE		
21	Eukaryotic translation initiation factor 3 subunit 2 - Mus musculus (Mouse)	83	28	36836.74	IF32_MOUSE	Q9QZD9	10
22	F-actin capping protein subunit alpha-1 - Mus musculus (Mouse)	92	51	33090.37	CAZA1_MOUSE	P47753	11
23	Histone cluster 1, H2bh - Mus musculus (Mouse)	43	51	13911.57	A2RTP6_MOUSE		
24	Histone cluster 1, H2bh - Mus musculus (Mouse)	34	35	13911.57	A2RTP6_MOUSE		
25	Hypothetical protein - Mus musculus (Mouse)	34	25	12290.56	Q8R177_MOUSE		
26	M-calpain large subunit - Mus musculus (Mouse)	30	45	4173.06	Q920R9_MOUSE		
27	M-calpain large subunit - Mus musculus (Mouse)	34	45	4173.06	Q920R9_MOUSE		
28	M-calpain large subunit - Mus musculus (Mouse)	29	45	4173.06	Q920R9_MOUSE		
29	M-calpain large subunit - Mus musculus (Mouse)	35	45	4173.06	Q920R9_MOUSE		
30	M-calpain large subunit - Mus musculus (Mouse)	35	45	4173.06	Q920R9_MOUSE		
31	M-calpain large subunit - Mus musculus (Mouse)	38	45	4173.06	Q920R9_MOUSE		
32	M-calpain large subunit - Mus musculus (Mouse)	34	45	4173.06	Q920R9_MOUSE		
33	Meprin 1 alpha - Mus musculus (Mouse)	40	11	86693.65	Q91WH9_MOUSE		
34	Methylcrotonoyl-CoA carboxylase beta chain, mitochondrial precursor - Mus musculus (Mouse)	176	46	61910.42	MCCC2_MOUSE		
35	Methylcrotonoyl-CoA carboxylase beta chain, mitochondrial precursor - Mus musculus (Mouse)	116	38	61910.42	MCCC2_MOUSE	Q3ULD5	12
36	Methylcrotonoyl-CoA carboxylase beta chain, mitochondrial precursor - Mus musculus (Mouse)	151	48	61910.42	MCCC2_MOUSE		
37	Myosin-9 - Mus musculus (Mouse)	74	10	227414.02	MYH9_MOUSE	Q8VDD5	13
38	NADH dehydrogenase [ubiquinone] iron-sulfur protein 2, mitochondrial precursor - Mus musculus (Mous	82	18	52990.80	NDUS2_MOUSE	Q91WD5	14
39	NADH-ubiquinone oxidoreductase 75 kDa subunit, mitochondrial precursor - Mus musculus	101	17	80723.93	NDUS1_MOUSE	Q91VD9	15

	(Mouse)						
40	Oxysterol binding protein 2 - Mus musculus (Mouse)	41	92	3507.68	Q5F210_MOUSE		
41	Peroxiredoxin-2 - Mus musculus (Mouse)	67	31	21936.12	PRDX2_MOUSE	Q61171	16
42	Peroxiredoxin-5, mitochondrial precursor - Mus musculus (Mouse)	62	42	22225.67	PRDX5_MOUSE	P99029	17
43	Peroxiredoxin-5, mitochondrial precursor - Mus musculus (Mouse)	108	50	22225.67	PRDX5_MOUSE		
44	Peroxiredoxin-5, mitochondrial precursor - Mus musculus (Mouse)	115	55	22225.67	PRDX5_MOUSE		
45	Peroxiredoxin-5, mitochondrial precursor - Mus musculus (Mouse)	108	45	22225.67	PRDX5_MOUSE		
46	Peroxiredoxin-5, mitochondrial precursor - Mus musculus (Mouse)	164	45	22225.67	PRDX5_MOUSE		
47	Peroxiredoxin-5, mitochondrial precursor - Mus musculus (Mouse)	160	56	22225.67	PRDX5_MOUSE		
48	Peroxiredoxin-5, mitochondrial precursor - Mus musculus (Mouse)	157	67	22225.67	PRDX5_MOUSE		
49	Peroxiredoxin-5, mitochondrial precursor - Mus musculus (Mouse)	146	55	22225.67	PRDX5_MOUSE		
50	Ppnx protein - Mus musculus (Mouse)	28	11	33504.96	Q8K3S0_MOUSE		
51	RAS-like family 11 member A - Mus musculus (Mouse)	34	7	27221.18	Q6IMB1_MOUSE		
52	RAS-like family 11 member A - Mus musculus (Mouse)	31	7	27221.18	Q6IMB1_MOUSE		
53	RAS-like family 11 member A - Mus musculus (Mouse)	29	7	27221.18	Q6IMB1_MOUSE		
54	RAS-like family 11 member A - Mus musculus (Mouse)	27	7	27221.18	Q6IMB1_MOUSE		
55	RAS-like family 11 member A - Mus musculus (Mouse)	34	7	27221.18	Q6IMB1_MOUSE		
56	RAS-like family 11 member A - Mus musculus (Mouse)	31	7	27221.18	Q6IMB1_MOUSE		
57	Septin-2 - Mus musculus (Mouse)	58	26	41727.36	SEPT2_MOUSE	P42208	18
58	Spectrin alpha chain, brain - Mus musculus (Mouse)	248	16	285220.58	SPTA2_MOUSE	P16546	19
59	Succinate dehydrogenase [ubiquinone] flavoprotein subunit, mitochondrial precursor - Mus musculus (	243	58	73622.58	DHSA_MOUSE	Q8K2B3	20
60	Succinate dehydrogenase [ubiquinone] flavoprotein subunit, mitochondrial precursor - Mus musculus (	225	52	73622.58	DHSA_MOUSE		

61	TRAV9D-3 - Mus musculus (Mouse)	39	24	12795.42	Q5R1G4_MOUSE		
62	Vacuolar ATP synthase catalytic subunit A - Mus musculus (Mouse)	205	53	68624.68	VATA_MOUSE	P50516	21
63	Vacuolar ATP synthase subunit B, brain isoform - Mus musculus (Mouse)	245	61	56856.98	VATB2_MOUSE	P62814	22

Table 1.8: mass spec analysis of a 2D gel of a DTT-eluted fraction from a lysate derived from mouse kidneys. The analysis is for the proteins remaining on the affinity column after acidic elution.

Spot #	Protein species	Score	% Coverage	Protein MW	Accession	Uniprot ID	# of species
1	0 day neonate cerebellum cDNA, RIKEN full-length enriched library, clone:C230058P07 product:cell di	31	27	12748.55	Q3TQ50_MOUSE		
2	10 days neonate cortex cDNA, RIKEN full-length enriched library, clone:A830014I19 product:weakly si	35	11	88533.14	Q8BLR8_MOUSE		
3	10-formyltetrahydrofolate dehydrogenase - Mus musculus (Mouse)	72	9	99501.84	FTHFD_MOUSE	Q8R0Y6	1
4	11 days embryo whole body cDNA, RIKEN full-length enriched library, clone:2700084K13 product:annexi	49	25	38926.90	Q9CZI7_MOUSE		
5	13 days embryo heart cDNA, RIKEN full-length enriched library, clone:D330037K14 product:cadherin 16	38	9	86851.68	Q3TPA4_MOUSE		
6	13 days embryo male testis cDNA, RIKEN full-length enriched library, clone:6030400N17 product:CGMP-	37	14	32360.93	Q8BJ62_MOUSE		
7	2810051F02Rik protein - Mus musculus (Mouse)	39	33	12483.39	Q91VT2_MOUSE		
8	3-hydroxyanthranilate 3,4-dioxygenase - Mus musculus (Mouse)	158	57	32954.63	3HAO_MOUSE	Q78JT3	2
9	3-hydroxyanthranilate 3,4-dioxygenase - Mus musculus (Mouse)	166	54	32954.63	3HAO_MOUSE		
10	3-hydroxyanthranilate 3,4-dioxygenase - Mus musculus (Mouse)	130	50	32954.63	3HAO_MOUSE		

11	40S ribosomal protein S12 - Mus musculus (Mouse)	66	34	14857.68	RS12_MOUSE	P63323	3
12	60 kDa heat shock protein, mitochondrial precursor - Mus musculus (Mouse)	100	42	61088.45	CH60_MOUSE	P63038	4
13	Abca7 protein - Mus musculus (Mouse)	28	14	34187.76	Q8R1I3_MOUSE		
14	Acetyl-coenzyme A synthetase 2-like, mitochondrial precursor - Mus musculus (Mouse)	89	13	75317.07	ACS2L_MOUSE	Q99NB1	5
15	Acid phosphatase 1, soluble - Mus musculus (Mouse)	35	24	18636.05	Q4VAI2_MOUSE		
16	Aconitate hydratase, mitochondrial precursor - Mus musculus (Mouse)	121	18	86151.30	ACON_MOUSE	Q99KI0	6
17	Activated spleen cDNA, RIKEN full-length enriched library, clone:F830207J03 product:yes-associated	36	20	25090.58	Q3U046_MOUSE		
18	Adenylate kinase isoenzyme 1 - Mus musculus (Mouse)	69	39	21640.16	KAD1_MOUSE	Q9R0Y5	7
19	Adult male cerebellum cDNA, RIKEN full-length enriched library, clone:1500019E20 product:hypothetic	107	63	28412.37	Q9DB29_MOUSE	Q9DB29	8
20	Adult male corpora quadrigemina cDNA, RIKEN full-length enriched library, clone:B230213G02 product:	32	12	24908.50	Q8BR60_MOUSE		
21	Adult male corpora quadrigemina cDNA, RIKEN full-length enriched library, clone:B230314C10 product:	33	30	14356.03	Q3USS7_MOUSE		
22	Adult male corpora quadrigemina cDNA, RIKEN full-length enriched library, clone:B230314C10 product:	40	39	14356.03	Q3USS7_MOUSE		
23	Adult male kidney cDNA, RIKEN full-length enriched library, clone:F530014F22 product:hypothetical G	29	27	15835.84	Q3UNU4_MOUSE		
24	Adult male liver tumor cDNA, RIKEN full-length enriched library, clone:C730013P19 product:heat shoc	45	12	56971.78	Q3UEM8_MOUSE		
25	Adult male testis cDNA, RIKEN full-length enriched library, clone:4922503G09 product:down-regulated	35	22	42230.41	Q3TTP7_MOUSE		
26	Aldh1a3 protein - Mus musculus (Mouse)	34	28	18949.69	Q810V9_MOUSE		
27	Aldh1a3 protein - Mus musculus (Mouse)	31	28	18949.69	Q810V9_MOUSE		
28	Aldh1a3 protein - Mus musculus (Mouse)	30	28	18949.69	Q810V9_MOUSE		

29	Aldh1a3 protein - Mus musculus (Mouse)	41	30	18949.69	Q810V9_MOUSE		
30	Aldh1a3 protein - Mus musculus (Mouse)	30	28	18949.69	Q810V9_MOUSE		
31	Aldh1a3 protein - Mus musculus (Mouse)	29	28	18949.69	Q810V9_MOUSE		
32	Aldh1a3 protein - Mus musculus (Mouse)	28	28	18949.69	Q810V9_MOUSE		
33	Alpha-enolase - Mus musculus (Mouse)	107	38	47453.34	ENOA_MOUSE	P17182	9
34	Alpha-enolase - Mus musculus (Mouse)	70	22	47453.34	ENOA_MOUSE		
35	Amine N-sulfotransferase - Mus musculus (Mouse)	113	53	35247.52	O35401_MOUSE	Q3UZZ6	10
36	Annexin A2 - Mus musculus (Mouse)	97	36	38936.95	ANXA2_MOUSE	P07356	11
37	Annexin A2 - Mus musculus (Mouse)	80	34	38936.95	ANXA2_MOUSE		
38	Aspartoacylase - Mus musculus (Mouse)	115	43	35777.96	ACY2_MOUSE	Q8R3P0	12
39	BC066135 protein - Mus musculus (Mouse)	26	23	18540.61	Q6NZH2_MOUSE		
40	Calcium/calmodulin-dependent serine protein kinase - Mus musculus (Mouse)	31	19	12768.50	A2ADQ1_MOUSE		
41	Cellular nucleic acid-binding protein - Mus musculus (Mouse)	66	40	20833.08	CNBP_MOUSE	P53996	13
42	Clathrin light polypeptide - Mus musculus (Mouse)	35	17	23521.36	A2AJ56_MOUSE		
43	Cofilin-1 - Mus musculus (Mouse)	92	34	18775.76	COF1_MOUSE	P18760	14
44	Cofilin-1 - Mus musculus (Mouse)	128	62	18775.76	COF1_MOUSE		
45	Copper chaperone for superoxide dismutase - Mus musculus (Mouse)	60	36	29463.62	CCS_MOUSE	Q9WU84	15
46	Cytidine deaminase - Mus musculus (Mouse)	82	74	16520.10	CDD_MOUSE	P56389	16
47	Dcpp1 protein - Mus musculus (Mouse)	36	28	18591.23	Q64097_MOUSE		
48	Dcpp1 protein - Mus musculus (Mouse)	28	28	18591.23	Q64097_MOUSE		
49	Dcpp1 protein - Mus musculus (Mouse)	32	28	18591.23	Q64097_MOUSE		
50	Destrin - Mus musculus (Mouse)	58	29	18851.61	DEST_MOUSE	Q9R0P5	17
51	Destrin - Mus musculus (Mouse)	63	29	18851.61	DEST_MOUSE		
52	Dihydropyrimidinase-related protein 2 - Mus musculus (Mouse)	180	37	62637.74	DPYL2_MOUSE	O08553	18
53	Dystrophin - Mus musculus (Mouse)	34	30	24726.51	Q9R0A2_MOUSE		
54	Elongation factor Tu, mitochondrial precursor - Mus musculus (Mouse)	139	30	49876.12	EFTU_MOUSE	Q8BFR5	19

55	Elongation factor Tu, mitochondrial precursor - Mus musculus (Mouse)	73	18	49876.12	EFTU_MOUSE		
56	ERO1-like protein alpha precursor - Mus musculus (Mouse)	102	30	54802.47	ERO1A_MOUSE	Q8R180	20
57	ERO1-like protein alpha precursor - Mus musculus (Mouse)	105	28	54802.47	ERO1A_MOUSE		
58	ES cells cDNA, RIKEN full-length enriched library, clone:2410004D02 product:similar to SERINE/THREO	28	14	43034.92	Q9CWU3_MOUSE		
59	Ezrin-radixin-moesin-binding phosphoprotein 50 - Mus musculus (Mouse)	72	25	38861.65	NHERF_MOUSE	P70441	21
60	Ezrin-radixin-moesin-binding phosphoprotein 50 - Mus musculus (Mouse)	69	27	38861.65	NHERF_MOUSE		
61	Ezrin-radixin-moesin-binding phosphoprotein 50 - Mus musculus (Mouse)	65	28	38861.65	NHERF_MOUSE		
62	Ezrin-radixin-moesin-binding phosphoprotein 50 - Mus musculus (Mouse)	109	38	38861.65	NHERF_MOUSE		
63	Ezrin-radixin-moesin-binding phosphoprotein 50 - Mus musculus (Mouse)	90	34	38861.65	NHERF_MOUSE		
64	Heat shock protein 84b - Mus musculus (Mouse)	46	5	83571.24	Q71LX8_MOUSE		
65	Hemoglobin subunit beta-1 - Mus musculus (Mouse)	120	73	15944.19	HBB1_MOUSE	P02088	22
66	Hemoglobin subunit beta-2 - Mus musculus (Mouse)	121	65	15982.30	HBB2_MOUSE	P02089	23
67	Heterogeneous nuclear ribonucleoprotein A3 - Mus musculus (Mouse)	102	25	39855.69	ROA3_MOUSE	Q8BG05	24
68	Heterogeneous nuclear ribonucleoprotein A3 - Mus musculus (Mouse)	107	30	39855.69	ROA3_MOUSE		
69	Heterogeneous nuclear ribonucleoprotein K - Mus musculus (Mouse)	78	26	51229.51	HNRPK_MOUSE	P61979	25
70	Inorganic pyrophosphatase - Mus musculus (Mouse)	138	70	33102.33	IPYR_MOUSE	Q9D819	26
71	Inorganic pyrophosphatase 2, mitochondrial precursor - Mus musculus (Mouse)	134	68	38546.32	IPYR2_MOUSE	Q91VM9	27
72	Inorganic pyrophosphatase 2, mitochondrial precursor - Mus musculus (Mouse)	99	40	38546.32	IPYR2_MOUSE		
73	Inorganic pyrophosphatase 2, mitochondrial precursor - Mus musculus (Mouse)	233	75	38546.32	IPYR2_MOUSE		

74	Interleukin 15 receptor alpha chain isoform 2D - Mus musculus (Mouse)	42	42	11211.70	Q810T6_MOUSE		
75	Leukocyte elastase inhibitor A - Mus musculus (Mouse)	95	27	42718.83	ILEUA_MOUSE	Q9D154	28
76	Leukocyte elastase inhibitor A - Mus musculus (Mouse)	147	32	42718.83	ILEUA_MOUSE		
77	Low-voltage-activated calcium channel alpha13.2 subunit - Mus musculus (Mouse)	42	41	12283.98	Q99P43_MOUSE		
78	Lung RCB-0558 LLC cDNA, RIKEN full-length enriched library, clone:G730038B15 product:similar to Msz	41	16	68198.96	Q3UML8_MOUSE		
79	Meprin 1 alpha - Mus musculus (Mouse)	50	15	86693.65	Q91WH9_MOUSE		
80	Meprin A subunit alpha precursor - Mus musculus (Mouse)	69	12	85226.89	MEP1A_MOUSE	P28825	29
81	Mitochondrial inner membrane protein - Mus musculus (Mouse)	80	13	84247.35	IMMT_MOUSE	Q8CAQ8	30
82	Mitochondrial inner membrane protein - Mus musculus (Mouse)	157	29	84247.35	IMMT_MOUSE		
83	NIMA - Mus musculus (Mouse)	32	100	4423.07	A2ATP0_MOUSE		
84	NOD-derived CD11c +ve dendritic cells cDNA, RIKEN full-length enriched library, clone:F630006F12 pr	36	22	33614.01	Q3TDV6_MOUSE		
85	Nucleoside diphosphate-linked moiety X motif 19 - Mus musculus (Mouse)	64	16	40798.59	NUD19_MOUSE	P11930	31
86	Nucleoside diphosphate-linked moiety X motif 19 - Mus musculus (Mouse)	94	50	40798.59	NUD19_MOUSE		
87	Nucleoside diphosphate-linked moiety X motif 19 - Mus musculus (Mouse)	113	47	40798.59	NUD19_MOUSE		
88	Nucleoside diphosphate-linked moiety X motif 19 - Mus musculus (Mouse)	121	50	40798.59	NUD19_MOUSE		
89	Nucleoside diphosphate-linked moiety X motif 19 - Mus musculus (Mouse)	72	22	40798.59	NUD19_MOUSE		
90	Osteoclast-like cell cDNA, RIKEN full-length enriched library, clone:I420027B09 product:fibulin 1,	36	13	82114.18	Q3TWK8_MOUSE		
91	Osteoclast-like cell cDNA, RIKEN full-length enriched library, clone:I420031B14 product:Weakly simi	212	32	57318.99	Q3TW96_MOUSE	Q3TW96	32
92	Patched homolog 1 splice variant 1B - Mus musculus (Mouse)	20	62	2565.30	Q5TLE8_MOUSE		
93	PDZ domain-containing protein 1 - Mus musculus (Mouse)	65	19	56862.78	PDZD1_MOUSE	Q9JIL4	33
94	PDZ domain-containing protein 1	72	34	56862.78	PDZD1_MOUSE		

	- Mus musculus (Mouse)						
95	Peptide methionine sulfoxide reductase - Mus musculus (Mouse)	88	59	26199.91	MSRA_MOUSE	Q9D6Y7	34
96	Peptide methionine sulfoxide reductase - Mus musculus (Mouse)	118	62	26199.91	MSRA_MOUSE		
97	Peptide methionine sulfoxide reductase - Mus musculus (Mouse)	88	68	26199.91	MSRA_MOUSE		
98	Peptide methionine sulfoxide reductase - Mus musculus (Mouse)	97	62	26199.91	MSRA_MOUSE		
99	Peptide methionine sulfoxide reductase - Mus musculus (Mouse)	114	72	26199.91	MSRA_MOUSE		
100	Peripheral myelin protein 2 - Mus musculus (Mouse)	30	22	15039.95	Q4KL10_MOUSE		
101	Peroxiredoxin 1 - Mus musculus (Mouse)	42	18	19085.78	A2AP14_MOUSE		
102	Peroxiredoxin 1 - Mus musculus (Mouse)	28	12	19085.78	A2AP14_MOUSE		
103	Peroxiredoxin-1 - Mus musculus (Mouse)	98	53	22390.44	PRDX1_MOUSE	P35700	35
104	Peroxiredoxin-1 - Mus musculus (Mouse)	161	67	22390.44	PRDX1_MOUSE		
105	Peroxiredoxin-1 - Mus musculus (Mouse)	91	49	22390.44	PRDX1_MOUSE		
106	Peroxiredoxin-1 - Mus musculus (Mouse)	78	35	22390.44	PRDX1_MOUSE		
107	Peroxiredoxin-1 - Mus musculus (Mouse)	141	59	22390.44	PRDX1_MOUSE		
108	Peroxiredoxin-1 - Mus musculus (Mouse)	96	40	22390.44	PRDX1_MOUSE		
109	Peroxiredoxin-1 - Mus musculus (Mouse)	115	48	22390.44	PRDX1_MOUSE		
110	Peroxiredoxin-1 - Mus musculus (Mouse)	92	41	22390.44	PRDX1_MOUSE		
111	Peroxiredoxin-1 - Mus musculus (Mouse)	157	67	22390.44	PRDX1_MOUSE		
112	Peroxiredoxin-1 - Mus musculus (Mouse)	131	63	22390.44	PRDX1_MOUSE		
113	Peroxiredoxin-1 - Mus musculus (Mouse)	154	67	22390.44	PRDX1_MOUSE		
114	Peroxiredoxin-1 - Mus musculus (Mouse)	143	67	22390.44	PRDX1_MOUSE		
115	Peroxiredoxin-1 - Mus musculus (Mouse)	170	67	22390.44	PRDX1_MOUSE		
116	Peroxiredoxin-1 - Mus musculus (Mouse)	162	63	22390.44	PRDX1_MOUSE		
117	Peroxiredoxin-1 - Mus musculus (Mouse)	154	63	22390.44	PRDX1_MOUSE		
118	Peroxiredoxin-1 - Mus musculus (Mouse)	159	67	22390.44	PRDX1_MOUSE		

119	Peroxiredoxin-1 - Mus musculus (Mouse)	177	67	22390.44	PRDX1_MOUSE		
120	Peroxiredoxin-1 - Mus musculus (Mouse)	175	67	22390.44	PRDX1_MOUSE		
121	Peroxiredoxin-1 - Mus musculus (Mouse)	180	63	22390.44	PRDX1_MOUSE		
122	Peroxiredoxin-2 - Mus musculus (Mouse)	58	22	21936.12	PRDX2_MOUSE	Q61171	36
123	Peroxiredoxin-2 - Mus musculus (Mouse)	68	45	21936.12	PRDX2_MOUSE		
124	Peroxiredoxin-2 - Mus musculus (Mouse)	99	55	21936.12	PRDX2_MOUSE		
125	Peroxiredoxin-2 - Mus musculus (Mouse)	73	36	21936.12	PRDX2_MOUSE		
126	Peroxiredoxin-2 - Mus musculus (Mouse)	67	24	21936.12	PRDX2_MOUSE		
127	Peroxiredoxin-4 - Mus musculus (Mouse)	129	63	31261.23	PRDX4_MOUSE	O08807	37
128	Peroxiredoxin-5, mitochondrial precursor - Mus musculus (Mouse)	102	37	22225.67	PRDX5_MOUSE	P99029	38
129	Peroxiredoxin-5, mitochondrial precursor - Mus musculus (Mouse)	58	24	22225.67	PRDX5_MOUSE		
130	Peroxiredoxin-5, mitochondrial precursor - Mus musculus (Mouse)	116	45	22225.67	PRDX5_MOUSE		
131	Peroxiredoxin-5, mitochondrial precursor - Mus musculus (Mouse)	147	46	22225.67	PRDX5_MOUSE		
132	Peroxiredoxin-5, mitochondrial precursor - Mus musculus (Mouse)	147	45	22225.67	PRDX5_MOUSE		
133	Peroxiredoxin-6 - Mus musculus (Mouse)	104	66	24969.02	PRDX6_MOUSE	O08709	39
134	Peroxiredoxin-6 - Mus musculus (Mouse)	100	52	24969.02	PRDX6_MOUSE		
135	Peroxiredoxin-6 - Mus musculus (Mouse)	95	45	24969.02	PRDX6_MOUSE		
136	Peroxiredoxin-6 - Mus musculus (Mouse)	69	27	24969.02	PRDX6_MOUSE		
137	Peroxisomal bifunctional enzyme - Mus musculus (Mouse)	77	15	78764.23	ECHP_MOUSE	Q9DBM2	40
138	Prdx2 protein - Mus musculus (Mouse)	37	22	21948.16	Q5M9N9_MOUSE		
139	Prdx2 protein - Mus musculus (Mouse)	43	22	21948.16	Q5M9N9_MOUSE		
140	Probable D-lactate dehydrogenase, mitochondrial precursor - Mus musculus (Mouse)	192	54	52499.42	LDHD_MOUSE	Q7TNG8	41
141	Probable D-lactate dehydrogenase, mitochondrial precursor - Mus musculus (Mouse)	96	32	52499.42	LDHD_MOUSE		

142	Probable D-lactate dehydrogenase, mitochondrial precursor - Mus musculus (Mouse)	187	55	52499.42	LDHD_MOUSE		
143	Probable D-lactate dehydrogenase, mitochondrial precursor - Mus musculus (Mouse)	116	32	52499.42	LDHD_MOUSE		
144	Probable D-lactate dehydrogenase, mitochondrial precursor - Mus musculus (Mouse)	79	21	52499.42	LDHD_MOUSE		
145	Probable D-lactate dehydrogenase, mitochondrial precursor - Mus musculus (Mouse)	116	23	52499.42	LDHD_MOUSE		
146	Probable D-lactate dehydrogenase, mitochondrial precursor - Mus musculus (Mouse)	122	26	52499.42	LDHD_MOUSE		
147	RIKEN cDNA D330038O06 gene - Mus musculus (Mouse)	35	10	62350.26	Q6PGD2_MOUSE		
148	Selenium-binding protein 1 - Mus musculus (Mouse)	115	39	53050.58	SBP1_MOUSE		
149	Selenium-binding protein 1 - Mus musculus (Mouse)	110	23	53050.58	SBP1_MOUSE		
150	Selenium-binding protein 1 - Mus musculus (Mouse)	60	11	53050.58	SBP1_MOUSE		
151	Selenium-binding protein 1 - Mus musculus (Mouse)	259	82	53050.58	SBP1_MOUSE		
152	Selenium-binding protein 1 - Mus musculus (Mouse)	270	81	53050.58	SBP1_MOUSE		
153	Selenium-binding protein 1 - Mus musculus (Mouse)	314	62	53050.58	SBP1_MOUSE	P17563	42
154	Selenium-binding protein 1 - Mus musculus (Mouse)	167	32	53050.58	SBP1_MOUSE		
155	Selenium-binding protein 1 - Mus musculus (Mouse)	95	21	53050.58	SBP1_MOUSE		
156	Selenium-binding protein 1 - Mus musculus (Mouse)	214	47	53050.58	SBP1_MOUSE		
157	Selenium-binding protein 1 - Mus musculus (Mouse)	212	48	53050.58	SBP1_MOUSE		
158	Selenium-binding protein 1 - Mus musculus (Mouse)	173	44	53050.58	SBP1_MOUSE		
159	Selenium-binding protein 2 - Mus musculus (Mouse)	78	20	53146.59	SBP2_MOUSE	Q63836	43
160	Stress-70 protein, mitochondrial precursor - Mus musculus (Mouse)	112	27	73767.84	GRP75_MOUSE	P38647	44
161	Succinate dehydrogenase complex, subunit B, iron sulfur - Mus musculus (Mouse)	56	35	32591.19	A2AA77_MOUSE		
162	Synapse-associated protein 1 - Mus musculus (Mouse)	76	17	41381.51	SYAP1_MOUSE	Q9D5V6	45
163	Synapse-associated protein 1 -	80	22	41381.51	SYAP1_MOUSE		

	Mus musculus (Mouse)						
164	Thioredoxin domain-containing protein 4 precursor - Mus musculus (Mouse)	97	35	47222.45	TXND4_MOUSE	Q9D1Q6	46
165	Thioredoxin-dependent peroxide reductase, mitochondrial precursor - Mus musculus (Mouse)	76	44	28337.49	PRDX3_MOUSE	P20108	47
166	Thioredoxin-dependent peroxide reductase, mitochondrial precursor - Mus musculus (Mouse)	61	36	28337.49	PRDX3_MOUSE		
167	Tubulin alpha-4A chain - Mus musculus (Mouse)	138	41	50633.65	TBA4A_MOUSE	P68368	48
168	Twinfilin-1 - Mus musculus (Mouse)	86	33	40282.56	TWF1_MOUSE	Q91YR1	49
169	Twinfilin-1 - Mus musculus (Mouse)	92	35	40282.56	TWF1_MOUSE		
170	Wiscott-Aldrich Syndrome protein homolog - Mus musculus (Mouse)	39	10	54568.45	Q61078_MOUSE		
171	Ywhaq protein - Mus musculus (Mouse)	50	28	28045.89	A3KML3_MOUSE		

Table 1.9: mass spec analysis of a 2D gel of an acid-eluted fraction from a mitochondrial lysate from mouse brains.

Spot #	Protein species	Protein MW	Mascot Score	% Coverage	Accession	Uniprot ID	# of species
3	ATP synthase subunit alpha, mitochondrial	59830	79	29	ATPA_MOUSE	Q03265	1
4	ATP synthase subunit alpha, mitochondrial	59830	92	34	ATPA_MOUSE		
5	ATP synthase subunit alpha, mitochondrial	59830	199	55	ATPA_MOUSE		
6	ATP synthase subunit alpha, mitochondrial	59830	228	58	ATPA_MOUSE		
7	ATP synthase subunit alpha, mitochondrial	59830	41	20	ATPA_MOUSE		
8	ATP synthase subunit beta, mitochondrial	56265	216	64	ATPB_MOUSE	P564804	2
9	ATP synthase subunit d, mitochondrial	18795	66	63	ATP5H_MOUSE	Q9DCX2	3
10	Cytochrome b-c1 complex subunit Rieske, mitochondrial	53446	47	27	UCRI_MOUSE	Q9CR68	4
20	Glyceraldehyde-3-phosphate dehydrogenase	36072	152	50	G3P_MOUSE	P16858	5
21	Glyceraldehyde-3-phosphate dehydrogenase	36072	110	56	G3P_MOUSE		

26	Isocitrate dehydrogenase [NAD] subunit gamma 1, mitochondrial	43157	42	25	IDHG1_MOUSE	P70404	6
27	NADH dehydrogenase [ubiquinone] iron-sulfur protein 2, mitochondrial	52991	51	25	NDUS2_MOUSE	Q91WD5	7
28	NADH dehydrogenase [ubiquinone] iron-sulfur protein 3, mitochondrial	30302	161	60	NDUS3_MOUSE	Q9DCT2	8
29	Pyruvate dehydrogenase E1 component subunit beta, mitochondrial	39254	90	47	ODPB_MOUSE	Q9D051	9

Table 1.10: mass spec analysis of a 2D gel of a DTT-eluted fraction from a mitochondrial lysate from mouse brains. The analysis is for the proteins remaining on the affinity column immediately after acidic elution took place.

Spot #	Protein species	Protein MW	Mascot Score	% Coverage	Accession	Uniprot ID	# of species
10	ATP synthase subunit alpha, mitochondrial	59830	184	55	ATPA_MOUSE	Q03265	1
11	ATP synthase subunit beta, mitochondrial	56265	108	57	ATPB_MOUSE	P564804	2
12	ATP synthase subunit beta, mitochondrial	56265	158	67	ATPB_MOUSE		
13	ATP synthase subunit d, mitochondrial	18795	51	54	ATP5H_MOUSE	Q9DCX2	3
16	Cytochrome b-c1 complex subunit 1, mitochondrial	53446	132	37	UCRI_MOUSE	Q9CR68	4
20	Glyceraldehyde-3-phosphate dehydrogenase	36072	76	33	G3P_MOUSE	P16858	5
21	Glyceraldehyde-3-phosphate dehydrogenase	36072	132	43	G3P_MOUSE		
22	Glyceraldehyde-3-phosphate dehydrogenase	36072	109	41	G3P_MOUSE		
25	Isocitrate dehydrogenase [NAD] subunit alpha, mitochondrial	40069	50	26	IDH3A_MOUSE	Q9D6R2	6
26	Peroxiredoxin-1	22390	103	57	PRDX1_MOUSE	P35700	7
27	Peroxiredoxin-1	22390	185	74	PRDX1_MOUSE		
28	Peroxiredoxin-2	21936	121	53	PRDX2_MOUSE	Q61171	8
29	Peroxiredoxin-4	31261	55	30	PRDX4_MOUSE	O08807	9
30	Peroxiredoxin-6	24969	36	24	PRDX6_MOUSE	O08709	10
31	Pyruvate dehydrogenase E1 component subunit beta, mitochondrial	39254	150	64	ODPB_MOUSE	Q9D051	11

Table 1.11: mass spec analysis of a 1D gel of an acid-eluted fraction from a mitochondrial lysate derived from mouse hearts.

Band #	Protein species	Accession	Uniprot ID	Mascot Score	% Coverage	Protein MW	# of species
1	ATP synthase subunit alpha, mitochondrial OS=Mus musculus GN	ATPA_MOUSE	Q03265	339	37	59716.00	1
2	Klra19 protein OS=Mus musculus GN=Klra19 PE=2 SV=1	Q9JHV3_MOUSE	Q9JHV3	37	31	31070.00	2
3	Ldhb protein OS=Mus musculus GN=Ldhb PE=2 SV=1	Q5M8R7_MOUSE	Q5M8R7	33	48	11317.00	3
4	NADH dehydrogenase [ubiquinone] 1 alpha subcomplex subunit 4	NDUA4_MOUSE	Q62425	46	24	9321.00	4
5	NADH-ubiquinone oxidoreductase 75 kDa subunit, mitochondrial	NDUS1_MOUSE	Q91VD9	132	18	79698.00	5
6	Nesprin-2 OS=Mus musculus GN=Syne2 PE=1 SV=2	SYNE2_MOUSE	Q6ZWQ0	56	4	782238.00	6

Table 1.12: mass spec analysis of a 1D gel of a DTT-eluted fraction fraction from a mitochondrial lysate derived from mouse hearts. The analysis is for the proteins remaining on the affinity column after acidic elution.

Band #	Protein species	Accession	Uniprot ID	Mascot Score	% Coverage	Protein MW	# of species
1	ATP synthase subunit beta, mitochondrial OS=Mus musculus GN=	ATPB_MOUSE	P56480	67	23	56265.00	1
2	Edem3 protein (Fragment) OS=Mus musculus GN=Edem3 PE=2 SV=1	Q8R1X5_MOUSE	Q8R1X5	33	35	6066.00	2
3	Keratin 15 OS=Mus musculus GN=Krt15 PE=3 SV=1	B1AQ77_MOUSE	B1AQ77	35	18	49463.00	3
4	Putative uncharacterized protein (Fragment) OS=Mus musculus	Q3UWR0_MOUSE	Q3UWR0	39	36	21988.00	4
5	Putative uncharacterized protein OS=Mus musculus GN=Zfp809 P	Q8BIL4_MOUSE	Q8BIL4	33	33	19729.00	5
6	Rac GTPase-activating protein 1	E9Q851_MOUSE	E9Q851	34	41	15467.00	6

Table 1.13: mass spec analysis of a 1D gel of a DTT-eluted fraction from a mitochondrial lysate derived from mouse skeletal muscles. The analysis is for the proteins remaining on the affinity column after acidic elution.

Band #	Protein species	Accession	Uniprot ID	Mascot Score	% Coverage	Protein MW	# of species
1	ATP synthase subunit alpha, mitochondrial OS=Mus musculus GN	ATPA_MOUSE	Q03265	107	16	59716.00	1
2	Keratin 15 OS=Mus musculus GN=Krt15 PE=3 SV=1	B1AQ77_MOUSE	B1AQ77	56	23	49463.00	2
3	Sarcoplasmic/endoplasmic reticulum calcium ATPase 1 OS=Mus m	AT2A1_MOUSE	Q8R429	63	6	109355.00	3
4	RNA-binding protein 39	D6RJ85_MOUSE	D6RJ85	33	43	6953.00	4

Supplementary tables 2. Interactors of Trx2 as identified by the proteomics and Y2H screens including those currently available in BioGRID.

Supplementary table 2.1. Cumulative protein interactions of mouse Trx2 as detected by acidic ("Acid") and DTT elutions ("DTT") in extracts from different mouse tissues. The table represents the combined data from all experiments with mitochondrial and total cell lysates. All proteins highlighted in green are of mitochondrial localization according to MitoCarta2.0. The DTT elutions in skeletal muscle correspond to two different experiments for total cell lysates (DTT 1, 2, analyzed by 2D electrophoresis) and an experiment where mitochondrial lysates were examined (DTT m, analyzed by 1D SDS PAGE). Cardiac and brain mitochondrial lysates (designation "m") were analyzed by 1D and 2D electrophoresis respectively. The raw data for this table are presented in Supplementary tables 1.1-1.13. Total tissue hits (right column) were calculated by the sum of each protein species detected in different tissues by Acid or DTT elutions. In the case of the DTT elutions of the skeletal muscle experiments (three columns), the respective interactome was calculated as the sum of all detected protein species and was considered as a single experiment (one column) in the calculation of total tissue hits.

# of protein species	Uniprot ID	Protein species	Lung		Skeletal muscle				Kidney		Cardiac muscle		Brain		Total # of tissues hits per elution per protein species
			Acid	DTT	Acid	DTT 1	DTT 2	DTT m	Acid	DTT	Acid m	DTT m	Acid m	DTT m	
1	P56480	ATP synthase subunit beta, mitochondrial	+		+		+		+			+	+	+	7
2	Q61171	Peroxiredoxin-2	+	+		+			+	+				+	6
3	Q03265	ATP synthase subunit alpha, mitochondrial	+		+	+		+			+		+	+	6
4	O08553	Dihydropyrimidinase-related protein 2		+					+	+			+	+	5
5	P16858	Glyceraldehyde-3-phosphate dehydrogenase	+		+	+	+						+	+	5
6	P17182	Alpha-enolase	+	+						+				+	4
7	P35700	Peroxiredoxin-1		+		+	+			+				+	4
8	O08807	Peroxiredoxin-4	+	+						+				+	4
9	O08709	Peroxiredoxin-6		+		+				+				+	4
10	P63038	60 kDa heat shock protein,				+	+			+				+	3

		mitochondrial													
11	P60710	Actin, cytoplasmic 1	+										+	+	3
12	P53996	Cellular nucleic acid-binding protein		+		+	+			+					3
13	P02088	Hemoglobin subunit beta-1		+		+	+			+					3
14	Q7TMM9	Tubulin beta-2A chain	+										+	+	3
15	P17563	Methanethiol oxidase/ Se-binding protein 1		+						+					2
16	O35226	26S proteasome non-ATPase regulatory subunit 4		+			+								2
17	Q99KI0	Aconitate hydratase, mitochondrial					+			+					2
18	P62737	Actin, aortic smooth muscle			+		+								2
19	Q9R0Y5	Adenylate kinase isoenzyme 1				+	+			+					2
20	P47738	Aldehyde dehydrogenase, mitochondrial	+						+						2
21	P23927	Alpha-crystallin B chain	+		+										2
22	P07356	Annexin A2		+						+					2
23	Q9DCX2	ATP synthase subunit d, mitochondrial											+	+	2
24	P21550	Beta-enolase			+		+								2
25	P18760	Cofilin-1		+						+					2
26	P56389	Cytidine deaminase							+	+					2
27	Q9CR68	Cytochrome b-c1 complex subunit Rieske, mitochondrial											+	+	2
28	Q9D7X3	Dual specificity protein phosphatase 3		+		+	+								2
29	P47753	F-actin-capping protein subunit alpha-1	+						+						2
30	P16045	Galectin-1		+		+	+								2
31	P62874	Guanine nucleotide-binding protein											+	+	2
32	B1AQ77	Keratin 15				+		+				+			2

33	Q9D154	Leukocyte elastase inhibitor A		+						+					2
34	Q3ULD5	Methylcrotonoyl-CoA carboxylase beta chain, mitochondrial	+						+						2
35	Q8VDD5	Myosin-9	+						+						2
36	Q91WD5	NADH dehydrogenase [ubiquinone] iron-sulfur protein 2, mitochondrial							+				+		2
37	Q91VD9	NADH-ubiquinone oxidoreductase 75 kDa subunit, mitochondrial							+		+				2
38	P99029	Peroxiredoxin-5, mitochondrial							+	+					2
39	Q9D051	Pyruvate dehydrogenase E1 component subunit beta, mitochondrial											+	+	2
40	P07724	Serum albumin	+	+											2
41	P38647	Stress-70 protein, mitochondrial				+	+			+					2
42	Q60864	Stress-induced-phosphoprotein 1		+		+	+								2
43	Q8K2B3	Succinate dehydrogenase [ubiquinone] flavoprotein subunit, mitochondrial			+				+						2
44	Q9D5V6	Synapse-associated protein 1		+						+					2
45	P20108	Thioredoxin-dependent peroxide reductase, mitochondrial				+				+					2
46	P17751	Triosephosphate isomerase			+	+	+								2
47	P20152	Vimentin	+	+											2
48	P50516	V-type proton ATPase catalytic subunit A	+						+						2
49	P62259	14-3-3 protein epsilon (	+						+						2
50	Q8K354	Carbonyl reductase [NADPH] 3	+	+											2

51	P07310	Creatine kinase M-type			+	+	+								2
52	Q9R0P5	Destrin (Actin-depolymerizing factor)		+						+					2
53	Q91VM9	Inorganic pyrophosphatase 2, mitochondrial		+						+					2
54	P70404	Isocitrate dehydrogenase [NAD] subunit gamma 1, mitochondrial	+										+		2
	Q63836	Selenium-binding protein 2	+							+					2
55	Q9D819	Inorganic pyrophosphatase								+					1
56	P58871	182 kDa tankyrase-1-binding protein		+											1
57	Q9CR00	26S proteasome non-ATPase regulatory subunit 9		+											1
58	Q78JT3	3-hydroxyanthranilate 3,4-dioxygenase								+					1
59	P63323	40S ribosomal protein S12								+					1
60	P62270	40S ribosomal protein S18							+						1
61	P62702	40S ribosomal protein S4, X isoform	+												1
62	P14206	40S ribosomal protein SA	+												1
63	Q99NB1	Acetyl-coenzyme A synthetase 2-like, mitochondrial								+					1
64	P68033	Actin, alpha cardiac muscle 1			+										1
65	P68134	Actin, alpha skeletal muscle			+										1
66	P63260	Actin, cytoplasmic 2												+	1
67	O54931	A-kinase anchor protein 2		+											1
68	P57780	Alpha-actinin-4 (Non-muscle alpha-actinin 4)							+						1
69	P61164	Alpha-centractin	+												1
70	P16460	Argininosuccinate synthase							+						1
71	Q8R3P0	Aspartoacylase								+					1
72	P12382	ATP-dependent 6-				+									1

		phosphofructokinase													
73	P47857	ATP-dependent 6-phosphofructokinase, muscle type					+								1
74	Q8VBT1	Beta-taxilin					+								1
75	Q8VCQ8	Caldesmon 1		+											1
76	P51125	Calpastatin (Calpain inhibitor)		+											1
77	Q08093	Calponin-2		+											1
78	Q9DAW9	Calponin-3		+											1
79	Q9DBC7	cAMP-dependent protein kinase type I-alpha regulatory subunit					+								1
80	P16015	Carbonic anhydrase 3				+	+								1
81	P08074	Carbonyl reductase													1
82	Q9WU84	Copper chaperone for superoxide dismutase								+					1
83	Q6P8J7	Creatine kinase S-type, mitochondrial				+	+								1
84	Q9CZ13	Cytochrome b-c1 complex subunit 1												+	1
85	Q9DB77	Cytochrome b-c1 complex subunit 2, mitochondrial	+												1
86	Q62425	Cytochrome c oxidase subunit NDUFA4									+				1
87	Q8R0Y6	Cytosolic 10-formyltetrahydrofolate dehydrogenase								+					1
88	Q62188	Dihydropyrimidinase-related protein 3	+												1
89	Q8BK84	Dual specificity phosphatase DUPD1				+									1
90	Q8R1X5	Edem3 protein										+			1

91	Q8BFR5	Elongation factor Tu, mitochondrial								+					1
92	P20029	Endoplasmic reticulum chaperone BiP											+		1
93	Q9D1Q6	Endoplasmic reticulum resident protein 44								+					1
94	Q8R180	ERO1-like protein alpha								+					1
95	Q9QZD9	Eukaryotic translation initiation factor 3 subunit I							+						1
96	O09164	Extracellular superoxide dismutase [Cu-Zn]		+											1
97	P47754	F-actin-capping protein subunit alpha-2	+												1
98	Q8BTM8	Filamin-A		+											1
99	P05064	Fructose-bisphosphate aldolase A			+										1
100	P13020	Gelsolin (Actin-depolymerizing factor)	+												1
101	P13707	Glycerol-3-phosphate dehydrogenase				+	+								1
102	P62827	GTP-binding nuclear protein Ran	+												1
103	P63017	Heat shock cognate 71 kDa protein											+		1
104	P14602	Heat shock protein beta-1			+										1
105	P02089	Hemoglobin subunit beta-2								+					1
106	Q8BG05	Heterogeneous nuclear ribonucleoprotein A3								+					1
107	Q60668	Heterogeneous nuclear ribonucleoprotein D0		+											1
108	Q9Z2X1	Heterogeneous nuclear ribonucleoprotein F		+											1
109	O35737	Heterogeneous nuclear ribonucleoprotein H		+											1

110	P61979	Heterogeneous nuclear ribonucleoprotein K								+					1
111	Q8R081	Heterogeneous nuclear ribonucleoprotein L		+											1
112	Q61249	Immunoglobulin-binding protein 1		+											1
113	P40936	Indolethylamine N-methyltransferase	+												1
114	Q9DB29	Isoamyl acetate-hydrolyzing esterase 1 homolog								+					1
115	Q9D6R2	Isocitrate dehydrogenase [NAD] subunit alpha, mitochondrial												+	1
116	O88844	Isocitrate dehydrogenase [NADP] cytoplasmic	+												1
117	P54071	Isocitrate dehydrogenase [NADP], mitochondrial	+												1
118	P11679	Keratin, type II cytoskeletal 8	+												1
119	Q9JHV3	Klra19 protein									+				1
120	Q5M8R7	Ldhb protein									+				1
121	Q61792	LIM and SH3 domain protein 1		+											1
122	P06151	L-lactate dehydrogenase A chain			+										1
123	P28825	Meprin A subunit alpha								+					1
124	Q8CAQ8	MICOS complex subunit Mic60								+					1
125	Q9D6Y7	Mitochondrial peptide methionine sulfoxide reductase								+					1
126	Q62234	Myomesin-1				+	+								1
127	Q9JHR4	Myosin heavy chain IIB				+	+								1
128	P05977	Myosin light chain 1/3, skeletal muscle isoform				+	+								1
129	Q9QVP4	Myosin regulatory light chain 2		+											1

130	P97457	Myosin regulatory light chain 2, skeletal muscle isoform				+	+								1
131	Q5XKE0	Myosin-binding protein C, fast-type				+	+								1
132	P70402	Myosin-binding protein H				+	+								1
133	Q9JIF9	Myotilin				+									1
134	P70441	Na(+)/H(+) exchange regulatory cofactor NHE-RF1								+					1
135	Q9JHL1	Na(+)/H(+) exchange regulatory cofactor NHE-RF2		+											1
136	Q9JIL4	Na(+)/H(+) exchange regulatory cofactor NHE-RF3								+					1
137	Q91XE4	N-acyl-aromatic-L-amino acid amidohydrolase							+						1
138	Q91YT0	NADH dehydrogenase [ubiquinone] flavoprotein 1, mitochondrial			+										1
139	Q9DCT2	NADH dehydrogenase [ubiquinone] iron-sulfur protein 3, mitochondrial											+		1
140	Q6ZWQ0	Nesprin-2									+				1
141	P11930	Nucleoside diphosphate-linked moiety X motif 19 (Nudix motif 19)								+					1
142	Q922B1	O-acetyl-ADP-ribose deacetylase MACROD1				+	+								1
143	Q9DBM2	Peroxisomal bifunctional enzyme								+					1
144	Q99K51	Plastin-3	+												1
145	P60335	Poly(rC)-binding protein 1		+											1
146	Q7TNG8	Probable D-lactate dehydrogenase, mitochondrial								+					1
147	Q99LX0	Protein/nucleic acid deglycase DJ-1				+	+								1

148	P35486	Pyruvate dehydrogenase E1 component subunit alpha, somatic form, mitochondrial											+		1
149	E9Q851	Rac GTPase-activating protein 1										+			1
150	Q01730	Ras suppressor protein 1	+												1
151	P24549	Retinal dehydrogenase 1	+												1
152	D6RJ85	RNA-binding protein 39				+		+							1
153	Q9WTM5	RuvB-like 2	+												1
154	Q8R429	Sarcoplasmic/endoplasmic reticulum calcium ATPase 1				+		+							1
155	Q8C1B7	Septin-11	+												1
156	P42208	Septin-2							+						1
157	O55131	Septin-7 (CDC10 protein homolog)	+												1
158	P16546	Spectrin alpha chain, non-erythrocytic 1							+						1
159	Q60598	Src substrate cortactin		+											1
160	Q3UZZ6	Sulfotransferase 1 family member D1								+					1
161	P26039	Talin-1		+											1
162	Q8BMS1	Trifunctional enzyme subunit alpha, mitochondrial		+											1
163	P20801	Troponin C, skeletal muscle (STNC)				+	+								1
164	Q8R112	Ttn protein				+	+								1
165	P68368	Tubulin alpha-4A chain								+					1
166	P99024	Tubulin beta-5 chain													1
167	Q91YR1	Twinfilin-1								+					1
168	Q3TW96	UDP-N-acetylhexosamine pyrophosphorylase-like protein 1								+					1
169	Q8BRB8	Uncharacterized protein		+											1

170	Q3UWR0	Uncharacterized protein										+			1
171	Q8BIL4	Uncharacterized protein										+			1
172	Q8C3W1	Uncharacterized protein C1orf198 homolog		+											1
173	P46735	Unconventional myosin-Ib	+												1
174	Q9WTI7	Unconventional myosin-Ic	+												1
175	Q8VDJ3	Vigilin		+											1
176	P62814	V-type proton ATPase subunit B, brain isoform							+						1
Sum of proteins per elution, of which (mitochondrial species)			40 (12)	46 (6)	15 (7)	43 (12)			22 (8)	50 (17)	6 (4)	6 (1)	16 (10)	19 (12)	
Common proteins between acidic-DTT elutions, of which (mitochondrial)			6 (3)		7 (5)				4 (2)		0		10 (6)		

Supplementary Table 2.2. Protein species interacting with Trx2 as revealed by a yeast two hybrid system from a human liver library.

Proteins highlighted in green are of mitochondrial localization (MitoCarta2.0).

#	Uniprot ID	Protein species	Gene name	Number of matches
1	P02675	Fibrinogen b chain precursor	FGB	6
2	P02679	Fibrinogen g chain precursor	FGG	1
3	P63261	g-actin	P63261	1
4	Q7Z406	Myosin heavy chain 14	MYH14	10
5	P29966	Myristoylated alanine rich protein kinase C substrate (MARCKS)	MARCKS	1
6	Q04206	NF-κB p65	RELA	1
7	Q14442	Phosphatidylinositol N-acetylglucosaminyltransferase subunit H	PIGH	1
8	P00747	Plasminogen	PLG	4

9	P07237	Protein Disulfide Isomerase	P4HB	1
10	Q53ET4	Serine hydroxymethyl transferase	SHMT1	1
11	P04004	Vitronectin, serum spreading factor	VTN	1

Supplementary Table 2.3. Protein species interacting with Trx2 as revealed by a yeast two hybrid system from a rat brain library.

Proteins highlighted in green are of mitochondrial localization (MitoCarta2.0).

#	Uniprot ID	Protein species	Gene name	Number of matches
1	P04644	40S ribosomal protein S17	Rps17	1
2	P61023	Calcineurin-like EF-hand protein	Chp1	1
3	P05503	Cytochrome c oxidase subunit 1 (mitochondrial)	Mtco1	2
4	Q78P75	Dynein light chain LC8-type 2 (Dynll2)	Dynll2	1
5	D4A314	GLIS family Zn finger 3	Glis3	1
6	Q00900	Human immunodeficiency virus type I enhancer-binding protein 2 homolog	Hivep2	1
7	Q4JFL8	Leukocyte common antigen-related phosphatase	LAR-PTP2	1
8		Mitochondrial 16S ribosomal RNA gene	mt-Rnr2	1

Supplementary Table 2.4. Protein species interacting with human Trx2 according to BioGRID.

Proteins highlighted in green are of mitochondrial localization (MitoCarta2.0).

#	UniProtKB	Protein species	Gene name
1	Q16540	39S ribosomal protein L23, mitochondrial (L23mt) (MRP-L23)	MRPL23
2	P62249	40S ribosomal protein S16	RPS16
3	P62917	60S ribosomal protein L8 (Large ribosomal subunit protein	RPL8

		uL2)	
4	P32969	60S ribosomal protein L9 (Large ribosomal subunit protein uL6)	RPL9
5	P08133	Annexin A6 (67 kDa calelectrin) (Annexin VI) (Annexin-6)	ANXA6
6	P63010	AP-2 complex subunit beta (AP105B) assembly protein complex 2 beta large chain	AP2B1
7	Q96M63	Coiled-coil domain-containing protein 114	CCDC114
8	P32321	Deoxycytidylate deaminase (EC 3.5.4.12) (dCMP deaminase)	DCTD
9	P40692	DNA mismatch repair protein Mlh1 (MutL protein homolog 1)	MLH1
10	Q9UNE7	E3 ubiquitin-protein ligase CHIP transferase CHIP	STUB1
11	P19474	E3 ubiquitin-protein ligase TRIM21	TRIM21
12	O95071	E3 ubiquitin-protein ligase UBR5	UBR5
13	P05062	Fructose-bisphosphate aldolase B (EC 4.1.2.13) (Liver-type aldolase)	ALDOB
14	P04150	Glucocorticoid receptor (GR) (Nuclear receptor subfamily 3 group C member 1)	NR3C1
15	O00461	Golgi integral membrane protein 4 (Golgi integral membrane protein, cis)	GOLIM4
16	Q96D09	G-protein coupled receptor-associated sorting protein 2 (GASP-2)	GPRASP2
17	P34931	Heat shock 70 kDa protein 1-like (Heat shock 70 kDa protein 1L) (Heat shock 70 kDa protein 1-Hom) (HSP70-Hom)	HSPA1L
18	Q9HCE1	Helicase MOV-10 (EC 3.6.4.13) (Armitage homolog) (Moloney leukemia virus 10 protein)	MOV10
19	Q12905	Interleukin enhancer-binding factor 2 (Nuclear factor of activated T-cells 45 kDa)	ILF2
20	Q12906	Interleukin enhancer-binding factor 3 (Double-stranded RNA-binding protein 76)	ILF3
21	P05783	Keratin, type I cytoskeletal 18 (Cell proliferation-inducing gene 46 protein) (Cytokeratin-18) (CK-18) (Keratin-18) (K18)	KRT18
22	Q6A162	Keratin, type I cytoskeletal 40 (Cytokeratin-40)	KRT40
23	P43364	Melanoma-associated antigen 11 (Cancer/testis antigen 1.11) (CT1.11) (MAGE-11 antigen)	MAGEA11

24	Q15555	Microtubule-associated protein RP/EB family member 2 (APC-binding protein EB2) (End-binding protein 2) (EB2)	MAPRE2
25	Q9UPY8	Microtubule-associated protein RP/EB family member 3 (EB1 protein family member 3) (EBF3) (End-binding protein 3) (EB3) (RP3)	MAPRE3
26	Q5JR59	Microtubule-associated tumor suppressor candidate 2 (Cardiac zipper protein)	MTUS2
27	Q9NS69	Mitochondrial import receptor subunit TOM22 homolog (hTom22) (1C9-2) (Translocase of outer membrane 22 kDa subunit homolog)	TOMM22
28	Q99683	Mitogen-activated protein kinase kinase kinase 5	MAP3K5
29	Q96HT8	MORF4 family-associated protein 1-like 1	MRFAP1L1
30	Q96CD2	Phosphopantothenoylcysteine decarboxylase (PPC-DC)	PPCDC
31	O95758	Polypyrimidine tract-binding protein 3 (Regulator of differentiation 1) (Rod1)	PTBP3
32	Q9UI14	Prenylated Rab acceptor protein 1 (PRA1 family protein 1)	RABAC1
33	P61289	Proteasome activator complex subunit 3 (11S regulator complex subunit gamma)	PSME3
34	Q52LJ0	Protein FAM98B	FAM98B
35	Q8IZU0	Protein FAM9B	FAM9B
36	Q8IZE3	Protein-associating with the carboxyl-terminal domain of ezrin (Ezrin-binding protein PACE-1) (SCY1-like protein 3)	SCYL3
37	Q9UJ41	Rab5 GDP/GTP exchange factor (RAP1)	RABGEF1
38	Q96HR9	Receptor expression-enhancing protein 6 (Polyposis locus protein 1-like 1)	REEP6
39	P49247	Ribose-5-phosphate isomerase (EC 5.3.1.6) (Phosphoriboisomerase)	RPIA
40	Q9GZL7	Ribosome biogenesis protein WDR12 (WD repeat-containing protein 12)	WDR12
41	Q8IUH3	RNA-binding protein 45 (Developmentally-regulated RNA-binding protein 1) (RB-1) (RNA-binding motif protein 45)	RBM45
42	Q9H0F6	Sharpin (Shank-associated RH domain-interacting protein) (Shank-interacting protein-like 1) (hSIPL1)	SHARPIN

43	O43805	Sjoegren syndrome nuclear autoantigen 1 (Nuclear autoantigen of 14 kDa)	SSNA1
44	Q01082	Spectrin beta chain, non-erythrocytic 1 (Beta-II spectrin) (Fodrin beta chain) (Spectrin, non-erythroid beta chain 1)	SPTBN1
45	P00441	Superoxide dismutase [Cu-Zn] (EC 1.15.1.1) (Superoxide dismutase 1) (hSod1)	SOD1
46	Q9NVV9	THAP domain-containing protein 1	THAP1
47	P10599	Thioredoxin (Trx) (ATL-derived factor) (ADF) (Surface-associated sulphydryl protein) (SASP)	TXN
48	Q9H3M7	Thioredoxin-interacting protein (Thioredoxin-binding protein 2) (Vitamin D3 up-regulated protein 1)	TXNIP
49	Q15654	Thyroid receptor-interacting protein 6 (TR-interacting protein 6) (TRIP-6) (Opa-interacting protein 1) (OIP-1) (Zyxin-related protein 1) (ZRP-1)	TRIP6
50	Q96CG3	TRAF-interacting protein with FHA domain-containing protein A	TIFA
51	Q04206	Transcription factor p65 (Nuclear factor NF-kappa-B p65 subunit) (Nuclear factor of kappa light polypeptide gene enhancer in B-cells 3)	RELA
52	P55072	Transitional endoplasmic reticulum ATPase (TER ATPase)	VCP
53	P67936	Tropomyosin alpha-4 chain (TM30p1) (Tropomyosin-4)	TPM4
54	Q6RW13	Type-1 angiotensin II receptor-associated protein (AT1 receptor-associated protein)	AGTRAP
55	P08621	U1 small nuclear ribonucleoprotein 70 kDa (U1 snRNP 70 kDa) (U1-70K) (snRNP70)	SNRNP70
56	Q9Y5K5	Ubiquitin carboxyl-terminal hydrolase isozyme L5 (UCH-L5) (EC 3.4.19.12) (Ubiquitin C-terminal hydrolase UCH37) (Ubiquitin thioesterase L5)	UCHL5
57	Q8N1B4	Vacuolar protein sorting-associated protein 52 homolog	VPS52
58	P08670	Vimentin	VIM
59	O43829	Zinc finger and BTB domain-containing protein 14 (Zinc finger protein 161 homolog)	ZBTB14

Supplementary Table 2.5. Four cliques in the disease network of Trx2 that relate ten different diseases.

Diseases in more than one clique are in bold. The numbering of cliques is arbitrary.

Clique 1	Gene name	Uniprot ID
TRIOSEPHOSPHATE ISOMERASE DEFICIENCY	TPI1	P17751
COMBINED OXIDATIVE PHOSPHORYLATION DEFICIENCY	TXN2	Q99757
LACTATE DEHYDROGENASE B DEFICIENCY	LDHB	Q5M8R7
PARKINSON'S DISEASE	PARK7	Q99LX0
Clique 2		
MITOCHONDRIAL COMPLEX III DEFICIENCY, NUCLEAR TYPE 5	UQCRC2	Q9DB77
MITOCHONDRIAL COMPLEX II DEFICIENCY	SDHA	Q8K2B3
COMBINED OXIDATIVE PHOSPHORYLATION DEFICIENCY	TXN2	Q99757
PYRUVATE DEHYDROGENASE COMPLEX DEFICIENCY	PDHA1	P35486
Clique 3		
ANEMIA, SIDEROBLASTIC	HSPA9	P38647
COMBINED OXIDATIVE PHOSPHORYLATION DEFICIENCY	TXN2	Q99757
LACTATE DEHYDROGENASE B DEFICIENCY	LDHB	Q5M8R7
Clique 4		
MITOCHONDRIAL COMPLEX II DEFICIENCY	SDHA	Q8K2B3
TRIOSEPHOSPHATE ISOMERASE DEFICIENCY	TPI1	P17751
COMBINED OXIDATIVE PHOSPHORYLATION DEFICIENCY	TXN2	Q99757
LACTATE DEHYDROGENASE B DEFICIENCY	LDHB	Q5M8R7